

DOKUZ EYLÜL UNIVERSITY
GRADUATE SCHOOL OF NATURAL AND APPLIED
SCIENCES

STEEL FIBER-MATRIX BOND
CHARACTERISTICS OF CEMENT BASED
COMPOSITES

by

Ahsanollah BEGLARIGALE

July, 2013

İZMİR

**STEEL FIBER-MATRIX BOND
CHARACTERISTICS OF CEMENT BASED
COMPOSITES**


**A Thesis Submitted to the
Graduate School of Natural and Applied Sciences of Dokuz Eylül University
In Partial Fulfillment of the Requirements for the Degree of Master of Science
in Civil Engineering, Construction Materials Program**

**by
Ahsanollah BEGLARIGALE**

**July, 2013
İZMİR**

M.Sc THESIS EXAMINATION RESULT FORM

We have read the thesis entitled “**STEEL FIBER-MATRIX BOND CHARACTERISTICS OF CEMENT BASED COMPOSITES**” completed by **AHSANOLLAH BEGLARIGALE** under supervision of **ASSOC. PROF. DR. HALİT YAZICI** and we certify that in our opinion it is fully adequate, in scope and in quality, as a thesis for the degree of Master of Science.



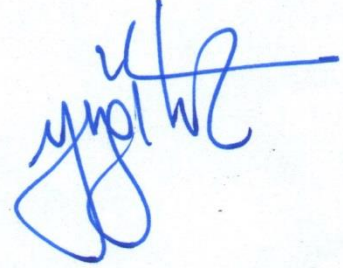
Assoc. Prof. Dr. Halit YAZICI

Supervisor



Assoc. Prof. Dr. Semsî YAZICI

(Jury Member)



Assist. Prof. Dr. Hüseyin YIGİTER

(Jury Member)



Prof. Dr. Ayşe OKUR

Director

Graduate School of Natural and Applied Sciences

ACKNOWLEDGMENTS

First and foremost I would like to express my deepest appreciation to my advisor, Assoc. Prof. Dr. Halit YAZICI, for his everlasting energy, valuable guidance, and wide knowledge that led to the completion of this research. I continuously received his personal support as much as his technical support. Herein, I would like to present my sincere thanks to him for all of his support.

Thanks are also given to Assist. Prof. Dr. Hüseyin YİĞİTER for his support throughout my master study. I am thankful to Research Assistant (MSc.) Çağlar YALÇINKAYA for his valuable helps and supports during my master study.

I would like to thank everyone in Civil engineering - Construction Materials department and laboratory of Dokuz Eylül University.

This thesis is a part of the TÜBİTAK MAG project No: 112M598. Special thanks to TÜBİTAK for their support and financial aids. The author acknowledges to Bekaert (Turkey), BASF (Turkey), DRACO, Sika (Turkey), POMZA EXPORT (POMEX), Modern Beton, Batı Beton, and Adana cement factory for their material supports.

Lastly I would like to give my sincere thanks and deepest appreciation to my life partner, my dear wife Avat MOUSHEKAF who I'm living for her. I would like to thank my family for all their love, patient, and support in my whole life.

Ahsanollah BEGLARIGALE

STEEL FIBER-MATRIX BOND CHARACTERISTICS OF CEMENT BASED COMPOSITES

ABSTRACT

The fiber-matrix bond characteristic is one of the most important factors which affect the mechanical properties of various steel fiber reinforced concretes (SFRC). Forasmuch as SFRC resists tensile forces as a composite material by its fiber and matrix phases, the fiber-matrix bond affects force transmission between them.

The aim of this research is to investigate some of the factors which affect the steel fiber-matrix bond characteristics by means of pull-out test. Ordinary mortar (OM) and reactive powder concrete (RPC) was used as main matrices. The effect of parameters such as end condition of fiber (smooth or hooked-end), embedment length, water/binder ratio, paste phase of RPC, steel-micro fiber, and curing conditions on fiber-matrix pull-out behavior were determined. The mechanical properties of the mixture were also analyzed.

In the second stage, the effect of some chemical admixtures on fiber-matrix bond characteristic of OM and RPC mixtures were investigated. Four polymer based, a corrosion inhibitor, and a waterproofing admixture were used in this stage of study. Additionally, fresh states, mechanical properties, chloride ion penetrability, and physical properties of the mixtures were determined.

Microstructural analysis was also performed to evaluate the microstructure of fiber-matrix interface of mixtures. Corrosion of steel fiber was also monitored by polarization technique which is widely utilized in the metallurgy and corrosion engineering.

Keywords: Pull-out test, bond characteristics, reactive powder concrete, steel fiber

ÇİMENTO ESASLI KOMPOZİTLERİN ÇELİK LİF-MATRİS ADERANSI ÖZELLİKLERİ

ÖZ

Çelik lifli betonların mekanik özelliklerini etkileyen en önemli faktörlerden biri lif-matris aderansıdır. Lifli betonlar kompozit malzeme oldukları dolayısıyla çekme kuvvetlerini lif ve matris ile kompozit bir davranışla karışılmaktadırlar. Bu sebepten dolayı aderans özellikleri lif ve matris arasında yük transferini etkileyebilmektedir.

Bu çalışmanın esas amacı çekip-çıkarma deneyi yöntemi ile lif-matris aderansını etkileyen bazı faktörlerin araştırılmasıdır. Matris olarak genelleksel çimento esaslı bir harç (OM) ve reaktif pudra beton (RPC) kullanılmıştır. Lifin kancalı ve kancasız durumu, lif gömme boyu, su/bağlayıcı oranı, hamur fazın etkisi, ve kür koşulları gibi parametrelerin lif-matris aderansında etkileri araştırılmıştır. Ayrıca karışımların mekanik özellikleri belirlenmiştir.

İkinci aşamada bazı kimyasal katkıların OM ve RPC karışımların lif-matris aderansı özelliklerinde etkisi araştırılmıştır. Dört farklı polimer, bir korozyon inhibitörü ve bir su geçirimsizlik sağlayan katkı kullanılmıştır. Ayrıca karışımların taze hal, mekanik ve fiziksel gibi özellikleri’de belirlenmiştir.

Lif-matris arayüzey özelliklerini daha detaylı irdelemek için iç yapı çalışmaları yapılmıştır. Ayrıca metalürji mühendisliği ve korozyon mühendisliğinin çalışmalarında kullanılan elektrokimyasal yöntemlerden polarizasyon tekniği ile çelik lif korozyon gelişimini izlenmiştir.

Anahtar Kelimeler: Çekme- çıkarma deneyi, aderans özellikleri, reaktif pudra beton, çelik lif

CONTENTS

	Page
THESIS EXAMINATION RESULT FORM	ii
ACKNOWLEDGEMENTS	iii
ABSTRACT	iv
ÖZ	v
LIST OF FIGURES	viii
LIST OF TABLES	xiv
CHAPTER ONE – INTRODUCTION	1
1.1 Aims and Scope	1
CHAPTER TWO – THE FIBER-MATRIX BOND CHARACTERISTICS.....	3
2.1 The Fiber-matrix Interface	3
2.2 Pull-out Behaviour	5
2.2.1 Effect of Matrix Type and Properties on Pull-out Behaviour.....	6
2.2.2 Effect of Fiber Type and Characteristics on Pull-out Behavior	8
2.2.3 Effect of Fiber Type and Characteristics on Pull-out Behavior	12
2.3 Pull-out Test Methods	13
CHAPTER THREE – EXPERIMENTAL	20
3.1 Purpose	20
3.2 Scope	20
3.3 Materials	21
3.4 Abbreviations	25
3.5 Production of Mixtures	28
3.5.1 Preparing of Mixtures	32

3.5.2 Casting	33
3.6 Pull-out Test	34
3.7 Microstructure Investigation	37
3.8 Corrosion of Steel Fibers	38
CHAPTER FOUR – RESULTS AND DISCUSSIONS	40
4.1 The Effect of Matrix Type, Fiber end Condition, Embedment Length, and W/C Ratio	40
4.1.1 Mechanical Properties of Mixtures	40
4.1.2 The Effect of End Condition and Embedment Length of Fiber	47
4.1.3 The Effect of Water/Binder Ratio on Pull-out Behavior	66
4.1.4 Microstructure Investigation	80
4.2 The Effect of Chemical Admixtures	87
4.2.1 Fresh State	87
4.2.2 Mechanical Properties	91
4.2.3 Chloride Penetration	94
4.2.4 Physical Properties of the Mixtures	96
4.2.5 Effect of Chemical Admixtures on Fiber-matrix Pull-out Behavior ...	108
4.2.6 Microstructure Investigation	116
4.2.7 Corrosion Measurement.....	125
CHAPTER FIVE – CONCLUSIONS	126
REFERENCES	129

LIST OF FIGURES

	Page
Figure 2.1 A schematic description of the fiber-matrix transition zone	3
Figure 2.2 Effect of silica fume on bond strength.....	4
Figure 2.3 SEM observation of fiber surface in various conditions	5
Figure 2.4 Pull-out peak load value of different SIFCON matrices 1	6
Figure 2.5 Pull-out peak load value of different SIFCON matrices 2	7
Figure 2.6 Effect of matrix strength on Pull-out behaviors	7
Figure 2.7 Effect of matrix strength on bond strength	8
Figure 2.8 Load–displacement curve averages for hooked and smooth fibers	9
Figure 2.9 Pull-out behavior under different embedment length (Hooked-end)	10
Figure 2.10 Pull-out behavior under different embedment length (smooth)	10
Figure 2.11 Different pullout mechanisms according to the geometry of fiber	12
Figure 2.12 SEM images of congestion of ASR products throughout the fiber-matrix interface	13
Figure 2.13 Pullout specimen and layout of fibers used by Chan & Chu (2003)	14
Figure 2.14 Pullout test setup (Chan & Chu, 2003)	15
Figure 2.15 Manufacturing process of specimen, details of steel plate, configuration and dimensions of specimen used by Lee, Kang, & Kim (2010)	16
Figure 2.16 Pullout apparatus used by Shannag, Brincker, & Hansen (1997)	17
Figure 2.17 Pull-out test used by Kima et al. (2013)	17
Figure 2.18 Specimen restraint diagram (pullout test) (Abu-Lebdeh et al., 2011) ...	18
Figure 2.19 The Apparatus for pull-out tests used by Aiello et al., (2009)	18
Figure 2.20 Pullout test apparatus used by Cunha, Barros, & Sena-Cruz (2010)	19
Figure 3.1 Hobart mixture	32
Figure 3.2 Fiber fixing apparatus	33
Figure 3.3 The flexural and compressive strength machines	34
Figure 3.4 The Schematic diagram of pull-out test setup	35
Figure 3.5 The test procedure of pull-out test	36
Figure 3.6 Fractured small samples (SEM).....	37
Figure 3.7 Wetting-drying cabin	38

Figure 3.8 Corrosion measurement system	39
Figure 4.1 Flexural strength of OM (0.5 W/C) and redesigned OM Mixtures	41
Figure 4.2 Compressive strength of OM (0.5 W/C) and redesigned OM Mixtures .	41
Figure 4.3 Flexural strength of RPC (0.2 W/B) and redesigned RPC Mixtures	42
Figure 4.4 Compressive strength of RPC (0.2 W/B) and redesigned RPC Mixtures	43
Figure 4.5 Flexural strength of reinforced RPC (0.2 W/B) mixtures	44
Figure 4.6 Compressive strength of reinforced RPC mixtures	44
Figure 4.7 Flexural strength of reinforced RPC (0.2 W/B) and redesigned RPC mixtures by steel-micro fiber	45
Figure 4.8 Compressive strength of reinforced RPC (0.2 W/B) and redesigned RPC mixtures by steel-micro fiber	45
Figure 4.9 Flexural and Compressive strength of paste phase of RPC (0.2 W/B) ...	46
Figure 4.10 Appearance of the hooked-end fiber before and after pull-out test	47
Figure 4.11 Pull-out load–displacement relationship of OM mixture with hooked-end fibers (7 days)	48
Figure 4.12 Pull-out load–displacement relationship of OM mixture with hooked-end fibers (28 days)	48
Figure 4.13 Pull-out load–displacement relationship of OM mixture with smooth fibers (7 days)	49
Figure 4.14 Pull-out load–displacement relationship of OM mixture with smooth fibers (28 days)	50
Figure 4.15 Pull-out peak load values of OM mixture	51
Figure 4.16 Flexural strength of OM (0.5 W/C) and redesigned OM Mixtures	51
Figure 4.17 Pull-out load–displacement relationship of redesigned OM mixture with 0.3 W/C ratio for hooked-end fibers (7 days)	52
Figure 4.18 Pull-out load–displacement relationship of redesigned OM mixture with 0.3 W/C ratio for hooked-end fibers (28 days)	53
Figure 4.19 Pull-out load–displacement relationship of redesigned OM mixture with 0.3 W/C ratio for smooth fibers (7 days)	54
Figure 4.20 Pull-out load–displacement relationship of redesigned OM mixture with 0.3 W/C ratio for smooth fibers (28 days)	54
Figure 4.21 Pull-out peak load values of redesigned OM with 0.3 W/C mixture	55

Figure 4.22 Pull-out debonding toughness values of redesigned OM with 0.3 W/C ratio mixture	56
Figure 4.23 Pull-out load–displacement relationship of RPC for hooked-end fibers (7 days)	57
Figure 4.24 Pull-out load–displacement relationship of RPC for hooked-end fibers (28 days)	57
Figure 4.25 Pull-out load–displacement relationship of RPC for smooth fibers (7 days)	58
Figure 4.26 Pull-out load–displacement relationship of RPC for smooth fibers (7 days)	59
Figure 4.27 Pull-out load–displacement relationship of RPC for smooth fiber with 4 cm embedment length (28 days)	60
Figure 4.28 Pull-out peak load values of RPC mixture	61
Figure 4.29 Pull-out debonding toughness values of RPC mixture	61
Figure 4.30 Pull-out load–displacement relationship of paste phase RPC for hooked-end fibers (7 days)	62
Figure 4.31 Pull-out load–displacement relationship of paste phase RPC for hooked-end fibers (28 days)	63
Figure 4.32 Pull-out load–displacement relationship of paste phase RPC for smooth fibers (7 days)	64
Figure 4.33 Pull-out load–displacement relationship of paste phase RPC for smooth fibers (28 days)	64
Figure 4.34 Pull-out peak load values of paste phase of RPC mixture	65
Figure 4.35 Pull-out debonding toughness values of paste phase of RPC mixture .	66
Figure 4.36 Pull-out load–displacement relationship of redesigned OM mixture in various W/C ratios (7 days water curing)	67
Figure 4.37 Pull-out load–displacement relationship of redesigned OM mixture in various W/C ratios (28 days water curing)	68
Figure 4.38 Pull-out load–displacement relationship of redesigned OM mixture in various W/C ratios (steam curing)	69
Figure 4.39 Pull-out load–displacement relationship of redesigned OM mixture in various W/C ratios (autoclave curing)	70

Figure 4.40 Pull-out peak load values of redesigned OM mixture in various W/C ratios	71
Figure 4.41 Debonding toughness values of redesigned OM mixture in various W/C ratios	71
Figure 4.42 Pull-out load–displacement relationship of redesigned RPC mixture in various W/C ratios (7 days water curing)	72
Figure 4.43 Pull-out load–displacement relationship of redesigned RPC mixture in various W/C ratios (28 days water curing)	73
Figure 4.44 Pull-out load–displacement relationship of redesigned RPC mixture in various W/C ratios (steam curing)	74
Figure 4.45 Pull-out load–displacement relationship of redesigned RPC mixture in various W/C ratios (autoclave curing)	75
Figure 4.46 Pull-out load–displacement relationship of RPC with 0.3 and 0.2 W/B ratio (autoclave curing)	75
Figure 4.47 Peak load values of redesigned RPC mixture in various W/C ratios ...	76
Figure 4.48 Debonding toughness values of RPC mixture in various W/C ratios ...	77
Figure 4.49 Pull-out load–displacement relationship of reinforced redesigned RPC mixture in various W/C ratios (7 days water curing)	78
Figure 4.50 Pull-out load–displacement relationship of reinforced redesigned RPC mixture in various W/C ratios (28 days water curing)	78
Figure 4.51 Pull-out peak load of RPC mixtures (R) and reinforced RPC mixtures (RF) at 7 and 28 days water curing	79
Figure 4.52 Pull-out debonding toughness of RPC mixtures (R) and reinforced RPC mixtures (RF) at 7 and 28 days water curing	80
Figure 4.53 SEM images of fiber-matrix interface of RPC after autoclave curing .	82
Figure 4.54 SEM images of fiber-matrix interface of RPC after autoclave curing .	83
Figure 4.55 EDS analysis of tobermorite gel observed in fiber-matrix interface of RPC (0.2 W/B ratio) mixture after autoclave curing	83
Figure 4.56 SEM images of fiber-matrix interface of RPC (0.3 W/B ratio) mixture after autoclave curing	84
Figure 4.57 SEM images of fiber-matrix interface of RPC (0.3 W/B ratio) mixture after autoclave curing	85

Figure 4.58 SEM images of fiber-matrix interface of redesigned RPC (0.4 W/B ratio) mixture after autoclave curing	86
Figure 4.59 The percentage of reduction in superplasticizer dosage for both OM and RPC mixtures	89
Figure 4.60 Unit weight of fresh OM mixtures	90
Figure 4.61 Unit weight of fresh RPC mixtures	91
Figure 4.62 Mechanical strength of chemical admixture containing OM mixtures	92
Figure 4.63 Mechanical strength of chemical admixture containing RPC mixtures	93
Figure 4.64 Rapid chloride ion penetration test result	94
Figure 4.65 Dry bulk density values	96
Figure 4.66 Porosity of OM mixtures	97
Figure 4.67 Porosity of RPC mixtures	98
Figure 4.68 Water absorption of OM mixtures	98
Figure 4.69 Water absorption of RPC mixtures	99
Figure 4.70 Capillary water absorption of F and OM control mixtures	100
Figure 4.71 Capillary water absorption of F and RPC control mixtures	101
Figure 4.72 Capillary water absorption of SI and OM control mixtures	102
Figure 4.73 Capillary water absorption of SI and RPC control mixtures	103
Figure 4.74 Capillary water absorption of SBR containing and OM control mixtures	104
Figure 4.75 Capillary water absorption of SBR containing and RPC control mixtures	105
Figure 4.76 Capillary water absorption of ADP containing and OM control mixtures	106
Figure 4.77 Capillary water absorption of ADP containing and RPC control mixtures	107
Figure 4.78 Pull-out load–displacement relationships of F and OM control mixtures	108
Figure 4.79 Pull-out load–displacement relationships of F and RPC control mixtures	109
Figure 4.80 Pull-out load–displacement relationships of SI and OM control mixtures	109

Figure 4.81 Pull-out load–displacement relationships of SI and RPC control mixtures	110
Figure 4.82 Pull-out load–displacement relationships of SBR containing and OM control mixtures	111
Figure 4.83 Pull-out load–displacement relationships of SBR containing and RPC control mixtures	112
Figure 4.84 Pull-out load–displacement relationships of ADP containing and OM control mixtures	113
Figure 4.85 Pull-out load–displacement relationships of ADP containing and RPC control mixtures	114
Figure 4.86 Pull-out peak load and debonding toughness of chemical admixture containing mixtures	115
Figure 4.87 SEM image of B2-N mixture	116
Figure 4.88 SEM image of Ca rich product observed in B2-N mixture	117
Figure 4.89 EDS analysis of the product which observed in air voids of B2-N mixture	118
Figure 4.90 SEM image of fiber-matrix interface of B2-N mixture	118
Figure 4.91 EDS analysis of the fiber-matrix interface of A2-N	119
Figure 4.92 SEM image of A2-N mixture	120
Figure 4.93 SEM image of A2-R mixture	121
Figure 4.94 SEM images of a) R2-R b) KM-R	122
Figure 4.95 SEM images of SI-N mixture	123
Figure 4.96 SEM images of SI-N mixture	124

LIST OF TABLES

	Page
Table 3.1 Physical, chemical and mechanical properties of cement and chemical composition of cement and silica fume	21
Table 3.2 Sieve analyses of aggregates	22
Table 3.3 Properties of polycarboxylic ether based superplasticizer	22
Table 3.4 Properties of steel fibers	23
Table 3.5 Properties of chemical admixtures	24
Table 3.6 Mix design of step one mixtures (kg/m ³)	27
Table 3.6 Mix design of second step mixtures (kg/m ³)	30
Table 4.1 Chloride Ion Penetrability Based on Charge Passed (ASTM C 1202)	94

CHAPTER ONE

INTRODUCTION

Cement based plain mortar and concrete are known as a brittle construction material which have low tensile strength. This poor behavior of these materials leads to crack under low levels of tensile strain. It has long been recognized that the behavior of such materials can be dramatically improved by the addition of steel or various discontinuous fiber. Steel fiber reinforced concrete (SFRC) is one the most popular composites which resists tensile forces by its fiber and matrix phases. The bond between fiber-matrix provides the stress transferring at the fiber–matrix phases. Mechanical properties of SFRC are dramatically influenced by the bond characteristics at the steel fiber–matrix interface. Some researchers have dealt with this important subject. However there are major lacks of information. Many parameters affect the bond characteristics of fiber–matrix. However, these parameters can be categorized in two main groups as follow:

- 1- Matrix characteristics
- 2- Fiber properties

This experimental study aims to assess the bond characteristics between steel fiber and cement based matrices. The effect of some of matrix and steel fiber properties was determined.

1.1 Aims and Scope

Ordinary mortar (OM) and reactive powder concrete (RPC) were used to evaluate the influence of matrix type. Steel fibers with two different end conditions (smooth and hooked-end) with various embedment lengths were used. The influence of water/binder ratio on pull-out behavior was also determined. Furthermore, four different curing were applied. Microstructure investigation was also carried out in this section of experimental program.

In second step of experimental program the effects of some chemical admixtures on pull-out behavior of steel fiber were determined. Additionally, fresh state, mechanical properties, physical characteristics, and chloride ion penetrability of all mixtures were determined. Microstructure investigation was also carried out in this step of experimental program. Furthermore, after specific wetting-drying cycles, the corrosion development of embedded fibers was also monitored by polarization technique.

CHAPTER TWO

THE FIBER-MATRIX BOND CHARACTERISTICS

This chapter summarizes the general knowledge, and the research studies that have been done on the fiber-matrix bond characteristics of cement based composites.

2.1 The Fiber-matrix Interface

The fiber-matrix interface characteristic (fiber-matrix transition zone) is the most effective factor which affects the bond strength. It is well known that the transition zone in the mature composite is quite porous and also filled with CH in direct contact with the fiber surface (Bentur & Diamond, 1985). These characteristics are similar to aggregate-matrix interfacial transition zone (Neville, 1995). Depend on bulk and fiber properties the CH layer can be 1 μm (duplex film) or much more massive (Bentur, Diamond, & Mindess, 1985). A schematic description of the transition zone showing the different layers is presented in Figure 2.1 (Bentur, Diamond, & Mindess, 1985).

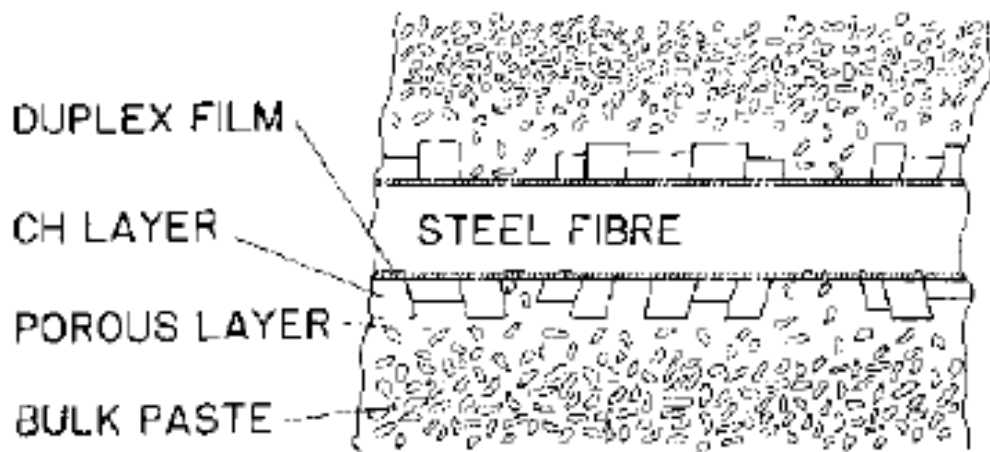


Figure 2.1 A schematic description of the fiber-matrix transition zone (Bentur, Diamond, & Mindess, 1985).

The density of this zone can be increased with supplementary cementitious materials (Bentur et al., 1995, Banthia, 1998, Chan and Li, 1997). Kayali (2004)

reported that using high volume fly ash improves the fiber-matrix interfacial transition zone. Furthermore, because of the pozzolanic effect of fly ash, the bond strength of fiber matrix increased. Chan & Chu (2004) evaluated the incorporation of silica fume in reactive powder to ameliorate the fiber-matrix interfacial properties. It can be concluded from their test result that the optimal silica fume content is between 20% and 30% (Figure 2.2). As shown in Figure 2.3 the microstructural analysis of the fibers revealed that other than longitudinal scratches as result of abrasion by the matrix during pullout process, the surface texture is very similar to that of a raw fiber, while fibers pulled out from the silica fume containing matrix have a different surface microstructure.

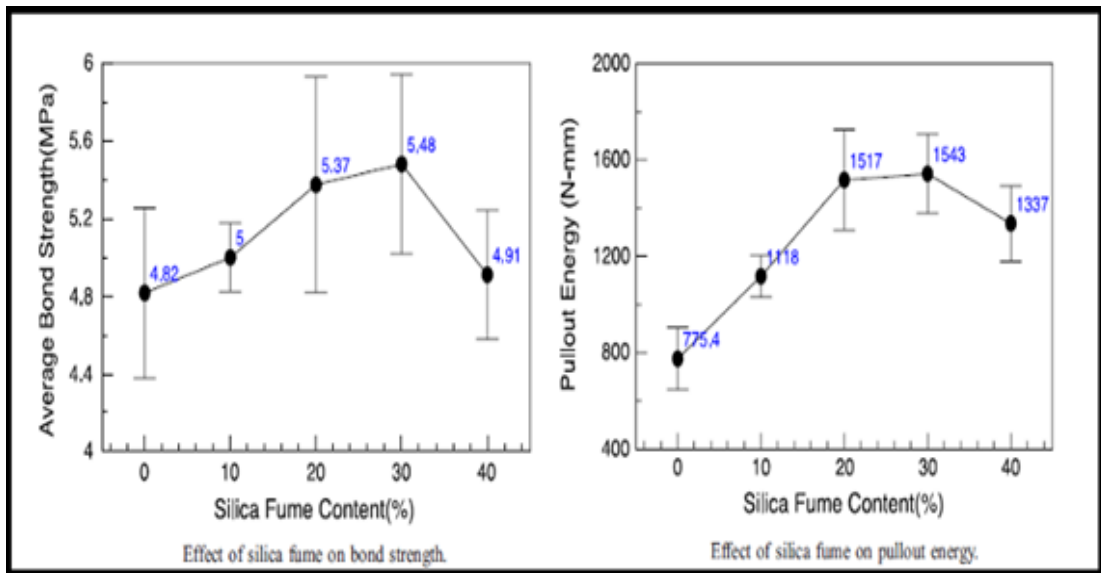


Figure 2.2 Effect of silica fume on fiber-RPC matrix bond strength and pullout energy (Chan & Chu, 2004).

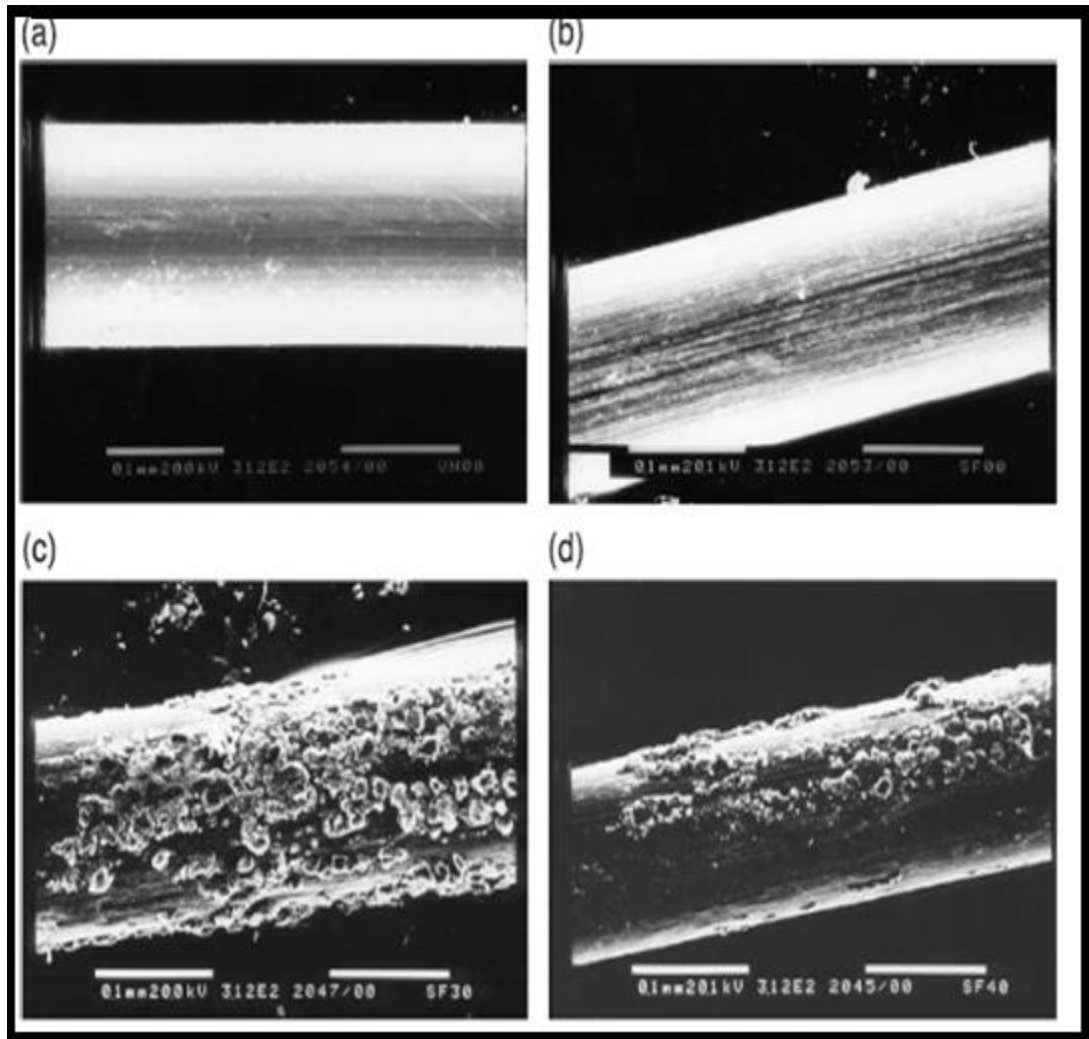


Figure 2.3 SEM observation of fiber surface in various conditions ($\times 300$): (a) raw fiber surface; (b) pullout fiber surface (0% silica fume content); (c) pullout fiber surface (30% silica fume content); (d) pullout fiber surface (40% silica fume content) (Chan & Chu , 2003).

2.2 Pull-out Behaviour

Many studies have been carried out on fiber pull-out behavior using different testing techniques to characterize the fiber-matrix bond characteristics of fiber-reinforced cementations composites. Generally it can be summarized from many researches that the pull-out behavior depends on both matrix and fiber characteristics.

2.2.1 Effect of Matrix type and Properties on Pull-out Behaviour

Parameters such as matrix strength, components, curing condition etc. have been studied intensively by some researchers. The effect of mix proportions of SIFCON matrix (slurry) and curing conditions on fiber pull-out behavior was investigated by Tuyan & Yazıcı (2012). It has been observed that improving the curing conditions and increasing strength of SIFCON matrix increased matrix-fiber bond strength. It can be indicated from their test results that high volume blast furnace slag replacement and decreasing water/binder ratio is significantly effective to improve fiber-matrix bond while the high volume fly ash replacement in the SIFCON matrix has a positive impact only in autoclave curing (Figure 2.4). Additionally, the fiber-matrix interface bond significantly increased as the curing condition improved. It was reported that autoclave curing was more effective than other curing conditions in terms of pull-out behavior while the steam curing is similar to the 28-day standard water curing (Figure 2.5).

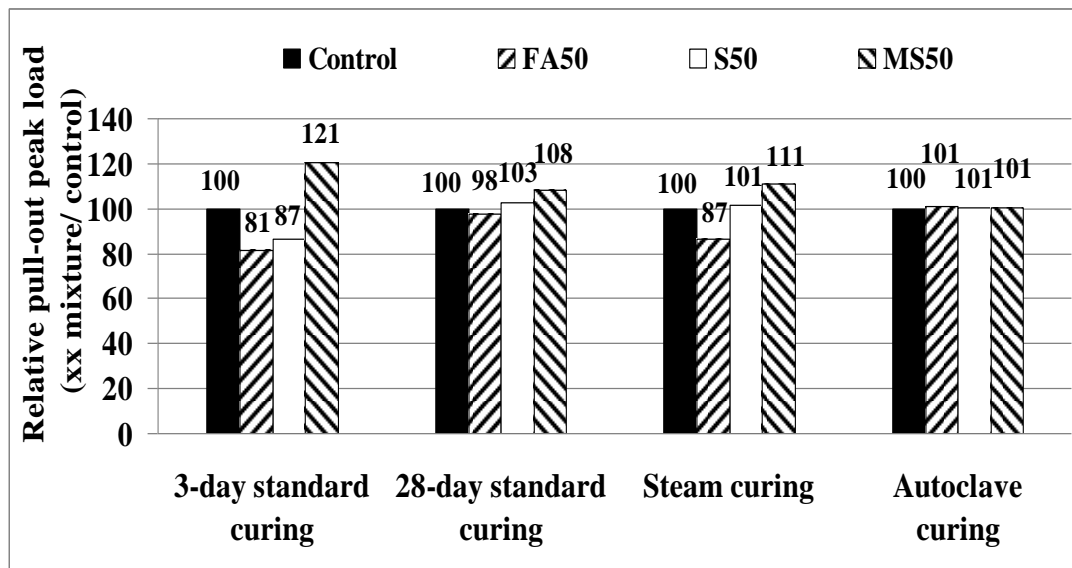


Figure 2.4 Pull-out peak load value of different SIFCON matrix under various curing conditions (Tuyan & Yazıcı, 2012).

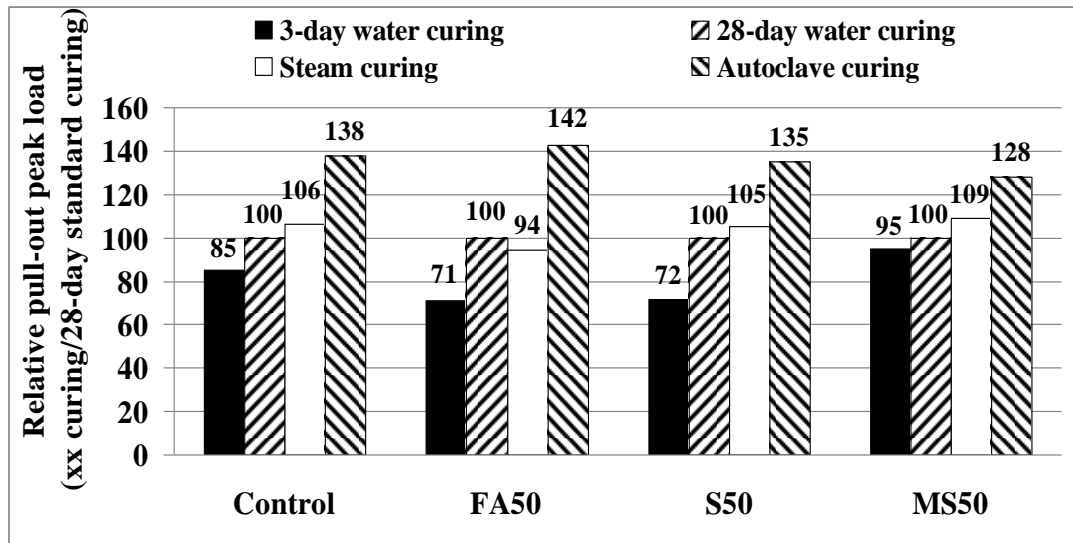


Figure 2.5 Pull-out behaviors of different SIFCON slurries under various curing conditions (Tuyan & Yazıcı, 2012).

The influence of matrix strength on both pull-out peak load and total pullout energy was also investigated by Abu-Lebdeh, Hamoush, Heard, & Zornig (2011). The pull-out peak load and total pull-out energy of very-high strength concrete increase as matrix strength increases (Figure 2.6). As shown in Figure 2.7 the positive effect of matrix strength on bond strength was also reported by Shannag, Brincker, & Hansen (1997).

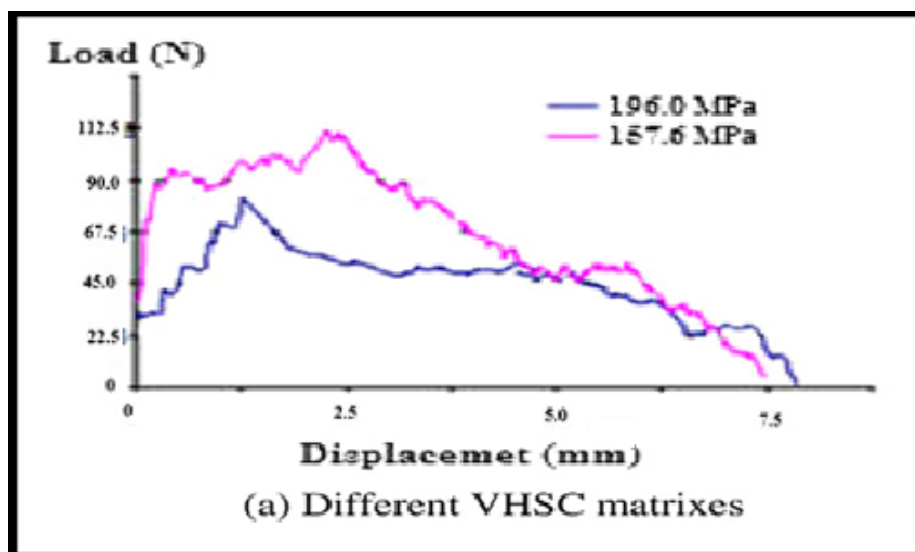


Figure 2.6 Effect of matrix strength on Pull-out behaviors (Abu-Lebdeh et al., 2011).

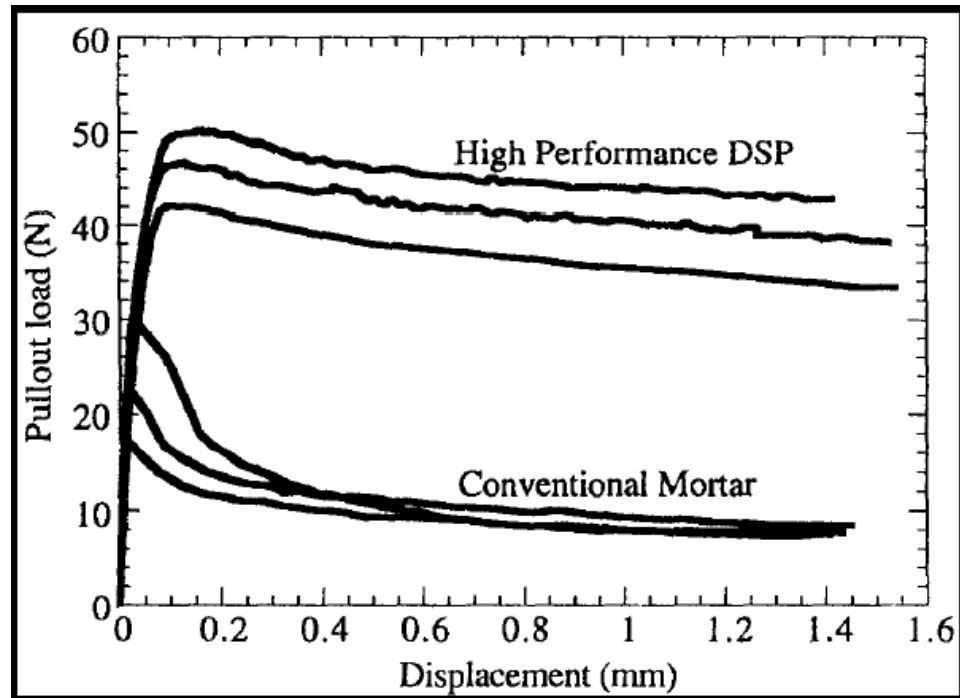


Figure 2.7 Effect of matrix strength on the pullout behavior of steel fibers from cement based matrices (Shannag, Brincker, Hansen, 1997).

2.2.2 Effect of Fiber Type and Characteristics on Pull-out Behavior

Effect of aspect ratio of steel fiber, embedded length and fiber type on pull-out behavior was studied by Tuyan & Yazıcı (2012). Peak load of hooked-end steel fibers was significantly higher than smooth steel fibers. The end condition of fiber was also investigated by Abu-Lebdeh et al. (2011) and similar result was reported (Figure 2.8).

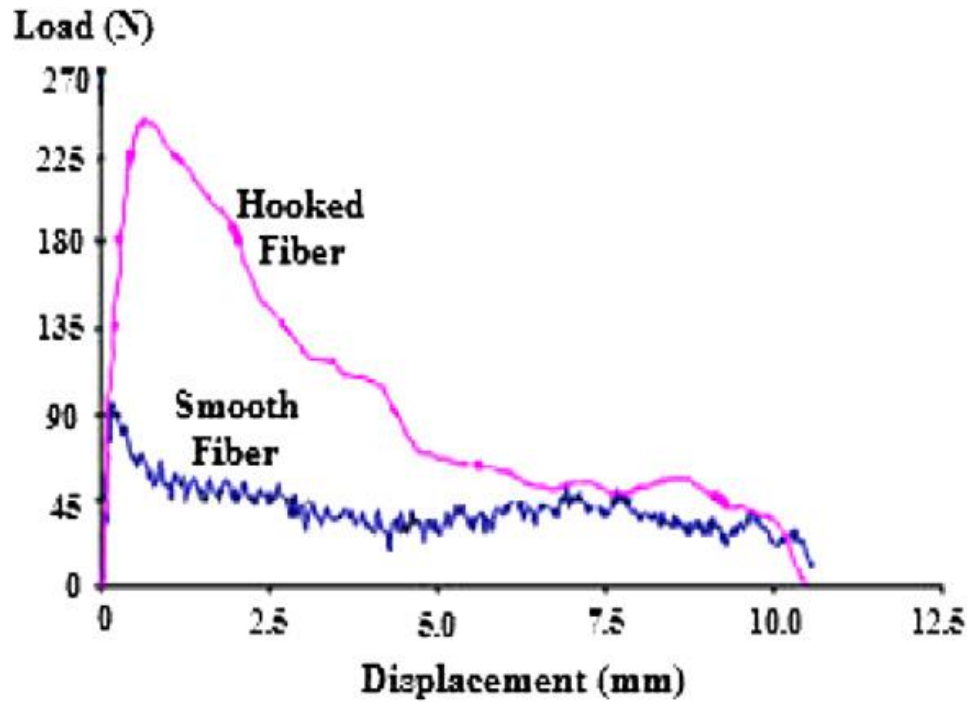


Figure 2.8 Load–displacement curve averages for hooked and smooth D fibers in VHSC with 12.7 mm embedment depth (1 in. = 25.4 mm; 1 N = 0.225 lb; 1 MPa = 145 psi) (Abu-Lebdeh et al., 2011).

Tuyan & Yazıcı (2012) reported that pull-out peak load and debonding toughness increased with increasing in embedment length of smooth and hooked-end fibers (Figures 2.9 and 2.10). Similar results were observed by Shannag, Brincker, & Hansen (1997). It was also observed that increasing the diameter of fiber have positive effect on bond strength between fiber and matrix.

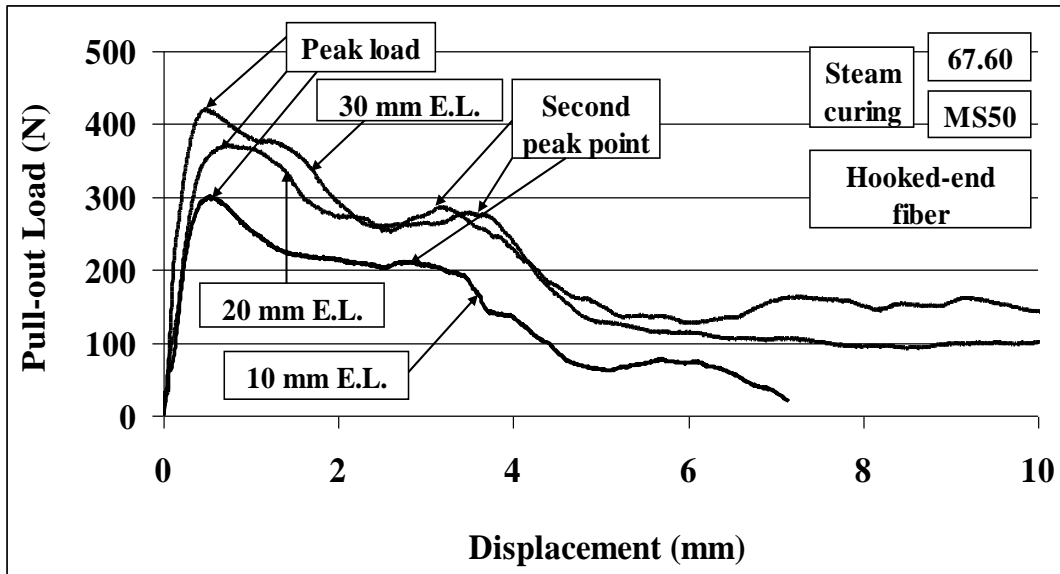


Figure 2.9 Pull-out load–displacement relationship under different embedment length (Hooked-end fiber) (Tuyan & Yazıcı, 2012).

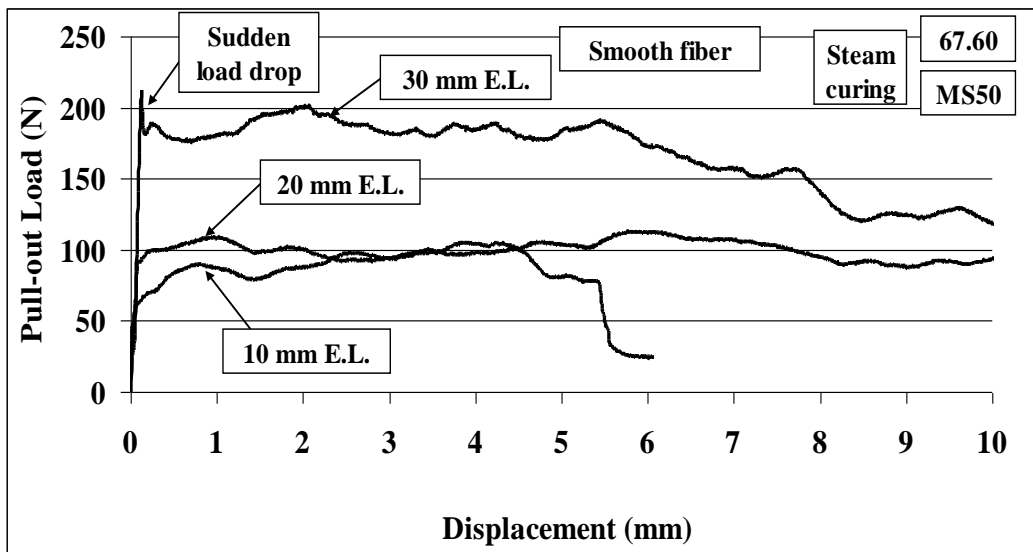


Figure 2.10 Pull-out load–displacement relationship under different embedment length (Smooth fiber) (Tuyan & Yazıcı, 2012).

Interfacial bond behavior of sisal fibers in cement based composites have been investigated by Silva, Mobasher, Soranakom, & Filho (2011). They dealt with the influence of fiber morphology and embedment length on the sisal fiber-cement matrix bond behavior. Their results indicated that sisal fiber morphology influences the bond strength significantly. It was found that the pull-out load increases as the embedment length of fiber increases.

Wu & Li (1999) have investigated the effect of plasma treatment on polyethylene fibers pull-out behavior. They reported that plasma treatment can lead to significant improvement in the pull-out behavior.

Lee, Kang, & Kim (2010) reported that the highest peak load was observed at an angle of 30 ° or 45 ° (the fiber inclination angles considered in the pullout tests were 0°, 15 °, 30 °, 45 °, and 60 °). They reported that pull-out peak load increased as the fibers were oriented at a more inclined angle.

The influence of sand / coarse aggregate (S/a) ratio on the interfacial bond strength of three high strength steel fibers (smooth, hooked, and twisted fiber) in concrete of nuclear power plants (NPP) was investigated by J. J Kim, D. J Kim, Kangb, & Lee (2013). They proved that deformed hooked and twisted steel fiber produced much higher interfacial bond strength than smooth steel fiber (Figure 2.11). Additionally, the highest maximum bond strength was observed in case of hooked-end fiber while twisted fiber generated the highest equivalent bond strength. As the S/a increased, both maximum and equivalent bond strength of twisted fiber showed much more increment compared to smooth and hooked-end fiber.

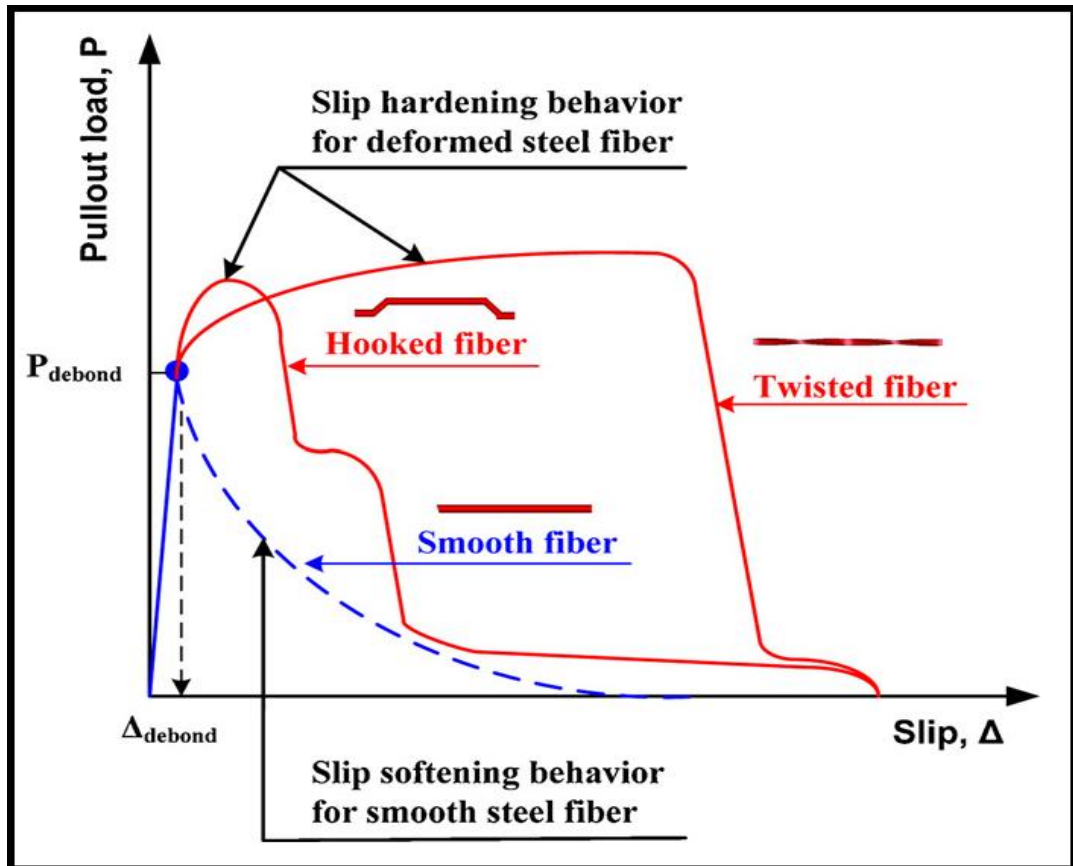


Figure 2.11 Different pullout mechanisms according to the geometry of steel fiber (Kima et al., 2013).

2.2.3 Effect of Durability Problems on Pull-out Behavior

Beglarigale & Yazıcı (2013) have investigated the effect of alkali silica reaction (ASR) on matrix-steel fiber bond characteristics. Test results indicate that the ASR gel congestion (Figure 2.12) in fiber-matrix interface increased the bond strength significantly during alkali exposure.

In recent years, bond characteristics of cement-based composites have been investigated by many researchers. However, there is a major lack of information about the effect of durability problems.

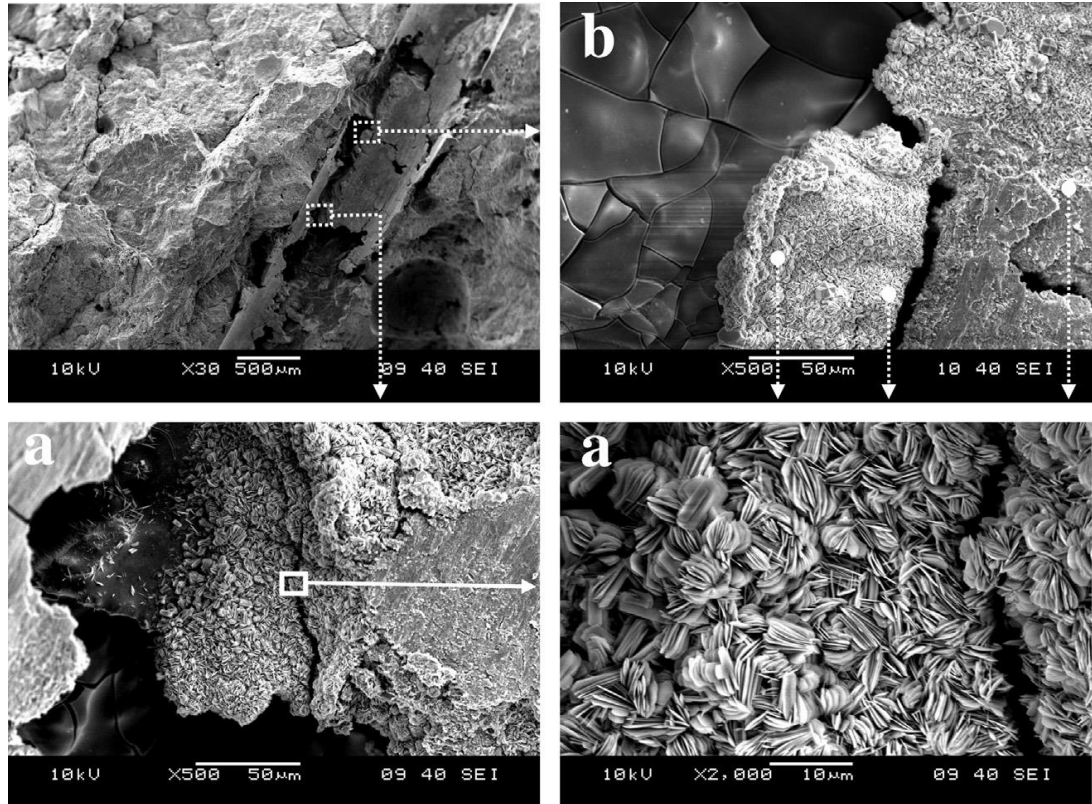


Figure 2.12 SEM images of congestion of ASR products throughout the fiber space after fiber pull-out test with a) rosette-type and b) cracked platy-crystals morphology (Beglarigale & Yazıcı, 2013).

2.3 Pull-out Test Methods

No standard test methods exist. In case of applying tensile force, pull-out tests methods can be classified into double-sided and single-sided tests, while it can be defined as single fiber or multiple fibers according to the number of fibers. This section presents procedures and setup of the pull-out test methods which have used by some researchers according to the available literature.

Chan & Chu (2003) have prepared a dog bone shape mold to prepare the fiber pull-out specimens (Figure 2.13). They arranged nine steel fibers on the matrix. The fibers were bent to form hooks on one end to ensure that the fibers will be pull out from the one half of the specimen. The surface of the section which cast firstly was lubricated to prevent adhesion to the other half. The matrix is then cast into the pull-out half one.

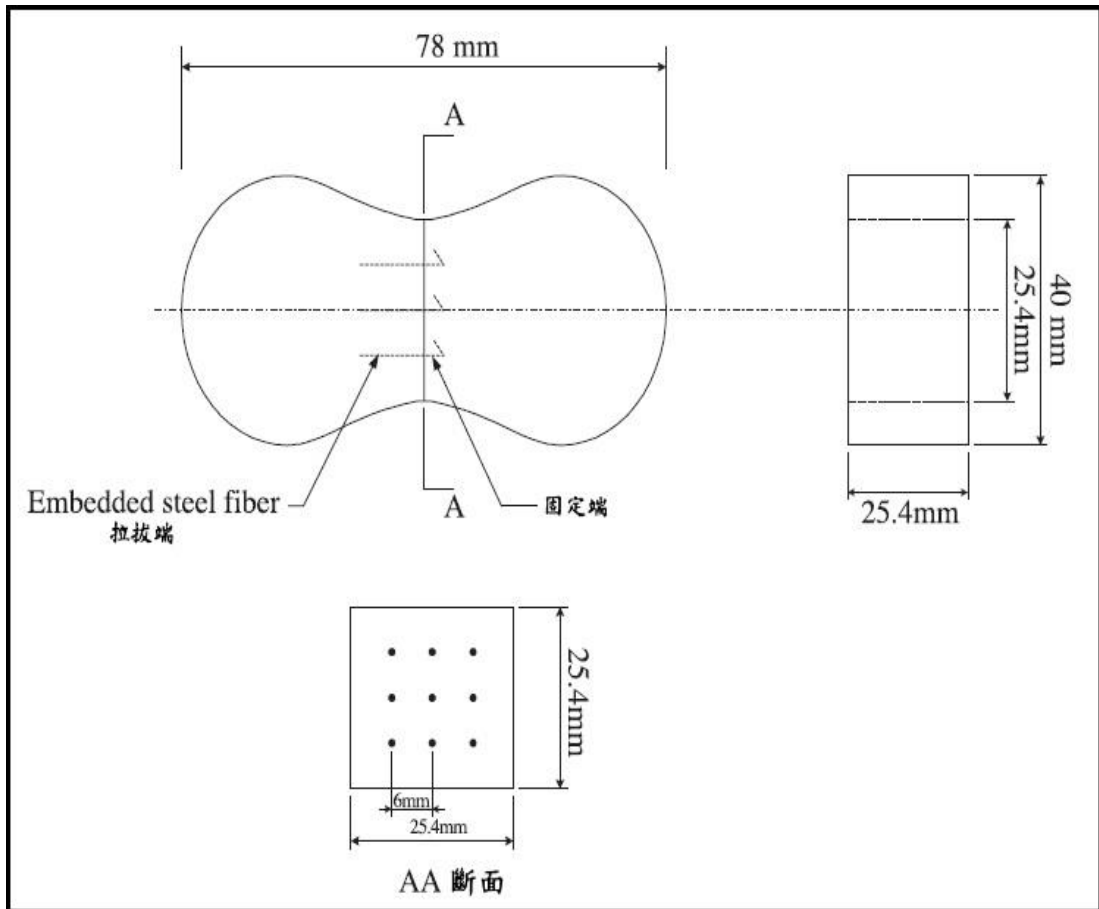


Figure 2.13 Pullout specimen and layout of fibers used by Chan & Chu (2003).

Figure 2.14 shows the pullout specimen fixtures and the LVDT fixtures of the pullout test setup. During fiber pullout tests, the pullout load and the fiber pullout distance were recorded by a load cell and the LVDT.

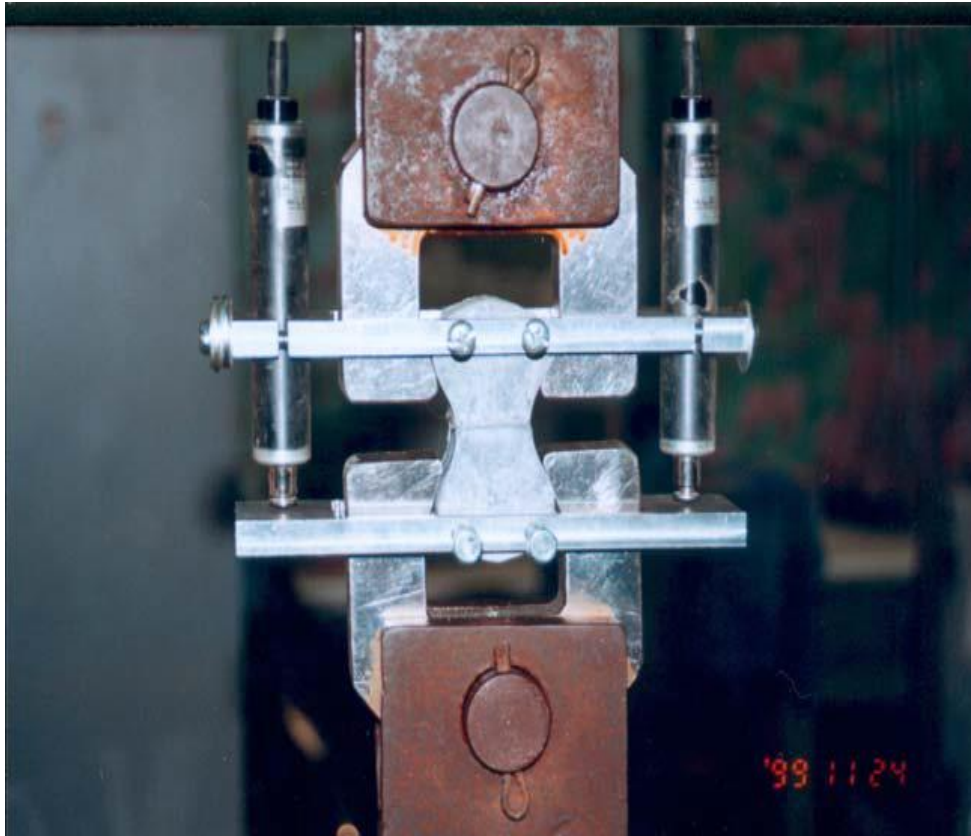


Figure 2.14 Pullout test setup (Chan & Chu, 2003).

Lee, Kang, & Kim (2010) prepared double-sided pullout specimens using multiple fibers (Figure 2.15). Firstly, PE sheet adhered to a steel plate and then fibers were placed into the plate. The plate divided the PVC mold before casting mortar on one face. After 24 hours the central steel plate was removed. Finally, the matrix is casted on the other face. The slip was measured by a clip gauge positioned at the center of the specimen.

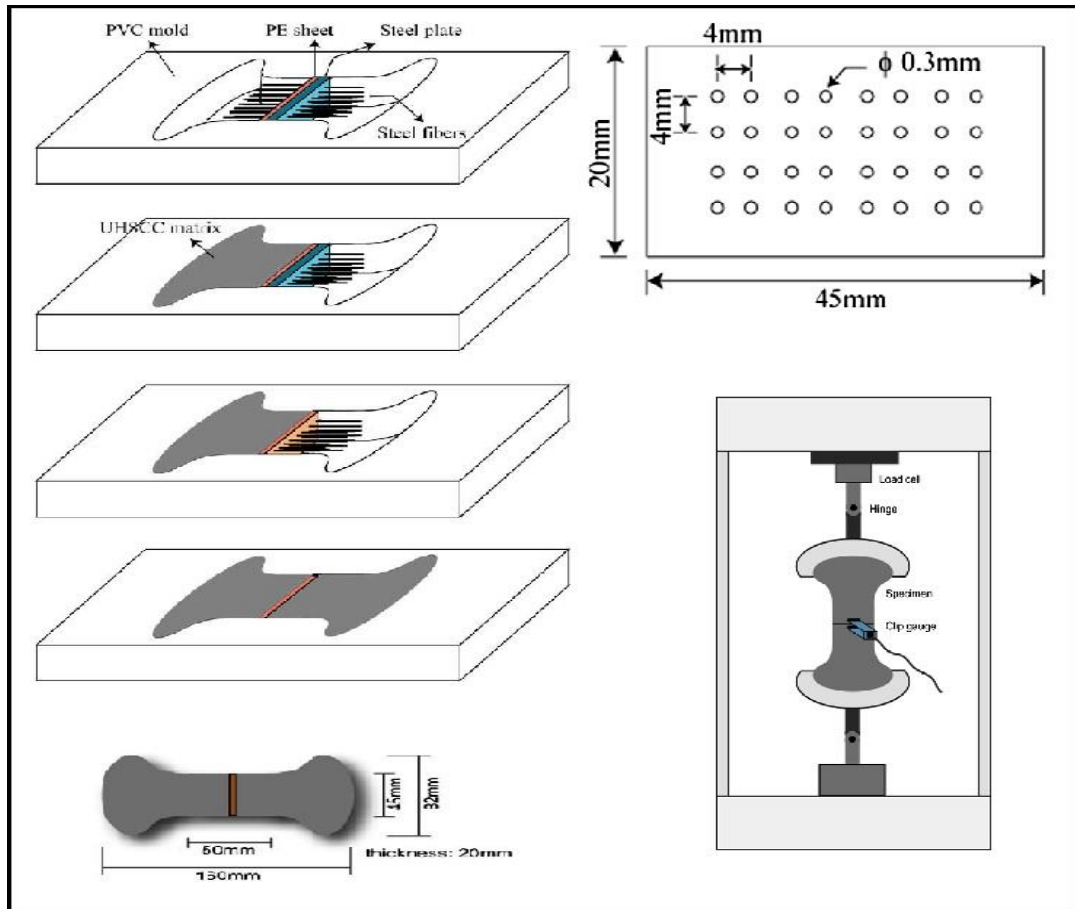


Figure 2.15 Manufacturing process of specimen, details of steel plate, configuration and dimensions of specimen used by Lee, Kang, & Kim (2010).

Shannag, Brincker, & Hansen (1997) have prepared prismatic shape of 25 mm x 23 mm x 19 mm specimens for pull-out test. They adjusted the steel fibers in a straight position in a specially designed mold, using a special apparatus. They have casted the specimens horizontally and the specimens were vibrated. The specimens were then covered with plastic sheets and cured at room temperature for 24 hours prior to demolding. A schematic diagram of the pull-out apparatus used in their study is shown in Figure 2.16.

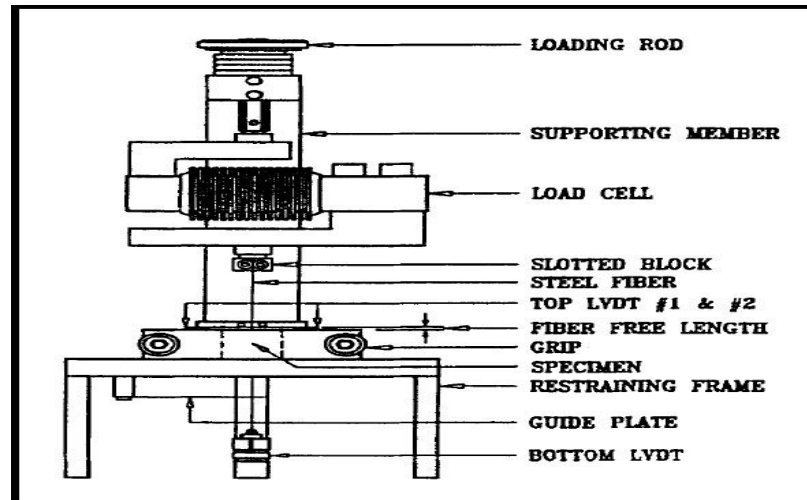


Figure 2.16 The fiber pullout apparatus used by Shannag, Brincker, & Hansen (1997).

Kima et al., (2013) have used single fiber pullout test for their research. Firstly, they pre-installed the fibers in a device and then placed in molds for pull-out samples (Figure 2.17). At the end, the matrix was casted into molds.

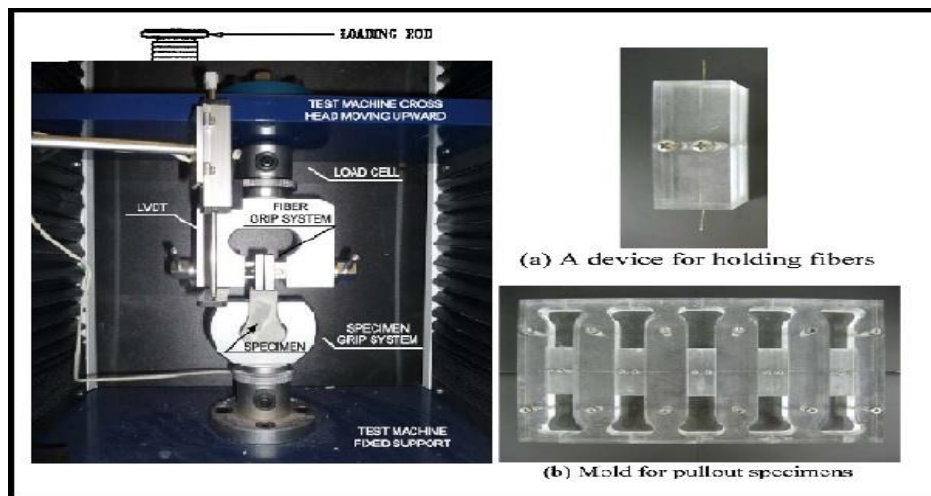


Figure 2.17 The pull-out test used by Kima et al., (2013).

Abu-Lebdeh et al. (2011) dealt with the pull-out behavior of single steel fiber from very-high strength concrete and normal strength concretes. The pull-out test specimens which they prepared consisted of six fibers for six single- fiber pull-out tests (Figure 2.18).

They used MTS testing machine (Figure 2.18) to carry out the pull-out test. The load cell used was a 9.78 KN load cell.

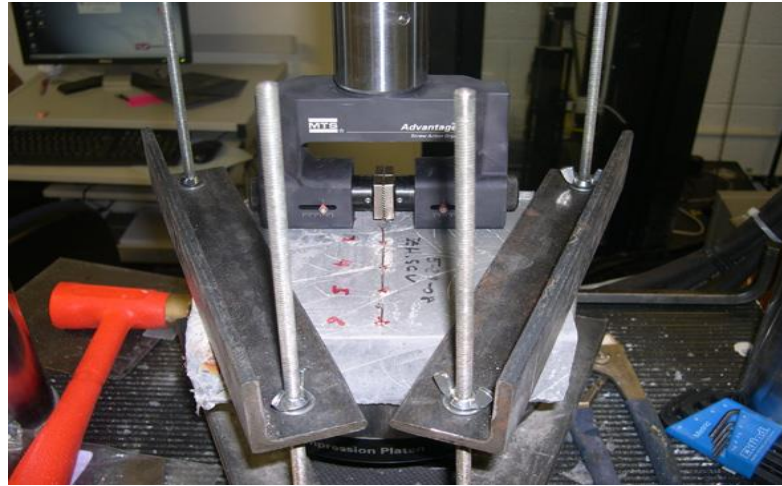


Figure 2.18 Specimen restraint diagram (pullout test) (Abu-Lebdeh et al., 2011).

Aiello, Leuzzi, Centonze, & Maffezzoli (2009) investigated the pull-out behavior of steel fibers recovered from waste tyres. They prepared a truncated cone specimen with a single steel fiber centrally embedded within it (Figure 2.19). They reinforced the free end of the fiber with aluminum tabs in order to prevent damage of the fiber within the gripping of the pull-out test apparatus (electro mechanic testing dynamometer LLOYD LR5K).

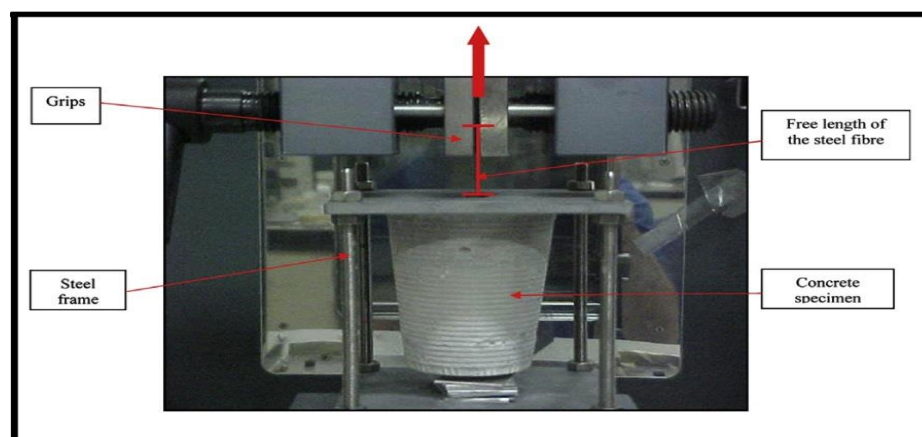


Figure 2.19 The Apparatus for pull-out tests used by Aiello et al., (2009).

Cunha, Barros, & Sena-Cruz (2010) have dealt with pull-out behavior of steel fiber in self-compacting concrete. They used a servo-hydraulic Lloyd LR30K machine with a capacity of 30 kN (Figure 2.20). They also used three LVDT's (linear stroke +/- 5mm) in order to measurement of the fiber pullout slip.

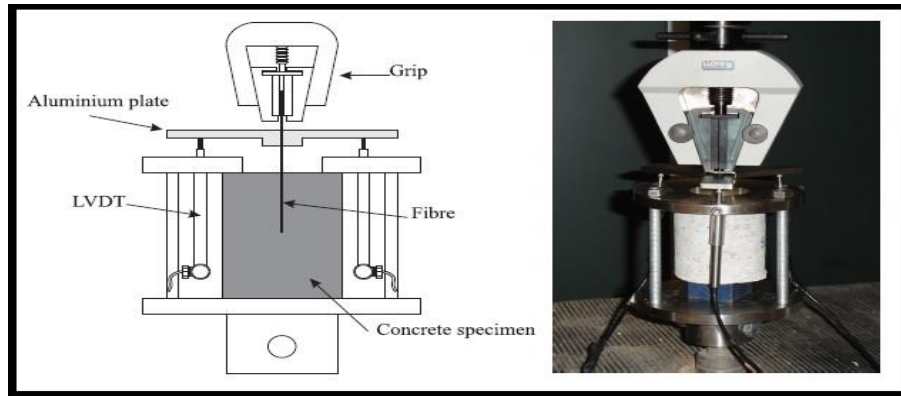


Figure 2.20 The Fiber pullout test apparatus used by Cunha, Barros, & Sena-Cruz (2010).

CHAPTER THREE

EXPERIMENTAL

This chapter presents the aim, scope, materials, and also experimental program of this research.

3.1 Purpose

The aim of this research is to evaluate the bond characteristics of steel fiber from ordinary mortar (OM) and reactive powder concrete matrix (RPC). Furthermore, the effect of some chemical admixtures on pull-out behavior was examined.

3.2 Scope

This thesis consists of two main steps:

1- The effect of four different (1, 2, 3, 4 cm) embedment length and end condition (Hooked-end and smooth) of steel fiber on pull-out behavior in both OM and RPC was determined. Influence of these parameters in case of decreasing W/C ratio of OM to 0.3 was also investigated. Furthermore, paste phase (binder + water) of RPC was also examined.

The effect water/cement ratio in three groups of matrixes was evaluated. The W/C ratio of mix design of OM was redesigned from 0.5 to 0.6, 0.4, and 0.3 and also the W/B ratio of mix design of RPC has been increased to 0.3, 0.4, 0.5, and 0.6 with and without steel micro fiber. Additionally, the study was carried out in four different curing conditions (7 and 28 water curing, steam, and autoclave curing). It should be noted that the mechanical properties of all matrixes were also determined.

1- In this step the effect of some chemical admixtures (SBR and ACR based polymers, a corrosion inhibitor, and a silica based water proofing admixture) on pull-out behavior of steel fiber-matrix from OM and RPC was studied. Furthermore, the

mechanical and physical characteristics of all mixture were investigated. Additionally, the corrosion rate of steel fiber exposed to corrosive environment was determined.

3.3 Materials

A Portland cement (CEM I 42.5R) was chosen for entire experimental study. The physical, chemical and mechanical properties of Portland cement and the silica fume used in RPC mix design is presented in Table 3.1. Two types of aggregate were used in experimental program. Crashed lime stone (1 – 5 mm) was used in ordinary mortar design and four different sizes (1-3, 0.5-1, 0-0.4, and 0-0.075 mm) of quartz aggregate was used in RPC mix design. Sieve analysis of aggregates is presented in Table 3.2.

A polycarboxylic ether based superplasticizer was used to reach the target workability. The properties of the superplasticizer are shown in Table 3.3. Two type of steel fiber were used in pull-out tests (Table 3.4). Furthermore, a type of brass-coated steel-micro fiber with 0.16 mm diameter, 6 mm length, and 37.5 aspect ratio were used.

Table 3.1 Physical, chemical and mechanical properties of cement and chemical composition of cement and silica fume.

Chemical Composition (%)			Properties of Cement	
	Cement	Silica Fume		
SiO ₂	19,90	92,25	Initial setting time (min)	170
Al ₂ O ₃	5,91	0,88	Final setting time (min)	225
Fe ₂ O ₃	2,10	1,98	Volume expansion (mm)	1.00
CaO	62,92	0,51	Specific surface(m²/kg)	
MgO	1,25	0,96	Cement (Blaine)	371
Na ₂ O	0,38	0,45	SF (m ² /kg) Nitrogen Ab.	20 000
K ₂ O	0,90	0.12	Compressive Strength of Cement (MPa)	
SO ₃	3,26	0,33	2 days	25
Cl ⁻	0,011	---	7 days	40
Loss on Ignition	3,94	---	28 days	50
Eq. Alkali	0,97		Potential composition (Bogue)	
			C ₃ S	56.97
			C ₂ S	12.60
			C ₃ A	12.02
			C ₄ AF	6.38

Table 3.2 Sieve analyses of aggregates.

Sieve size (mm)	Quartz aggregate			Sieve size (mm)	Crushed limestone aggregate 1 – 5 mm
	1-3 mm	0.5 – 1 mm	400 µm		
8	100.0	100.0	100.0	8	100.0
4	100.0	100.0	100.0	4	97.3
2	53	100.0	100.0	2	63.7
1	0	74	100.0	1	36.1
0.5	0	0	100.0	0.5	15.3
0.25	0	0	76.0	0.25	1.7
0.125	0	0	8.4	0.106	0.4
0.09	0	0	5.9		
0.075	0	0	4.0		
0.063	0	0	2.1		
0.053	0	0	1.7		

Table 3.3 Properties of polycarboxylic ether based superplasticizer.

Form	liquid
Color	yellow to brown
pH value	5 – 7 (20 °C)
boiling temperature	approx. 100 °C
Density	1.06 g/cm ³ (20 °C)
Solubility in water	miscible
Viscosity, dynamic	< 200 mPa.s (20 °C)

Table 3.4 Properties of steel fibers.

Code	Length (L) (mm)	Diameter (d) (mm)	Aspect Ratio (L/d)	Tensile Strength (N/mm²)
80.60	60	0,75	80	1050
48.50	50	1,05	48	1000
Micro	6	0.16	37.5	2100-2200

Two types of polymers (styrene-butadiene rubber (SBR) and acrylic dispersion based polymer (ADP)) which are common in construction industry were used in this thesis. Two type of SBR and two type of ADP were used as polymers. A waterproofing (WP) admixture with chemical base of an aqueous colloidal blend of inorganic silicate and fatty acids were also used. Additionally, the properties of nitrogen containing organic and inorganic substances (alkanolamine) based corrosion inhibitor (CIN) and all chemical admixture used in this study are presented in Table 3.5.

Table 3.5 Properties of chemical admixtures.

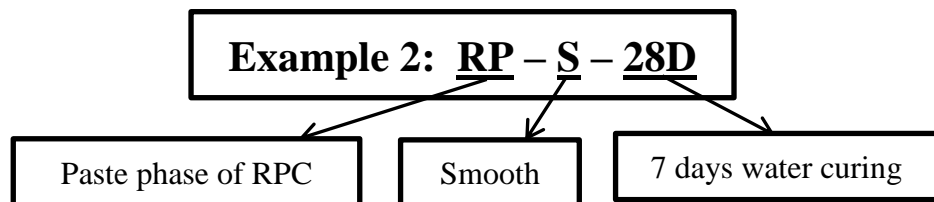
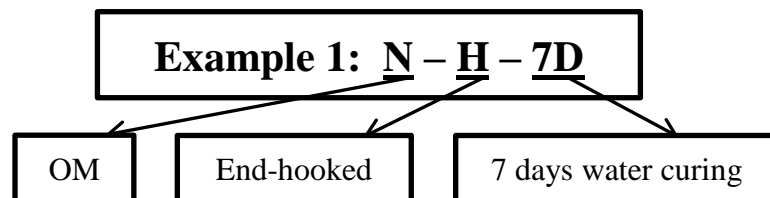
Properties	SBR		ADP		WP	CIN
	SBR 1	SBR 2	ADP 1	ADP 2	WP	CIN
Appearance	White liquid emulsion	White liquid	White	White	Liquid, yellow	Green liquid
Density	1.01 ±0.01 kg/ lt	1.015±0.01 kg/l	1.08 kg/liter	0.98 kg/ lt	1,015 – 1,055 kg/l	1.0625±0.005 kg/l
pH value	8-12	8-12	-	8	~ 10±1	9.3-10.3
Chloride Content	≤%0.1 (TS EN 480-10)	-	-	-	-	Max.% 0.1
Solid content	%23+/-3	%33- 35	42%	-	-	-
Application temperature	+5°C /+35°C	-	+5°C +35°C	-	-	-
freezing point	-5°C	-5°C	-	-	-	-15 °C
Recommend dosage by producer	2-5% of cement	2-5% of cement	1.5% of cement	1-1.5% of cement	3% of cement	12 kg/m ³ of concrete

3.4 Abbreviations

The specimens which were prepared to examine the effect of fiber end condition and embedment length were abbreviated as follow:

- 1- 7 days water curing = 7D
- 2- 28 days water curing = 28D
- 3- Ordinary mortar (0.5 W/C ratio) = N
- 4- RPC = R
- 5- The mixture which were prepared by decreasing W/C ratio of OM from 0.5 to 0.3 = 0.3N

- 6- RPC paste phase = RP
- 7- Smooth fiber = S
- 8- Hooked-end fiber = H



The chemical admixtures names and dosages were abbreviated as follow:

1. 5% of SBR1 = A1
2. 15% of SBR1 = A2
3. 5% of SBR2 = B1
4. 15% of SBR2 = B2
5. 1.5% of ADP1 = R1
6. 5% of ADP1 = R2
7. 1.5% of ADP2 = L1
8. 5% of ADP2 = L2
9. 3 % WP = SI
10. CNI = F

Two control mixtures for each OM and RPC were prepared as follow:

KN: Control mixture which was cured for 28 days in 20±2°C water (Normal curing). This control mixture was prepared in order to compare with corrosion inhibitor containing mixture.

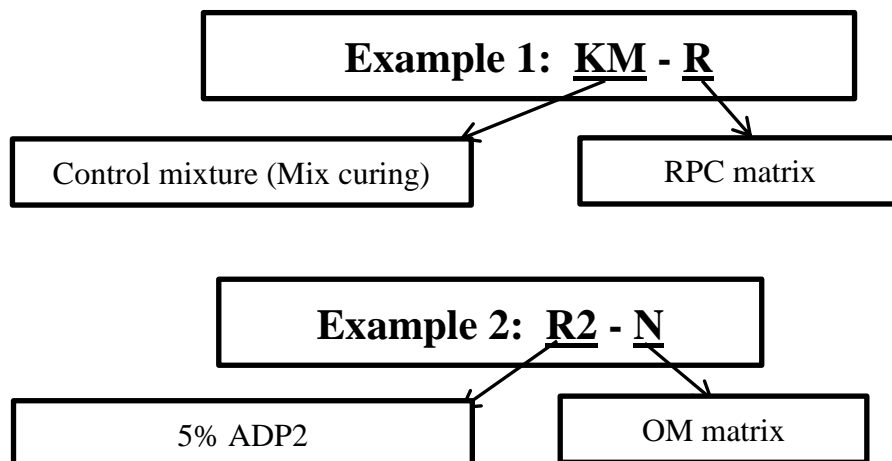
KM: Control mixture which was cured for 7 days in 20±2°C and 21 reminder days in air (Mix curing). This control mixture was prepared in order to compare with polymer and WP containing mixtures.

The matrixes were also abbreviated as follow:

- 1- Ordinary mortar = N
- 2- RPC = R

The mixtures in second section which were prepared to evaluate the effect of chemical admixtures were also abbreviated as follow:

- Chemical admixtures name and dosage – matrix type (OM or RPC)



3.5 Production of Mixtures

Mix design of ordinary mortar (OM) and RPC are presented in Table 3.6. An OM with 0.5 W/C ratio and a RPC with 0.2 W/B ratio were designed to examine the effect of end condition and embedment length of steel fiber on bond characteristic of fiber-matrix. The effect of these parameters was also investigated in paste phase of RPC and a mix design of high strength ordinary mortar with 0.3 w/c ratio. The mix design of these mixtures was also presented in Table 3.6.

In this step of study the fibers with 60 mm length, 0.75 mm diameter were used. This type of steel fiber produce as hooked-end, however, to evaluate the effect of end condition of fiber, the hooked-end of fiber were smooth by cutting the end of the fibers. The smooth and hooked-end fibers were embedded in four different lengths (1, 2, 3, 4 cm).

Table 3.6 Mix design of step one mixtures (kg/m³).

Mixtures	Water	Cement	Silica Fume	Aggregate				SP/C (%)	
				Lime Stone 0-05 mm	Quartz (mm)				
					1-3	0.5-1	0-0.4		0-0.075
O-0.3	150	500	-	1687	-	-	-	-	4.2
O-0.4	202	500	-	1588	-	-	-	-	1.4
O-0.5	250	500	-	1473	-	-	-	-	0.8
O-0.6	300	500	-	1352	-	-	-	-	0
R-0.2	184	824	107	-	609	348	174	87	2.2
R-0.3	249	724	107	-	570	310	174	87	1.1
R-0.4	294	624	107	-	556	296	174	87	0.55
R-0.5	315	524	107	-	575	314	174	87	0.01
R-0.6	318	424	107	-	609	348	174	87	-
Paste-0.2	355	1590	207	-	-	-	-	-	1.3

To evaluate the effect of W/C ratio on pull-out behavior of steel fiber-matrix, the mix design of OM and RPC were redesigned. The cement content (500 kg/m³) of OM design were fixed, but the W/C ratio were increased to 0.6 and decreased to 0.4 and 0.3. Furthermore, the mix design of RPC was redesigned. The Water/Binder

ratio was increased to 0.3, 0.4, 0.5, and 0.6. The 0-0.4 and 0-0.075 sizes of quartz aggregate and silica fume dosage of mixtures were fixed, while the cement dosage were decreased as the W/B ratio increased. Additionally, the redesigned RPC mixtures were also reinforced by 2% steel-micro fibers. The mix designs of all these mixtures are presented in Table 3.6.

The effect of W/C ratio was carried out in four different curing conditions. After casting, a series of specimens were kept for 24h in $20\pm 2^{\circ}\text{C}$ and after that were demolded and cured in water for seven days and others were cured for 28 days. The temperature of curing water was fixed in $20\pm 2^{\circ}\text{C}$. Another series of specimens were subjected to steam curing. 6 h after casting the molds were put in steam curing cabin. After 6h the temperature of the cabin was reach to 100°C and the specimens were kept in this condition for 12h. After cooling the specimens were tested. The autoclave curing regime is different from other curing conditions. After casting, a series of specimens were kept for 24h in $20\pm 2^{\circ}\text{C}$ and after that were demolded. The specimens were put in autoclave cabin. The temperature was adjusted to 210°C and steam presure was adjusted to 2 MPa. The specimens were cured for 12h in autoclave cabin. It must be noted that hooked-end fiber with 30 mm embedment length were used to evaluating the effect of W/B ratio on bond characteristics.

In step two OM with 0.5 W/C ratio and RPC with 0.2 W/B ratio were selected as base mixture to evaluate the effect of chemical admixtures. Furthermore, the fiber with 50 mm length and 1.05 mm diameter was used in this step. The embedment length of fiber in this section was adjusted to 25 mm. SBR and ADP latex polymers were used in two dosages. The 5% were selected as a first dosage of mixtures and 15% of cement weight were also selected as second dosage of SBR containing mixtures for both OM and RPC. In case of ADP latex polymers 1.5% and 5% of cement weight were chosen. Furthermore, 3% of cement weight were chosen as WP admixture dosage.

According to the literature polymers need both water and air curing (R. U Wang, P. M Wang, & Li, 2005; Çolak, 2005; Kim & Robertson, 1997). Because of this fact

the polymer containing mixtures were cured for seven days in water and after that were cured in air for 21 days. WP containing mixture was also cured in this curing regime.

12 kg/m³ producer recommended dosage were chosen for corrosion inhibitor containing mixture. The specimens were cured in water for 28 days. It must be noted that the water that was add to mixture from chemical admixture were subtract from mix design water. The mix design of this section is presented in Table 3.7.

Table 3.7 Mix design of second step mixtures (kg/m³).

Mixtures	Water	Chemical Admixture - ADD/C %	Cement	Silica Fume	Aggregate				SP/C (%)	
					Lime Stone 0-5 mm	Quartz (mm)				
						1-3	0.5-1	0-0.4		0-0.075
KN-N	250	0	500	-	1466	-	-	-	-	1.2
KM-N	250	0	500	-	1466	-	-	-	-	1.2
A1-N	237	SBR1-5%	500	-	1470	-	-	-	-	1
A2-N	213	SBR1-15%	500	-	1470	-	-	-	-	0.9
B1-N	237	SBR2-5%	500	-	1470	-	-	-	-	1
B2-N	213	SBR2-15%	500	-	1470	-	-	-	-	0.9
L1-N	246	ADP1-1.5%	500	-	1469	-	-	-	-	1
L2-N	238	ADP1-5%	500	-	1471	-	-	-	-	0.8
R1-N	246	ADP2-1.5%	500	-	1469	-	-	-	-	1
R2-N	238	ADP2-5%	500	-	1471	-	-	-	-	0.8
F-N	242	CNI-12 kg/m ³	500	-	1474	-	-	-	-	1.2
SI-N	243	WP-3%	500	-	1466	-	-	-	-	1.2
KN-R	184	0	824	107	-	603	347	174	87	2.2
KM-R	184	0	824	107	-	603	347	174	87	2.2
A1-R	160	SBR1-5%	824	107	-	608	347	174	87	2.1
A2-R	114	SBR1-15%	824	107	-	611	347	174	87	1.8
B1-R	160	SBR2-5%	824	107	-	608	347	174	87	2.1
B2-R	114	SBR2-15%	824	107	-	611	347	174	87	1.8
L1-R	177	ADP1-1.5%	824	107	-	605	347	174	87	2.1
L2-R	161	ADP1-5%	824	107	-	614	347	174	87	1.7
R1-R	177	ADP2-1.5%	824	107	-	605	347	174	87	2.1
R2-R	161	ADP2-5%	824	107	-	614	347	174	87	1.7
F-R	178	CNI-12 kg/m ³	824	107	-	606	347	174	87	2.2
SI-R	170	WP-3%	824	107	-	605	347	174	87	2.2

3.5.1 Preparing of Mixtures

The mixtures were mixed by Hobart mixer (Figure 3.1). Preparing of OM and RPC mixtures was different from each other. In case of OM the dry ingredients of each mixture were premixed for two minute to achieve homogeneous dry components. Then, half of the mixing water was added to the dry mixture, while the remaining water was being mixed with the required amount of superplasticizer and then poured into the mixer. After normal speed for about 1 minute, mixing continued for another 3 min in high speed and the workability of each mixture was controlled with mini-flow table test. The required amount of superplasticizer used to achieve 150 ± 10 mm flow table values in all mixtures.

In case of RPC, the dry ingredients of each mixture were premixed for 5 minute. Then, half of the mixing water was added to the dry mixture, while the remaining water was being mixed with the required amount of superplasticizer and then poured into the mixer after 5 min normal speed mixing. After that, mixing continued for another 10 min in high speed and the workability of each mixture was controlled with mini-flow table test. The required amount of superplasticizer used to achieve 220 ± 10 mm flow table values in all RPC mixtures. It must be noted that chemical admixtures were mixed with mixture water.



Figure 3.1 Hobart mixer.

3.5.2 Casting

The mixtures that were prepared for the pull-out test were poured into 50x50x50 mm cubic molds in two layers with 30sec applying vibration for each layer. After placing final layer, single steel fiber was centrally embedded into the fresh mixture by an apparatus which allowed the fiber become perpendicular to the surface of the specimen and adjusts the desired embedment length into the matrix and then vibration was applied for 30sec (Figure 3.2). In addition, in order to determine the flexural and compressive strength of the matrix phase 40x40x160 mm prismatic specimens and 50x100 mm cylinders to subject to the rapid chloride permeability test. The broken half-prisms after three point flexural test were tested in uniaxial compression (loading area is 40x40 mm) (Figure 3.3).



Figure 3.2 Fiber fixing apparatus.



Figure 3.3 The flexural and compressive strength machines.

3.6 Pull-out Test

The fiber-matrix bond characteristics were determined by applying single-fiber pull-out test that is common method used and analyzed by some researchers. The Schematic diagram of pull-out test setup used in this study is presented in Figure 3.4. Capacity of the load-cell was 6 kN. The pull-out test specimen was fixed to the frame on the bottom platen while the free end of the fiber was held by the fiber mounting plate. The matrix remained rigid while the fiber mounting plate moved upward with a rate of 1 mm/min under closed loop control test procedure as shown in Figure 3.5. During the slip of fiber from the matrix, corresponding load values were recorded by the load-cell that was connected to a computer. Some important parameters such as peak pull-out load, displacement at the peak load and debonding toughness (slip

energy) were find out by analyzing the Pull-out load versus end displacement curves plotted using the data from the test.

Each data presented here are the average test results of three specimens for flexural strength and four specimens for pull-out test values. Compressive strength results are the average of six samples that were left from bending test. On the other hand, pull-out load-displacement curves were drawn using with one specimen graph that represents closest to the average pull-out performance.

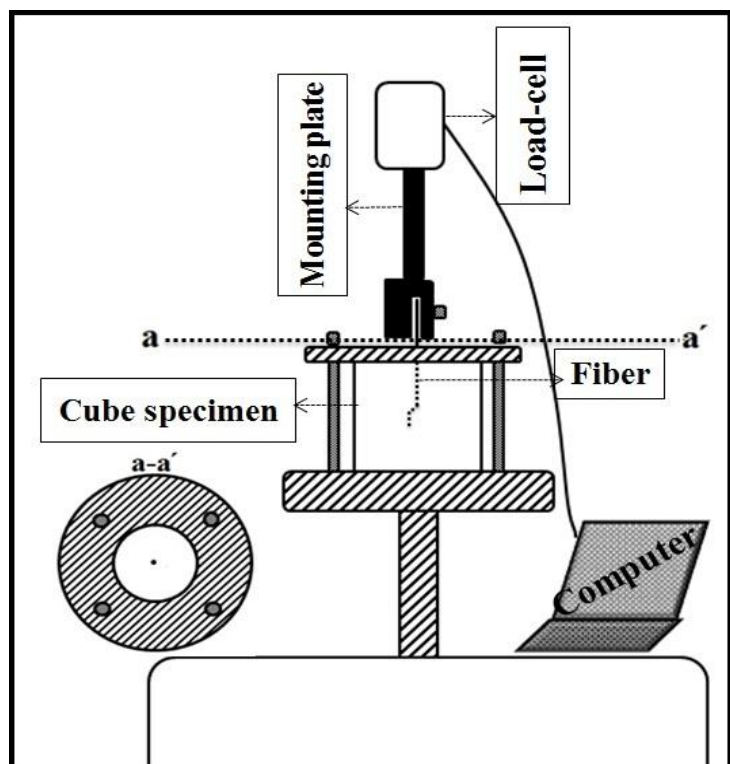


Figure 3.4 The Schematic diagram of pull-out test setup.

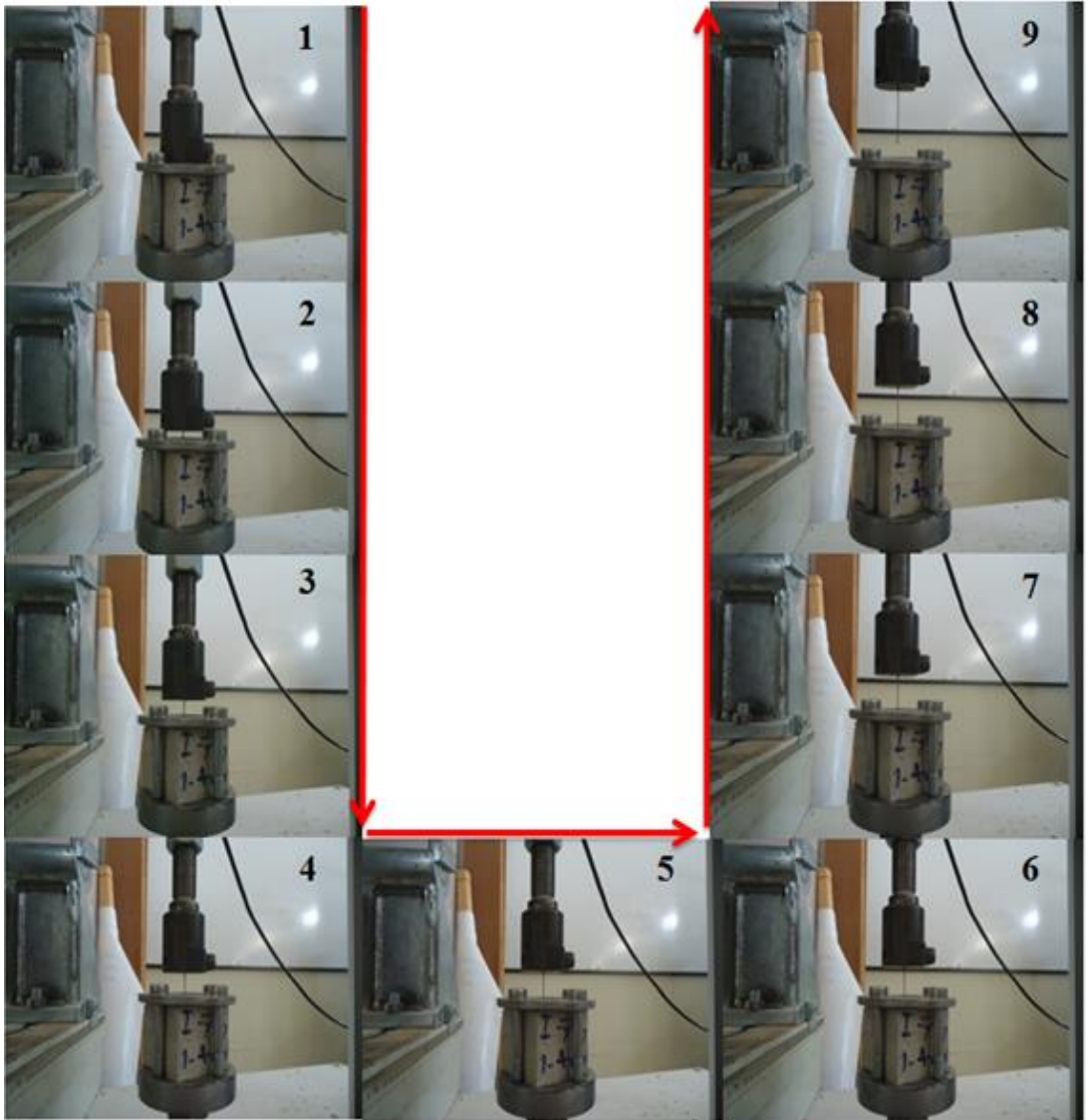


Figure 3.5 The test procedure of pull-out test.

3.7 Microstructure Investigation

The microstructure of the fiber-matrix interfaces were studied by using JEOL JSM 6060 electron microscope (SEM). The samples for SEM analysis were prepared by taking small pieces from the fiber-matrix interface zone.

Original microstructure and morphology of the products were observed on fractured surfaces using secondary electron imaging. Fractured small samples were mounted on the SEM stubs using carbon paint (Figure 3.6); the samples were coated with gold. The SEM study was carried out by using an accelerating voltage of 10 kV. Scanning electron microscopy (SEM) and energy dispersive spectrometry (EDS) analyses were attempted to identify the composition of materials and their morphology.



Figure 3.6 Fractured small samples were mounted on the SEM stubs using carbon paint.

3.8 Corrosion of Steel Fibers

To determine the effect of corrosion of steel fiber on bond characteristics of steel fiber-matrix two series of specimens were subjected to the wetting-drying cycle under corrosive environment. Furthermore, a series of specimens was also put in water to achieve the same maturity with the specimens in cabin. After specific wetting-drying cycles, the corrosion development of embedded fibers was monitored by polarization technique which is widely utilized in the metallurgy and corrosion engineering.

After 28-day water curing an electric wire was soldered to the embedded steel fiber and the surface of fiber were covered by five epoxy layer. At the end cubes and prisms specimens were put in wetting-drying cycle cabin exposure to 3.5% NaCl solution (Figure 3.7).



Figure 3.7 Wetting-drying cabin.

A cycle of the cabin consists as follow:

- 120 min wetting (20° C %3,5 NaCl)
- 180 min drying (20° C normal air)

Corrosion measurements were performed by a three-electrode system. Gamry REF600 Potentiostat/Galvonastat/ZRA system was used in measurements. Reference electrode is saturated calomel reference electrode and is graphite counter electrode. Electrolytic media for measurement was also carried out in 3.5% NaCl solution (Figure 3.8).

Firstly, the open circuit potential of the test specimens was determined. Secondly, polarization in anodic direction with direct currant was applied to specimens. Results were analyzed by Tafel analysis systems.

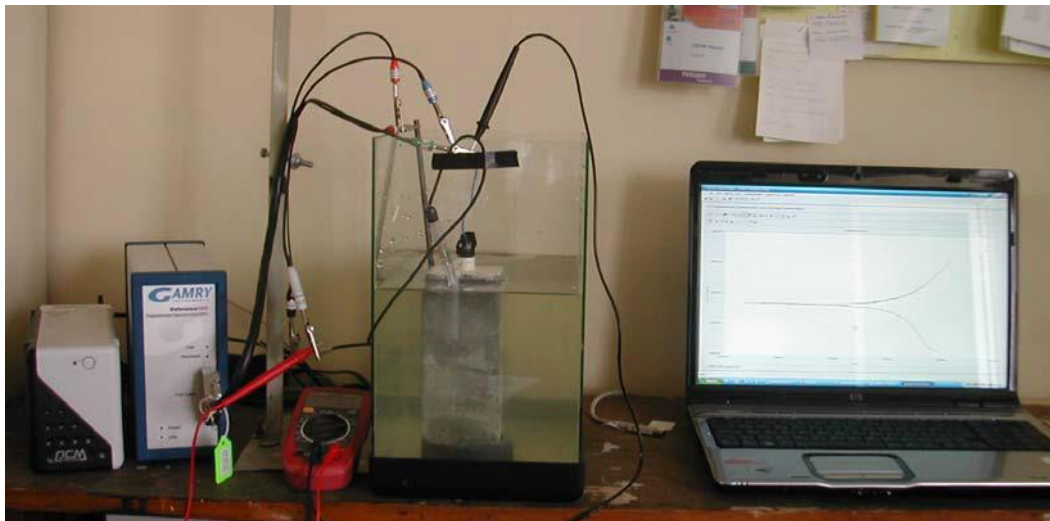


Figure 3.8 Corrosion measurement system.

CHAPTER FOUR

RESULTS AND DISCUSSIONS

4.1 The Effect of Matrix Type, Fiber End Condition, Embedment Length, and W/C Ratio

4.1.1 Mechanical Properties of Mixtures

Flexural strength of OM (0.5 W/C) and redesigned OM mixtures in various curing conditions are shown in Figure 4.1. It can be indicated from Figure 4.1 that the strength of mixture were increased as decreasing the W/C ratio. This behavior is similar in all curing conditions. Flexural strength of all mixtures in 28 days water curing was raised compared to the 7 days strengths. This behavior shows that cement hydration is dominant in 28 days. As shown in Figure 4.1, except 0.3W/C mixture the flexural strength of mixture were lower compared to the 28 days. The cement based composites with higher W/C ratio and without any mineral additives is more sensitive in steam curing. The thermal shock in early age of specimens caused micro cracks which is dangerous in case of flexural strength. Flexural strength of specimens in steam curing decreased by 1-30 % compared to the 28-day water curing.

Flexural strength of autoclave cured specimens of all mixture were strongly decreased as results of this fact that SiO₂ sources is the most important factor in terms of autoclave curing (Odler, 2004). This remarkable strength loss is more visible in mixtures that have higher W/C ratio. Flexural strength of specimens in autoclave curing decreased by 32-81 % compared to the 28-day water curing.

Compressive strength of OM (0.5 W/C) and redesigned OM mixtures in various curing conditions are shown in Figure 4.2. It can be indicated from test results that mechanism of compressive strength of all mixture is similar to the flexural strength in all curing condition. The significant point of this section is the extremely negative effect of autoclave curing as a result of low cement dosage and absence of SiO₂ sources (Please see the microstructure investigation section).

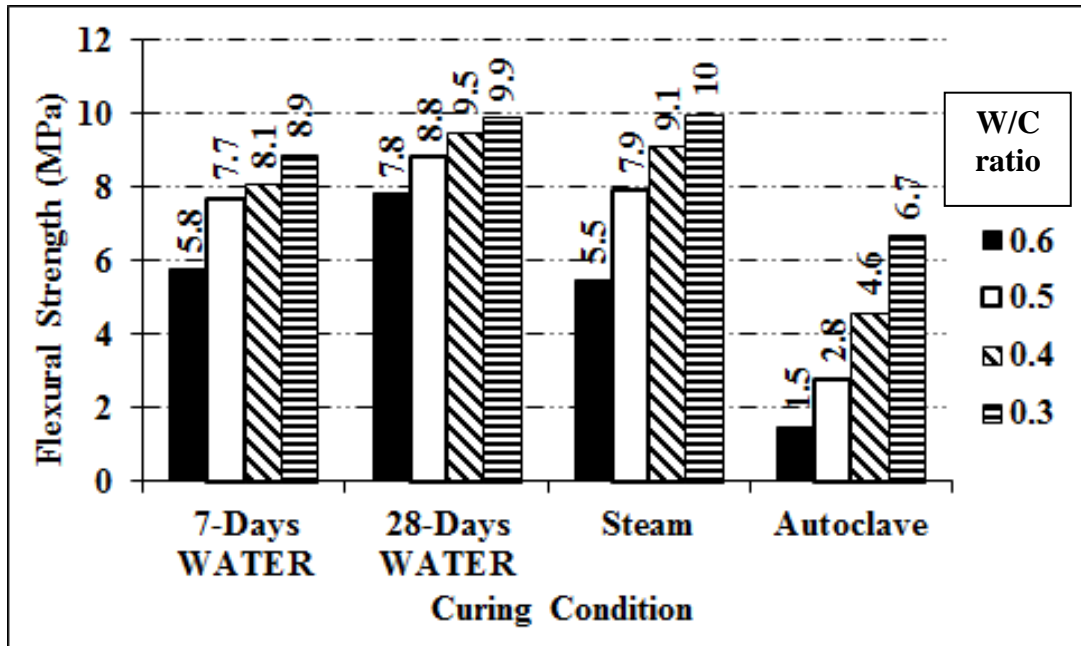


Figure 4.1 Flexural strength of OM mixture with different W/C ratio.

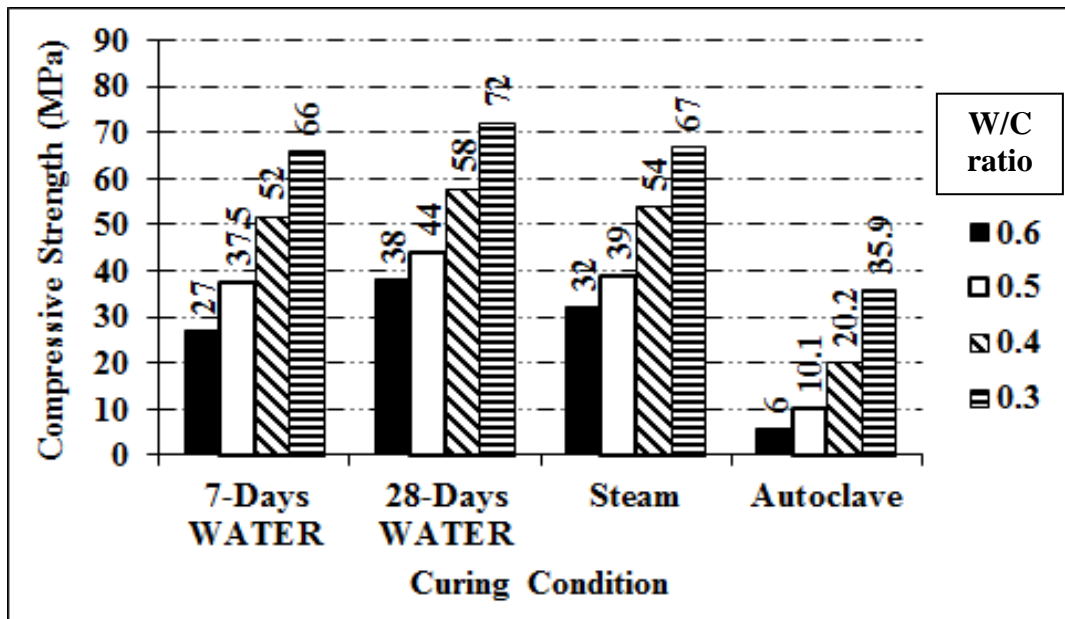


Figure 4.2 Compressive strength of OM mixture according to the W/C ratio.

Flexural strength of RPC (0.2 W/B) and redesigned RPC mixtures in various curing conditions are shown in Figure 4.3. It can be indicated from Figure 4.3 strength of mixture was increased as decreasing the W/B ratio. Additionally, the strength of all mixture was increased with longer water curing. Because of dense micro structure as a result of high cement dosage, low W/B ratio, incorporation of

silica fume, and low CaO/SiO₂ ratio by addition of silica components, the strength of RPC with 0.2 W/B ratios is remarkable higher than other mixtures (Chan & Chu, 2011; Lehmann, Fontana, & Muller, 2009; Richard & Cheyrezy, 1995, 1994). The behavior of mixture in steam curing is just similar to the OM mixtures, while the strength of RPC and the redesigned mixture with 0.3 and 0.4 W/C ratios was increased (3-19 %) in autoclave curing. Existence of SiO₂ component (silica fume and quartz powder), low W/B ratio and high cement content leads to formation of calcium SiO₂ hydrate (C-S-H) phases and tobermorite gel (Please study the microstructure investigation section). The flexural strength of specimens with 0.5 and 0.6 W/B ratios was decreased (10-11 %) compared to 28 days water cured once. However, they have SiO₂ component, the low cement content and higher W/B ratio leads to this strength loss. It must be noted that flexural strength is more sensitive in case of heat curing.

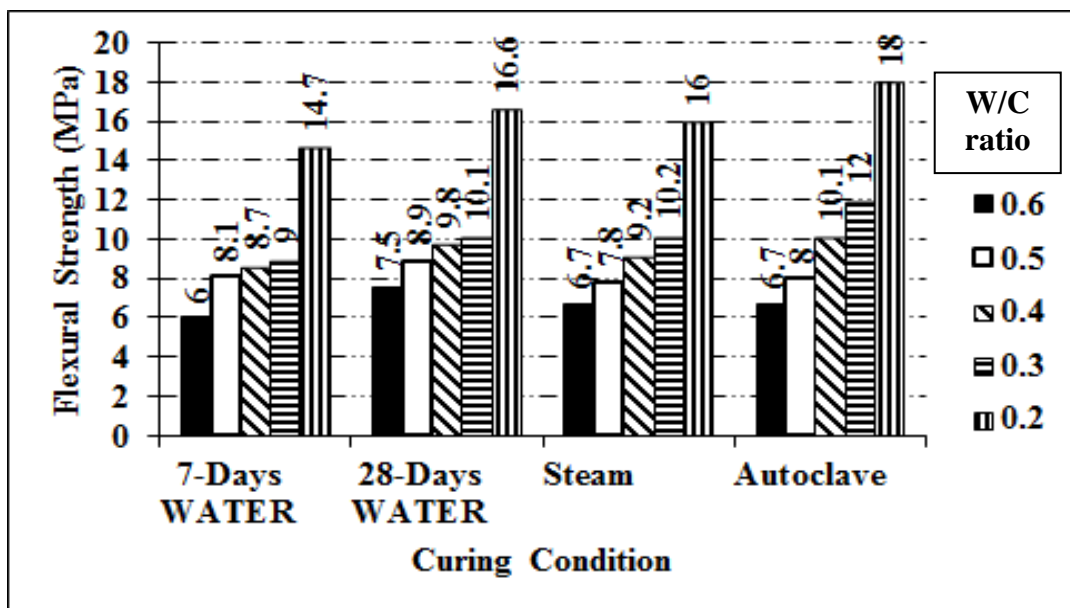


Figure 4.3 Flexural strength of RPC (0.2 W/B) and redesigned RPC mixtures.

Compressive strength of RPC (0.2 W/B) and redesigned RPC mixtures in various curing conditions are shown in Figure 4.4. It can be indicated from test results that mechanism of compressive strength of all mixture is similar to the flexural strength in 7 and 28 water curing and steam curing. The compressive strength of all mixture in autoclave curing was increased significantly (15-46 %). It can be concluded that

existence of SiO₂ components is more effective in case of compressive strength even in high W/C ratio and low cement content.

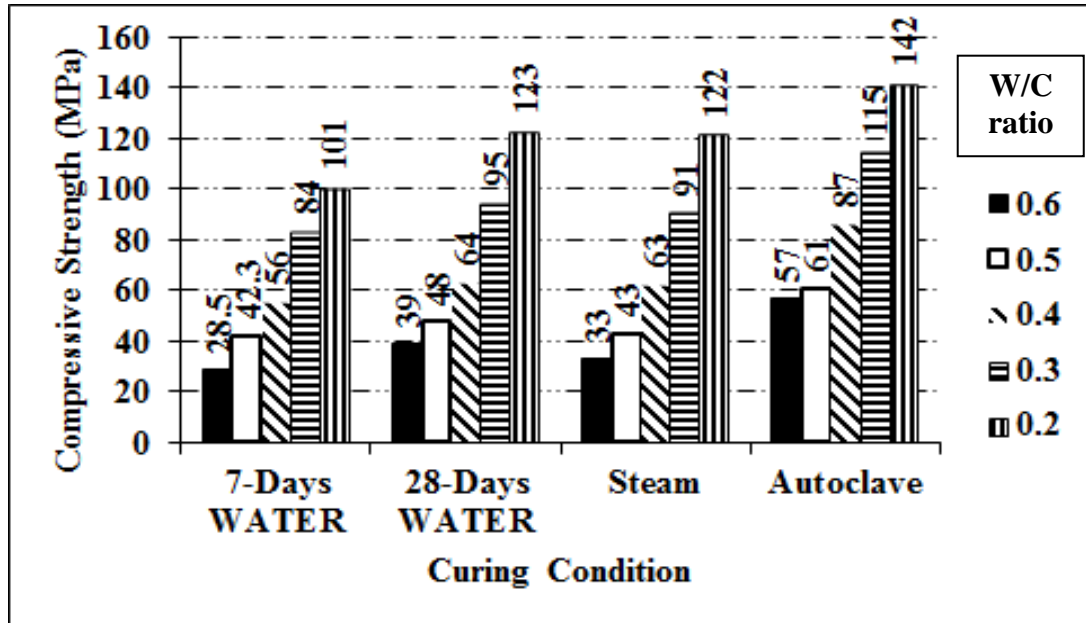


Figure 4.4 Compressive strength of RPC (0.2 W/B) and redesigned RPC mixtures.

Flexural and compressive strength of RPC (0.2 W/B) and redesigned RPC mixtures reinforced by 2% steel-micro are presented in Figures 4.5 and 4.6, respectively. Additionally, the test result of 28-day water cured specimens of redesigned RPC mixtures and reinforced once was computed in Figures 4.7 and 4.8. It can be indicate from test results that incorporation of steel-micro fiber increased both flexural and compressive strength.

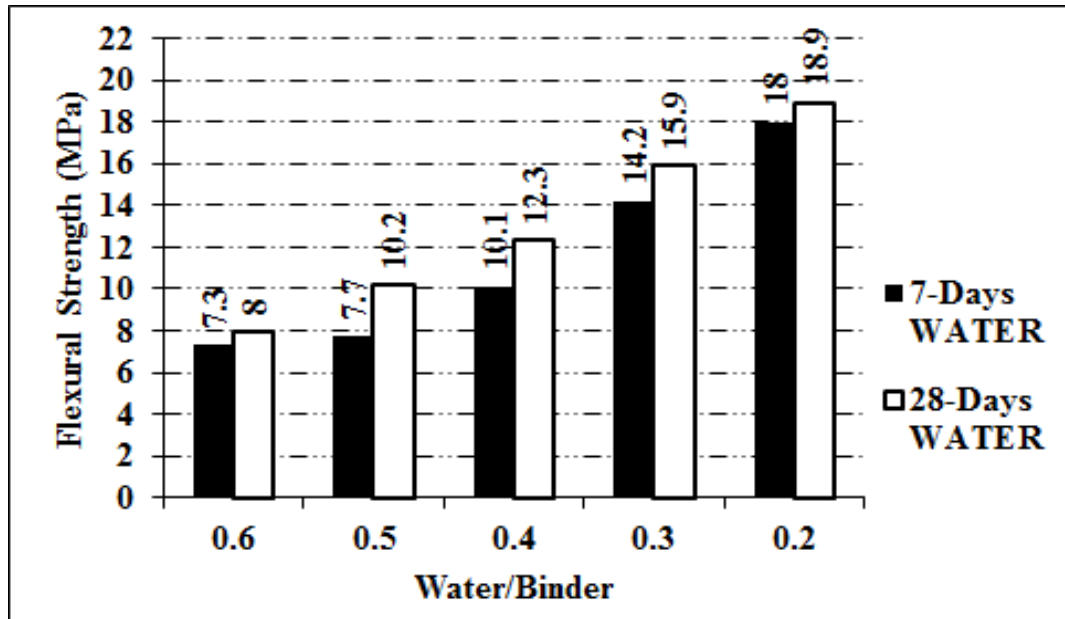


Figure 4.5 Flexural strength of reinforced RPC (0.2 W/B) and redesigned RPC mixtures with steel-micro fiber.

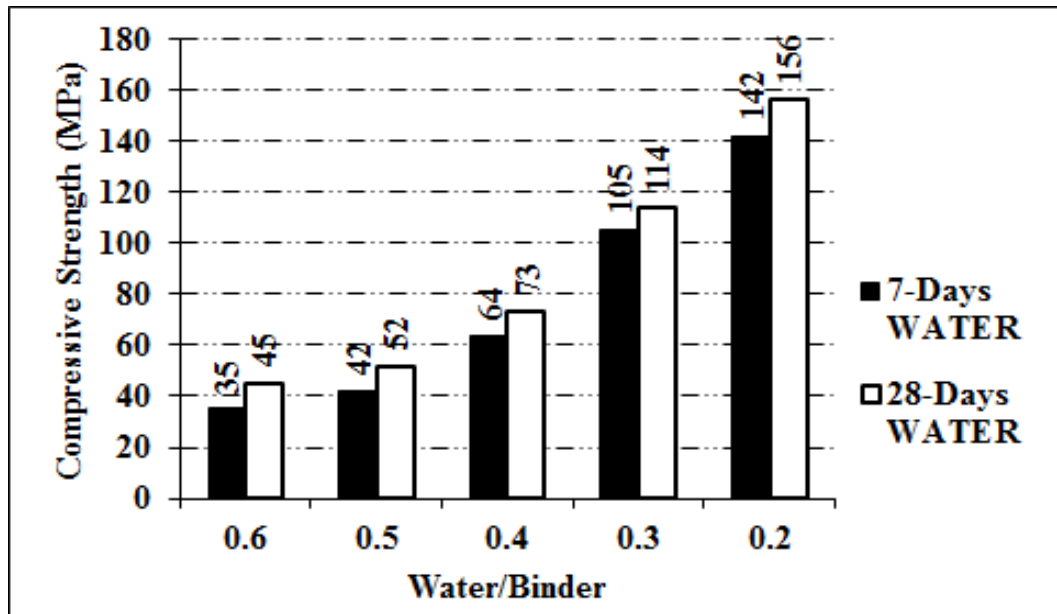


Figure 4.6 Compressive strength of reinforced RPC (0.2 W/B) and redesigned RPC mixtures with steel-micro fiber.

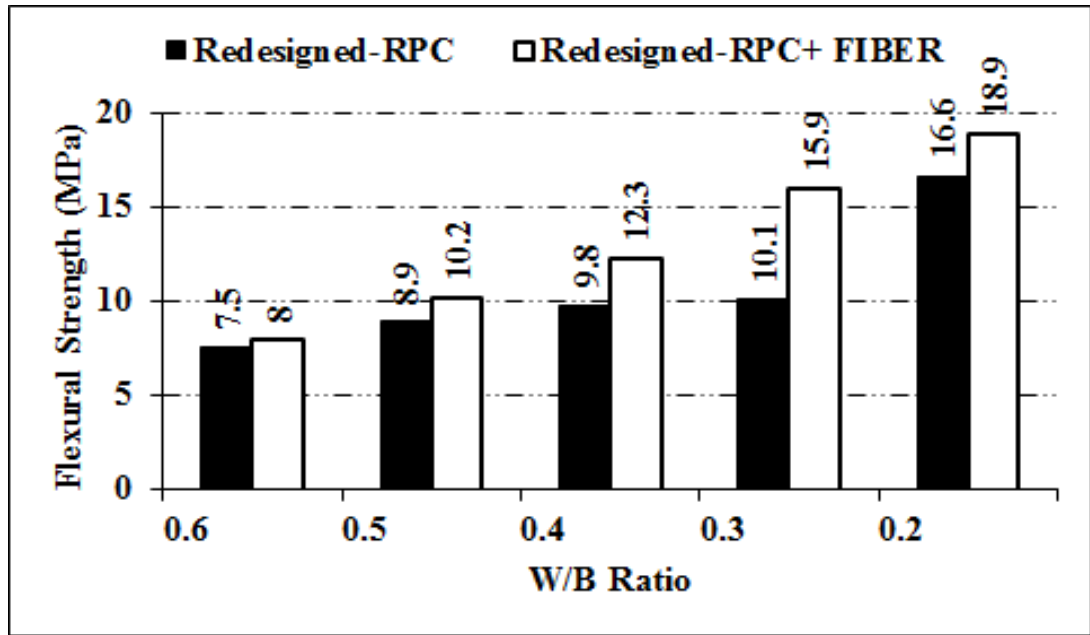


Figure 4.7 Flexural strength of reinforced RPC (0.2 W/B) and redesigned RPC mixtures with steel-micro fiber.

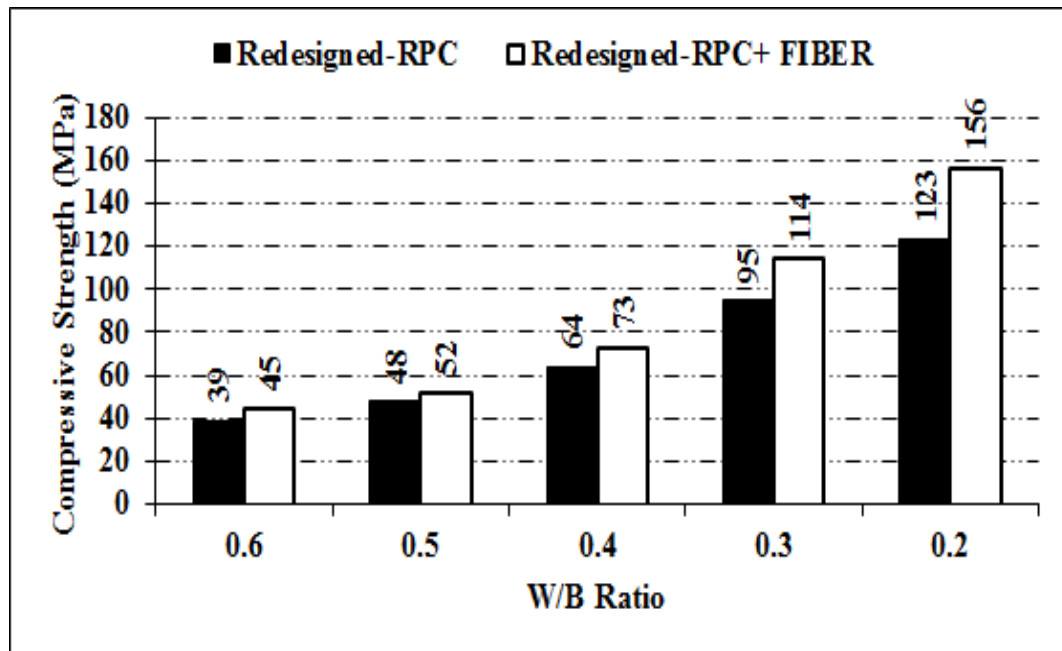


Figure 4.8 Compressive strength of reinforced RPC (0.2 W/B) and redesigned RPC mixtures with steel-micro fiber.

This behavior is due to crack-bridging effect of steel-micro fiber under loading. Due to higher bond strength of fiber-matrix in low W/C ratio, the strength increment of mixture with low W/B ratio was more pronounced.

Flexural and compressive strength of paste phase (binder + water) of RPC (0.2 W/B) are presented in Figure 4.9. It can be seen from Figure 4.9 that both flexural and compressive strengths of paste phase of RPC is lower than RPC. Excessive cement content (1590 kg/m^3) of the mixture leads to occurring high hydration heat in early ages of specimens. Thermal shock leads to micro cracking in specimens. On the other hand shrinkage occurs strongly as a result of very high cement dosage. Lack of aggregate is the other reason of these problems.

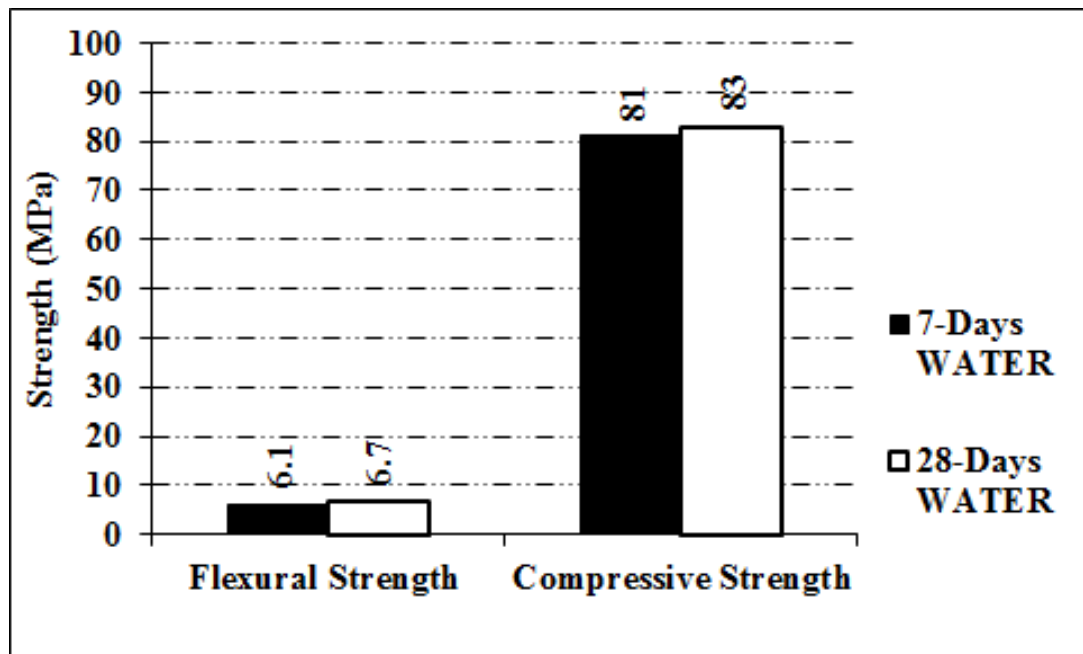


Figure 4.9 Flexural and Compressive strength of paste phase of RPC (0.2 W/B).

4.1.2 The Effect of End Condition and Embedment Length of Fiber

The appearance of the hooked-end fiber before and after pull-out test is shown in Figure 4.10. The pull-out test load – displacement curves of OM mixture with hooked-end fiber in various embedment lengths of fiber after 7 and 28 days water curing are presented in Figures 4.11 and 4.12, respectively. It can be seen from curves the combination of two different mechanisms constitutes the pull-out behavior: debonding of the surround interface and frictional slip of the fiber. Firstly, the embedment length of fibers is fully debonded (from outer surface to the interior of specimen), then the fiber pull-out occurs under frictional resistance (Cunha, Barros, & Sena-Cruz, 2010). High pull-out peak load indicates the good bond between matrix and steel fiber. It can be stated that, fiber shows elongation until the peak load without the initiation of a considerable debonding. Second peak point in the descending part of hooked-end fiber is related to the mechanical interlock of hooked end. This behavior is also reported by some researchers (Armelin & Banthia, 1997; Cunha, Barros, & Sena-Cruz, 2010). The additional peak points were also observed in the load-displacement graphs of some mixtures. This behavior may be related to the effect of aggregate (especially coarser aggregate 1-4 mm) on frictional resistance of fiber-matrix. This behavior was not reported in SIFCON matrix which has aggregate smaller than 1 mm (Tuyan & Yazıcı, 2012).



Figure 4.10 The appearance of the hooked-end fiber before and after pull-out test.

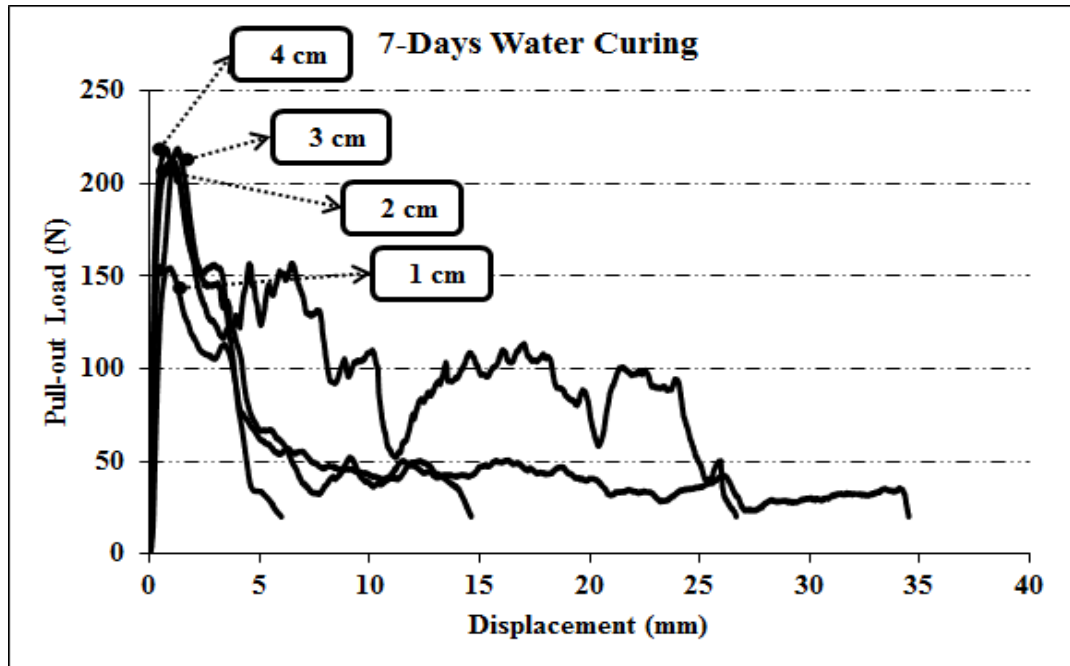


Figure 4.11 Pull-out load–displacement relationship of OM mixture with hooked-end fibers according to the embedment length (7 days).

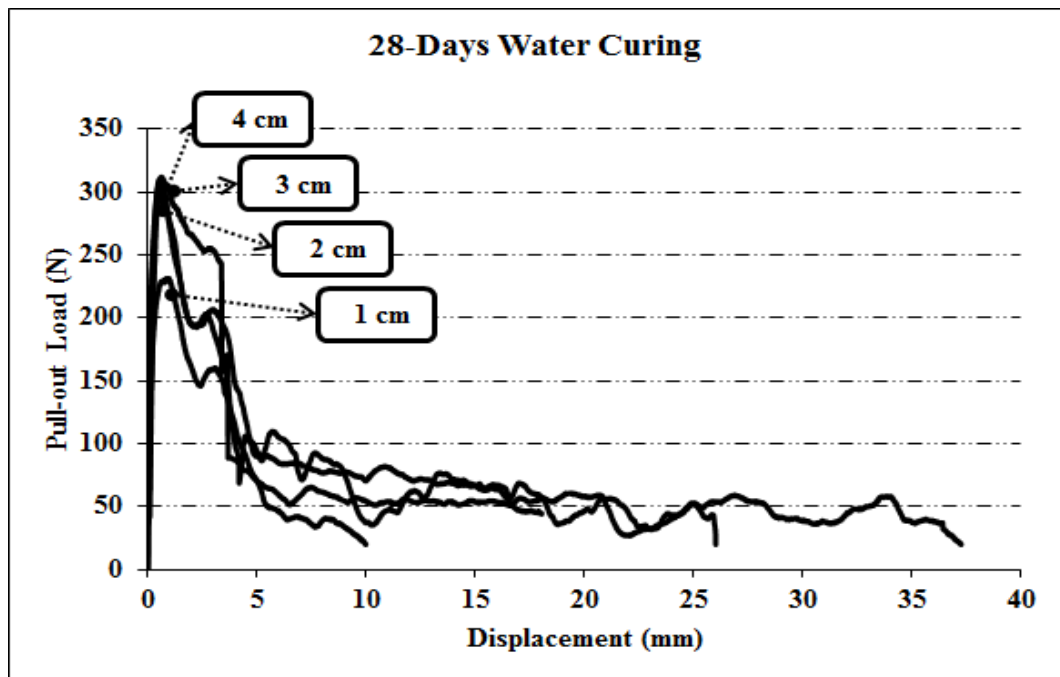


Figure 4.11 Pull-out load–displacement relationship of OM mixture with hooked-end fibers according to the embedment length (28 days).

It can be indicated from Figures 4.11 and 4.12 that pull-out peak load of hooked-end fibers in 2, 3, and 4 embedment lengths is approximately similar, while the peak load of fiber with 1 cm embedment length is lower than others in OM mixture.

The pull-out test load – displacement curves of OM mixture with smooth fiber in various embedment lengths of fiber after 7 and 28 days water curing are presented in Figures 4.13 and 4.14, respectively.

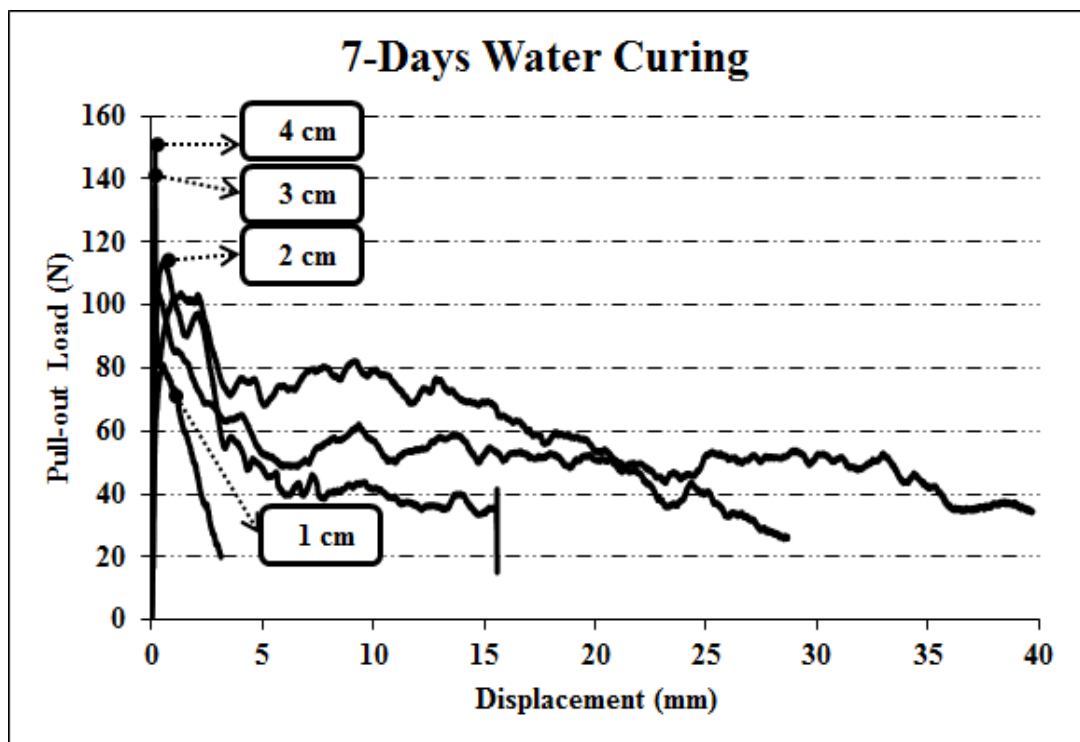


Figure 4.13 Pull-out load–displacement relationship of OM mixture with smooth fibers according to the embedment length (7 days).

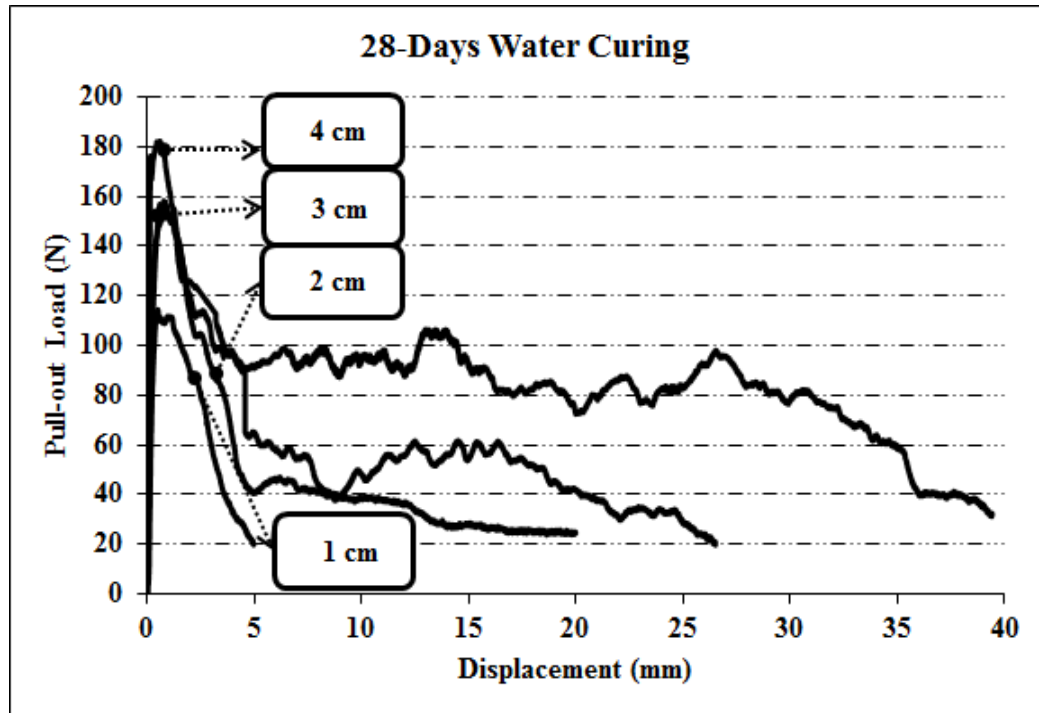


Figure 4.14 Pull-out load–displacement relationship of OM mixture with smooth fibers according to the embedment length (28 days).

As can be seen from curves the pull-out behavior of smooth fiber is different from hooked-end once. The fiber pull-out of smooth fiber occurs under frictional resistance. In most of the time after peak load sudden load drop was observed in descending part of smooth fiber graph. Additionally, the peak load and debonding toughness of the fibers was increased as embedment length increased in OM mixture.

Average peak load and debonding toughness in different embedment lengths for hooked-end and smooth steel fibers of OM mixture are presented in Figures 4.15 and 4.16. Debonding toughness values were determined by measuring the area underneath the pull-out load–displacement curve. It can be seen from figures that pull-peak load and debonding toughness of both smooth and hooked-end fiber were increased in 28 days compared to the 7-day once. However, it is obvious that pull-out peak load development is more obvious in case of hooked-end fiber than smooth once. In case of hooked-end fibers the pull-out peak load and debonding toughness values were increased compared to the 1 cm embedment length by 26-30 % and 40-

65 %, respectively. However, these increments were 35-45 % and 78-95 % for smooth fibers.

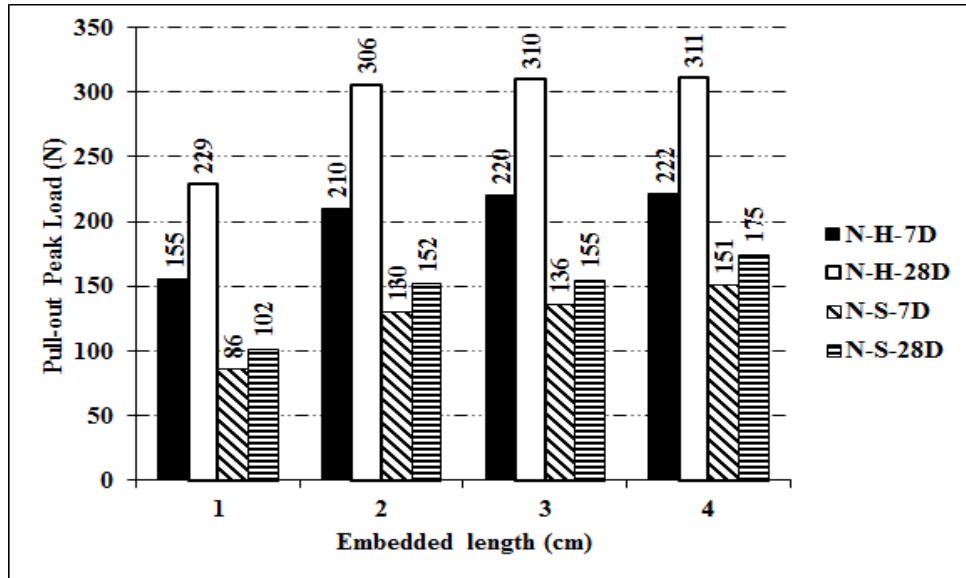


Figure 4.15 Pull-out peak load values of OM mixture.

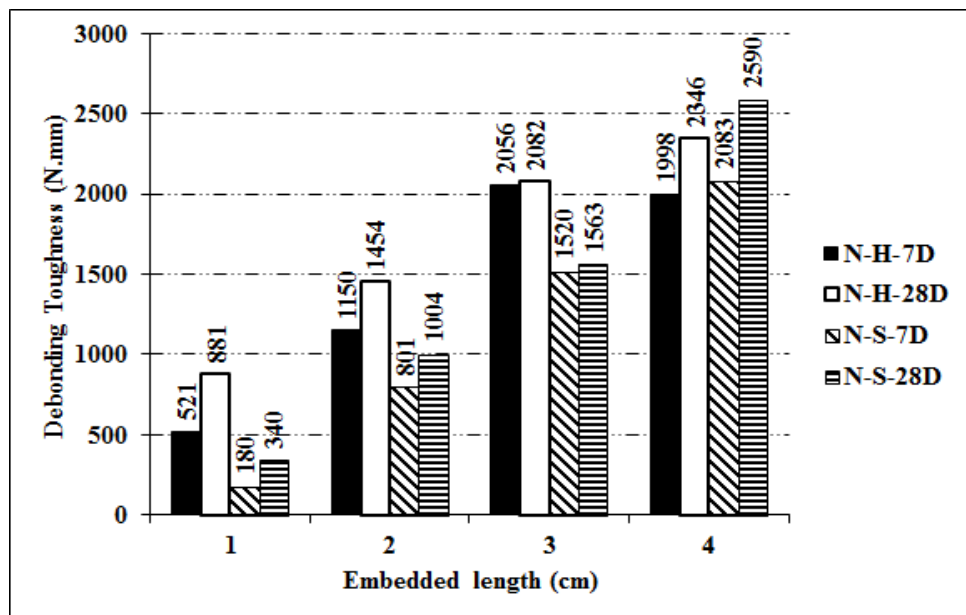


Figure 4.16 Pull-out debonding toughness values of OM mixture.

The pull-out test load – displacement curves of redesigned OM with 0.3 W/C ratio mixture for hooked-end fiber in various embedment lengths after 7 and 28 days water curing are presented in Figures 4.17 and 4.18, respectively.

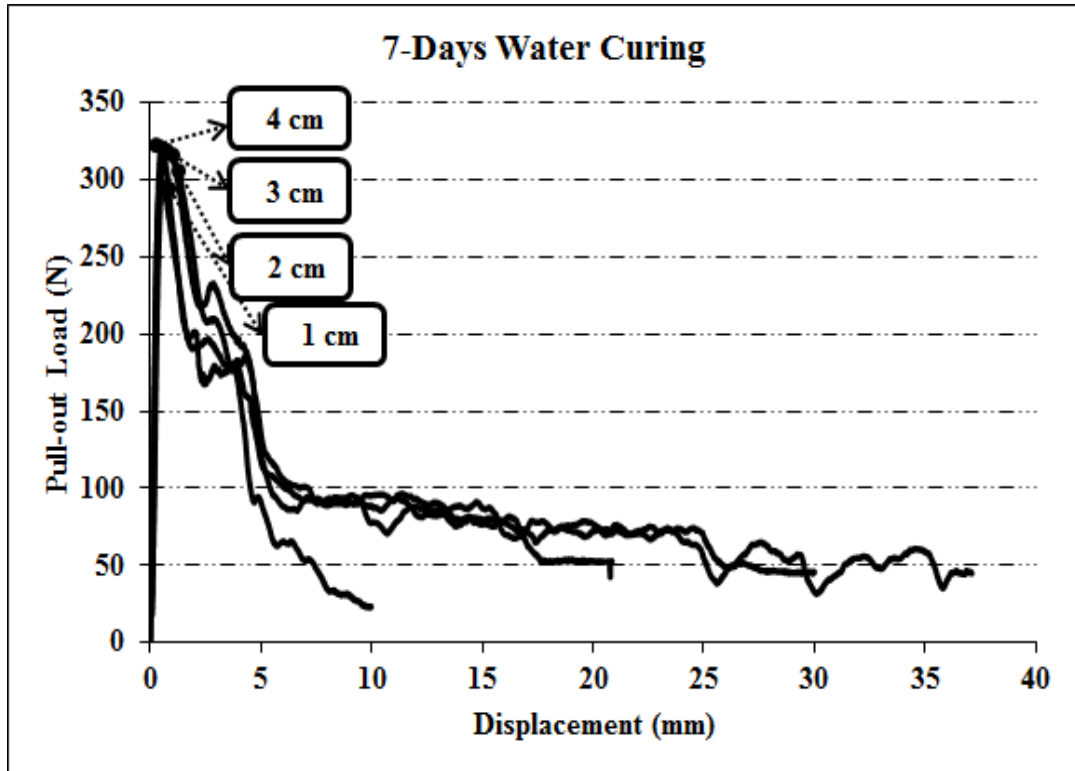


Figure 4.17 Pull-out load–displacement relationship of redesigned OM mixture with 0.3 W/C ratio for hooked-end fibers according to the embedment length (7 days).

It can be seen from Figures 4.17 and 4.18 that the pull-out load–displacement relationship of 0.3W/C OM mixture is approximately similar to the OM mixture for hooked-end fiber. However, there are some differences such as higher pull-out peak load and debonding toughness values and high peak load value even for 1 cm embedment length. It can be explained by low W/C ratio which leads to better bond strength between steel fiber and matrix. This behavior is valid in both 7 and 28 days water curing. In other words decreasing W/C ratio, increasing bond strength decreased the importance of embedment length of the fiber into the matrix.

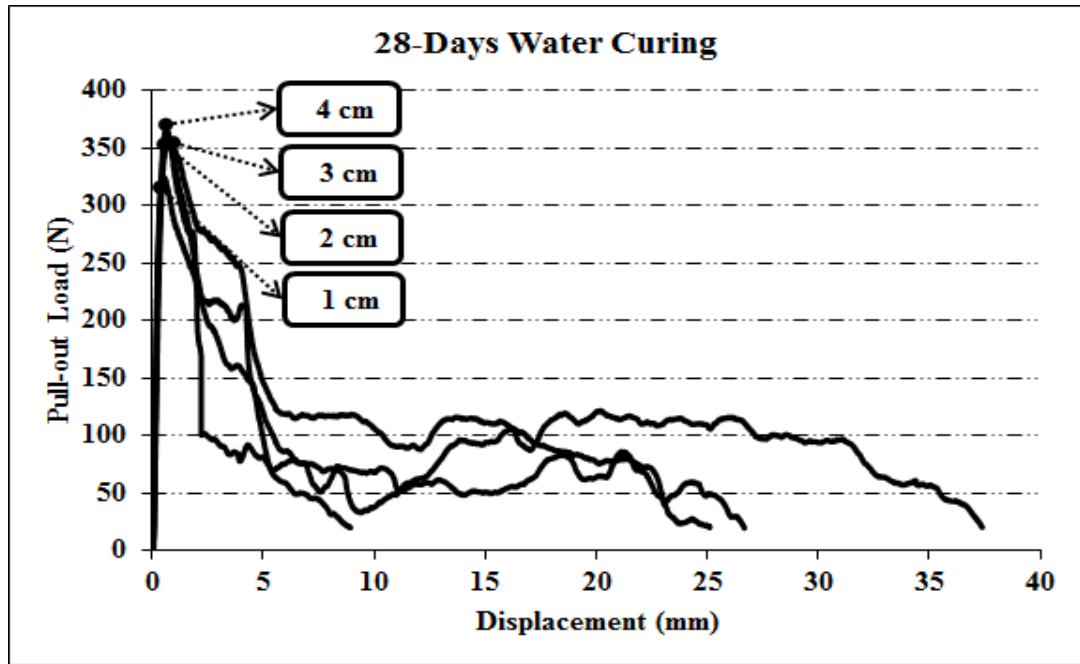


Figure 4.18 Pull-out load–displacement relationship of redesigned OM mixture with 0.3 W/C ratio for hooked-end fibers according to the embedment length (28 days).

The pull-out test load – displacement curves of redesigned OM with 0.3 W/C ratio mixture for smooth fiber in various embedment lengths after 7 and 28 days water curing are presented in Figures 4.19 and 4.20, respectively.

As can be seen from Figures 4.19 and 4.20 the pull-out load–displacement relationship of 0.3W/C OM mixture is similar to the OM mixture for hooked-end fiber. The maximum pull-out load increased as the embedment length increased in both 7 and 28 water curing. However, the pull-out peak load of fibers with 4, 3, and 2 cm (smooth fiber) are close to each other, while this behavior was not observed in case of OM mixture. It must be noted that 1 cm embedment length is extremely insufficient for smooth fiber just like OM mixture.

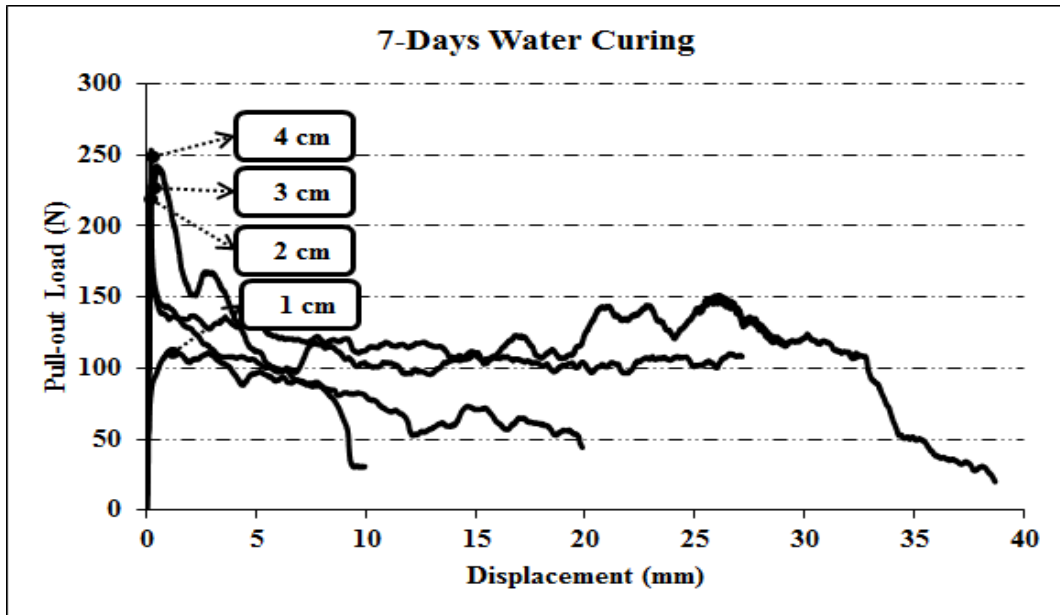


Figure 4.19 Pull-out load–displacement relationship of redesigned OM mixture with 0.3 W/C ratio for smooth fibers according to the embedment length (7 days).

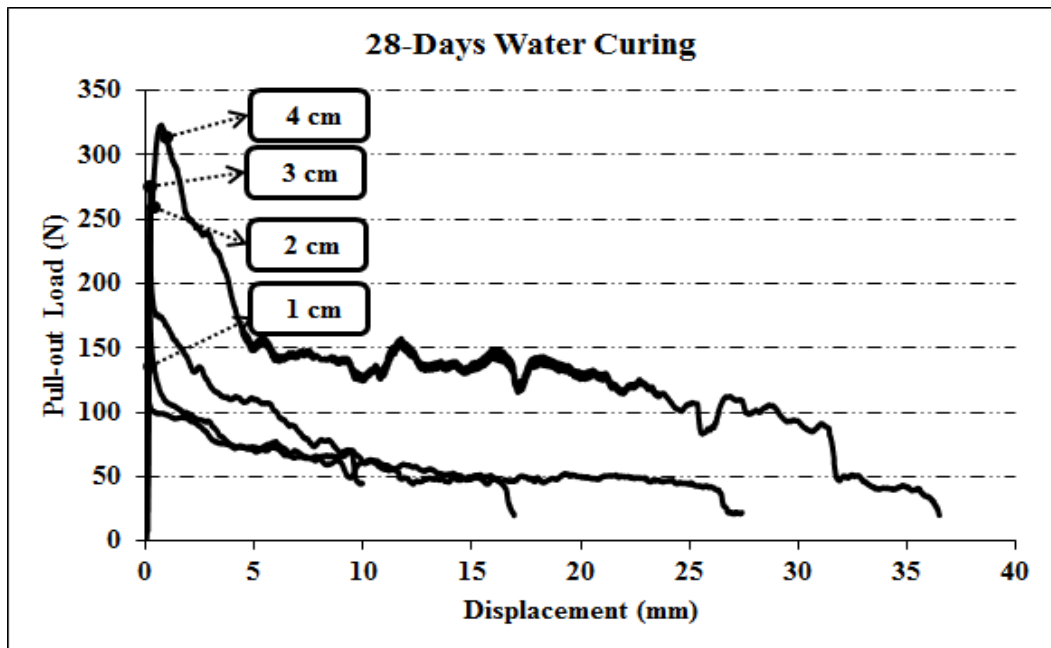


Figure 4.20 Pull-out load–displacement relationship of redesigned OM mixture with 0.3 W/C ratio for smooth fibers according to the embedment length (28 days).

Average peak load and debonding toughness in different embedment lengths for hooked-end and smooth steel fibers of redesigned OM with 0.3 W/C ratio mixture are presented in Figures 4.21 and 4.22. It can be seen from figures that pull-peak load and debonding toughness of both smooth and hooked-end fiber were increased in 28 days compared to the 7-day once. However, it is obvious that pull-out peak load development is more obvious in case of hooked-end fiber than smooth once.

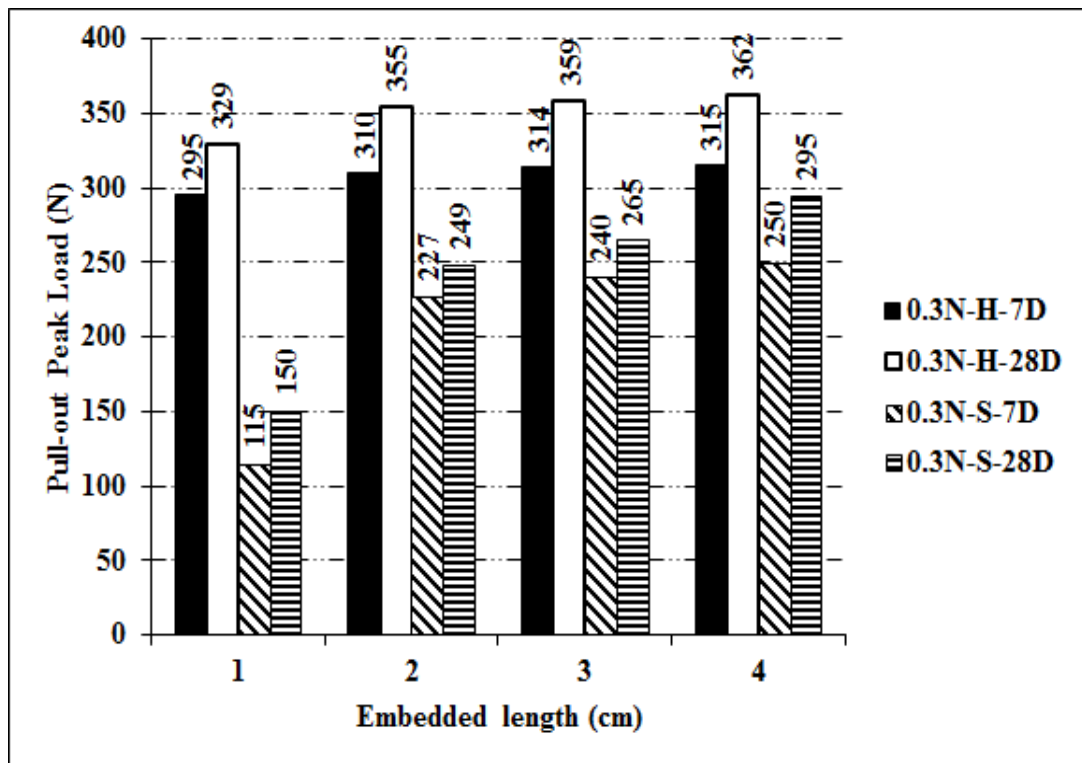


Figure 4.21 Pull-out peak load values of redesigned OM with 0.3 W/C ratio mixture.

As shown in Figures 4.21 and 4.22 both pull-out peak load and debonding toughness of all embedment lengths were increased at 28-day compared to the 7-day once. It must be mentioned that 1 cm embedment length is not sufficient in terms of smooth fiber, while this behavior is not valid in case of hooked-end fiber. The better performance of hooked-end fiber is more obvious in 1 cm embedment length. In case of hooked-end fibers the pull-out peak load and debonding toughness values were increased compared to the 1 cm embedment length by 5-9 % and 45-65 %, respectively. However, these increments were 40-54 % and 60-80 % for smooth fibers.

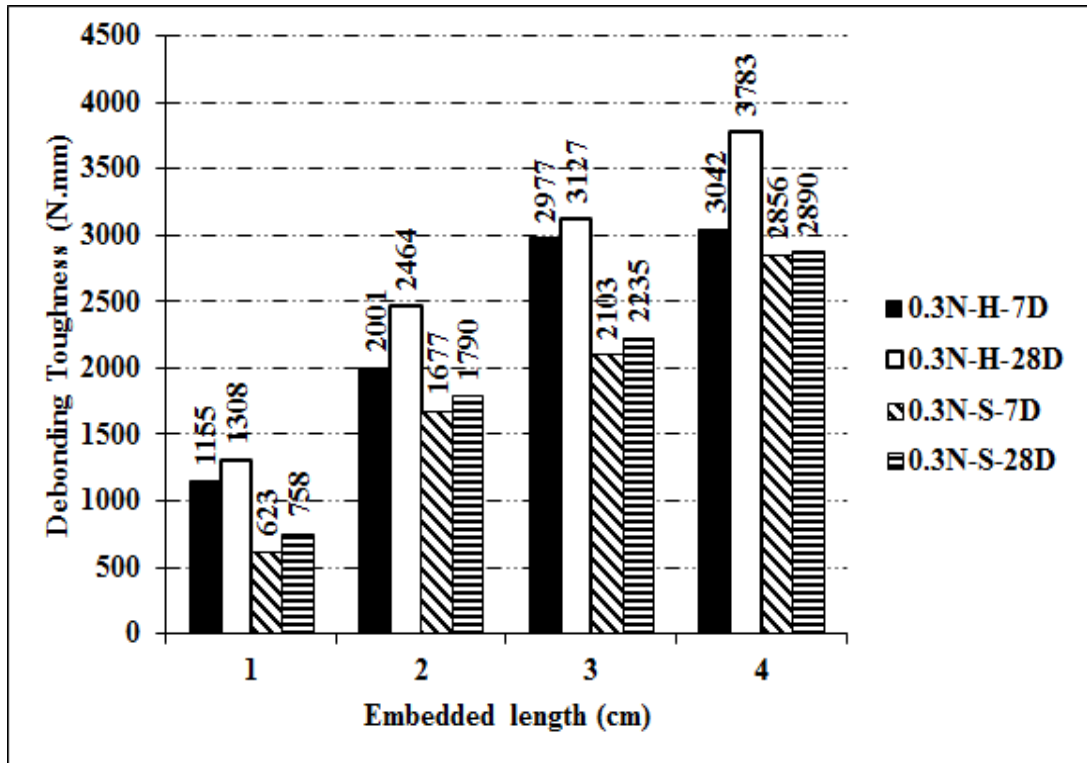


Figure 4.22 Pull-out debonding toughness values of redesigned OM with 0.3 W/C ratio mixture.

The pull-out test load – displacement curves of RPC mixture for hooked-end fiber in various embedment lengths after 7 and 28 days water curing are presented in Figures 4.23 and 4.24, respectively. As can be seen from Figures 4.23 and 4.24 the pull-out peak load and debonding toughness of RPC is much more than OM and even 0.3W/C OM mixtures. The dense microstructure and low W/B ratio leads to better bond characteristic of hooked-end steel fiber and RPC matrix. Furthermore, existence of silica fume has a positive effect in bond between steel-fiber and RPC matrix (Chan & Chu 2003). It must be noted that there is no excessive difference in peak load of each embedment length; however, the peak load was increased as the embedment length increased.

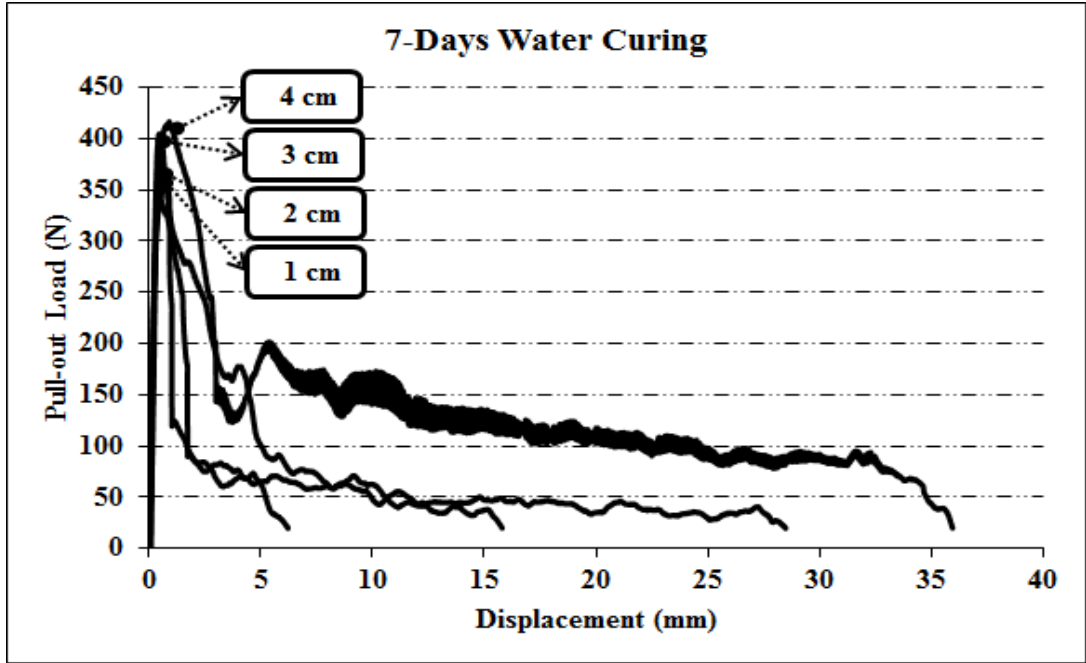


Figure 4.23 Pull-out load–displacement relationship of RPC for hooked-end fibers according to the embedment length (7 days).

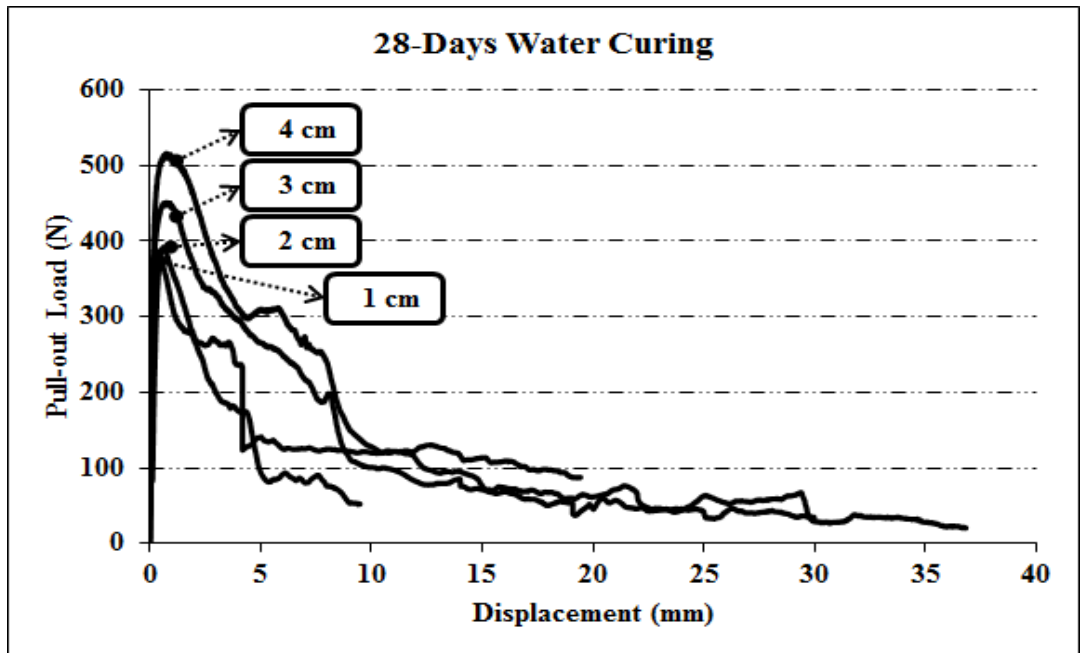


Figure 4.24 Pull-out load–displacement relationship of RPC for hooked-end fibers according to the embedment length (28 days).

The pull-out test load – displacement curves of RPC mixture for smooth fiber in various embedment lengths after 7 and 28 days water curing are presented in Figures 4.25 and 4.26, respectively.

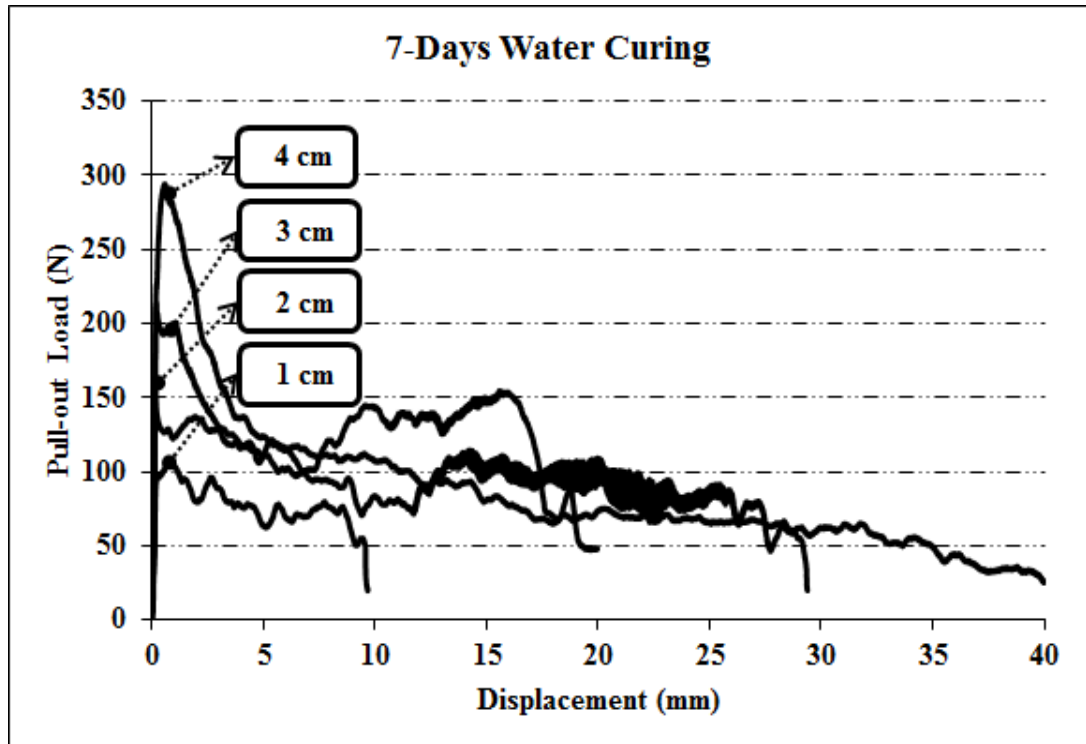


Figure 4.25 Pull-out load–displacement relationship of RPC for smooth fibers according to the embedment length (7 days).

As shown in Figures 4.25 and 4.26 the pull-out performance of smooth fiber in RPC matrix is better than OM and even than 0.3W/C OM matrixes in both 7 and 28 days. However, except 4 cm embedment length at 28 days this increment is not as much as hooked-end fibers once. Similar to the other mixtures the peak load and debonding toughness were increased as embedment length increased. This behavior is much more obvious in 28 days water curing. As mentioned later the 1 cm embedment is not sufficient in case of smooth fiber, so similar result can be seen in RPC.

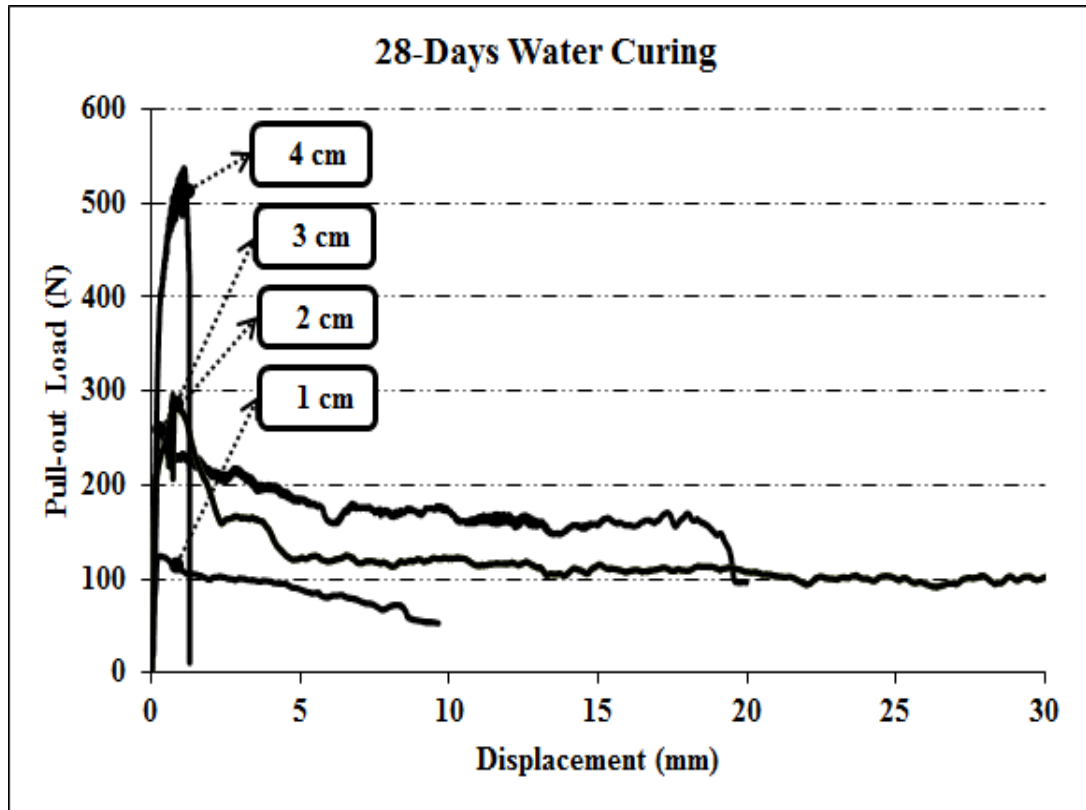


Figure 4.26 Pull-out load–displacement relationship of RPC for smooth fibers according to the embedment length (28 days).

The pull-out behavior of smooth fiber with 4 cm embedment length of RPC at 28 days was different compared to other specimens (Figure 4.27). As can be seen from Figure 4.27 the smooth fiber ruptured after approximately 1.3 mm displacement. Pull-out load–displacement curves after debonding of the surround interface (300 – 400 N load), frictional slip of the fiber was begun and the load increased with a wave form appearance. Because of the dense microstructure of interface of fiber-RPC matrix, fiber rupture was occurred in 4 cm embedment length of smooth fiber after 28-day water curing. This means bond strength between RPC matrix and fiber is higher than tensile strength of fiber itself.

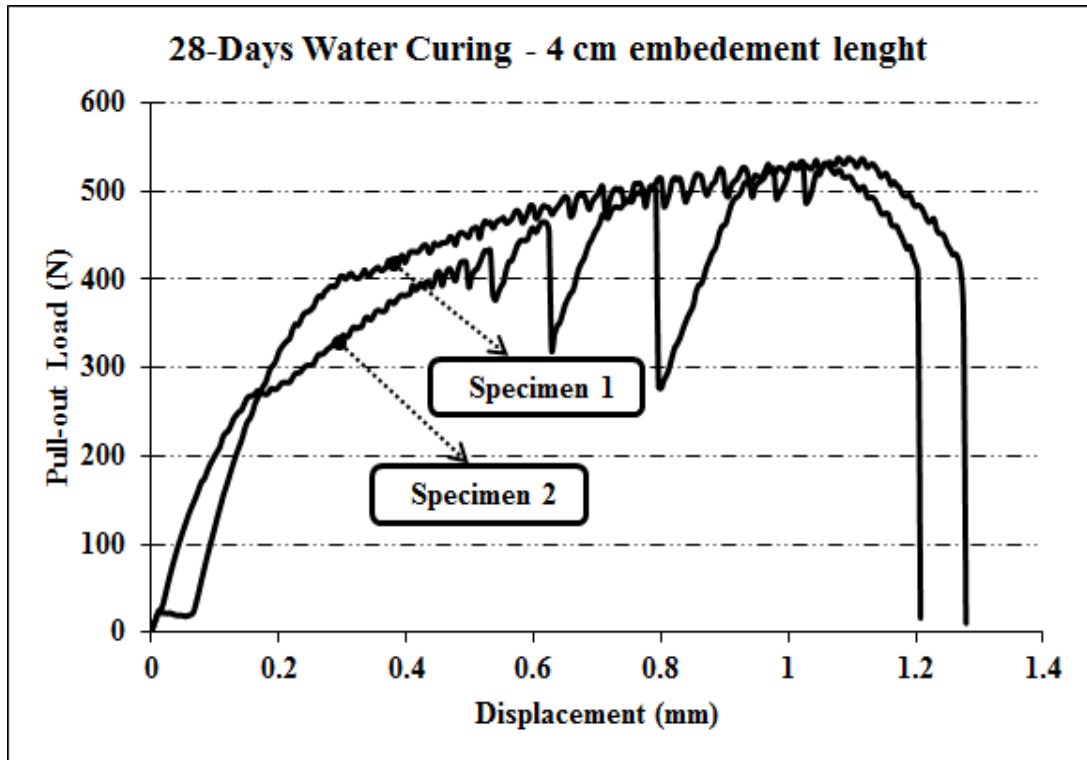


Figure 4.27 Pull-out load–displacement relationship of RPC for smooth fiber with 4 cm embedment length (28 days).

Average peak load and debonding toughness in different embedment lengths for hooked-end and smooth steel fibers of RPC mixture are presented in Figures 4.28 and 4.29. It can be seen from Figures 4.28 and 4.29 that except 4 cm embedment length the pull-out peak load of hooked-end specimens is much higher than smooth once. However, debonding toughness is more complex. The debonding toughness of hooked-end fiber is much higher than smooth once in case of 1 cm as a result of this fact that 1 cm embedment length for smooth fiber is extremely insufficient. In case of 2 and 3 cm embedment lengths, this behavior is just opposite to the 1 cm once. As mentioned earlier, the smooth fibers with 4 cm embedment length were ruptured after approximately 1.3 mm displacement, so the debonding toughness value is very low.

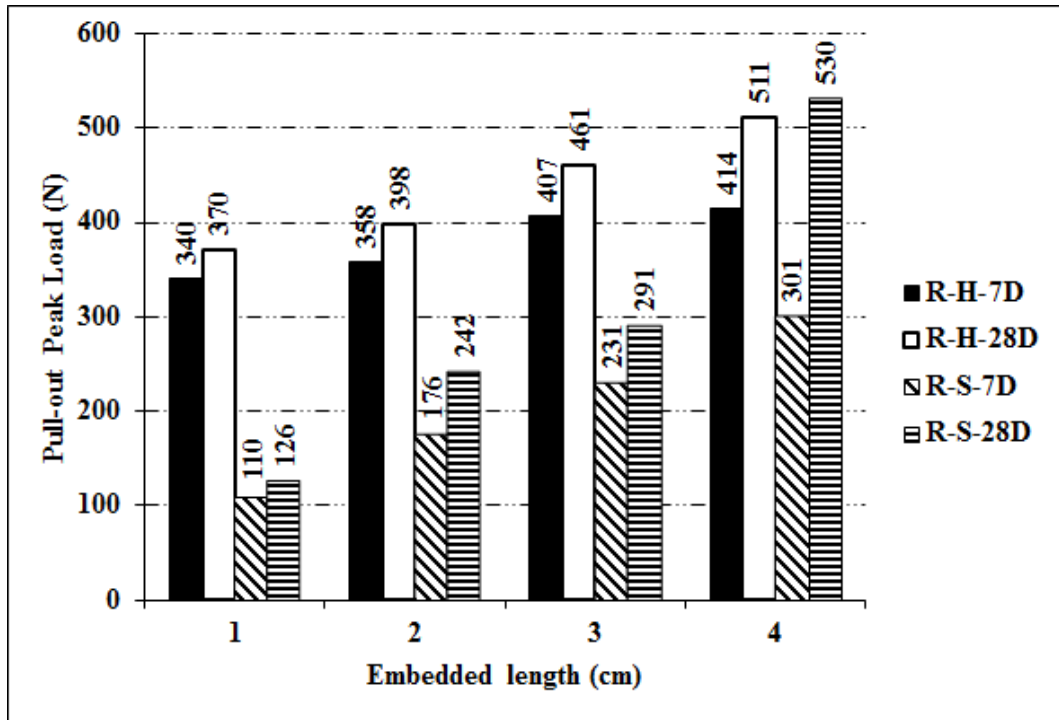


Figure 4.28 Pull-out peak load values of RPC mixture.

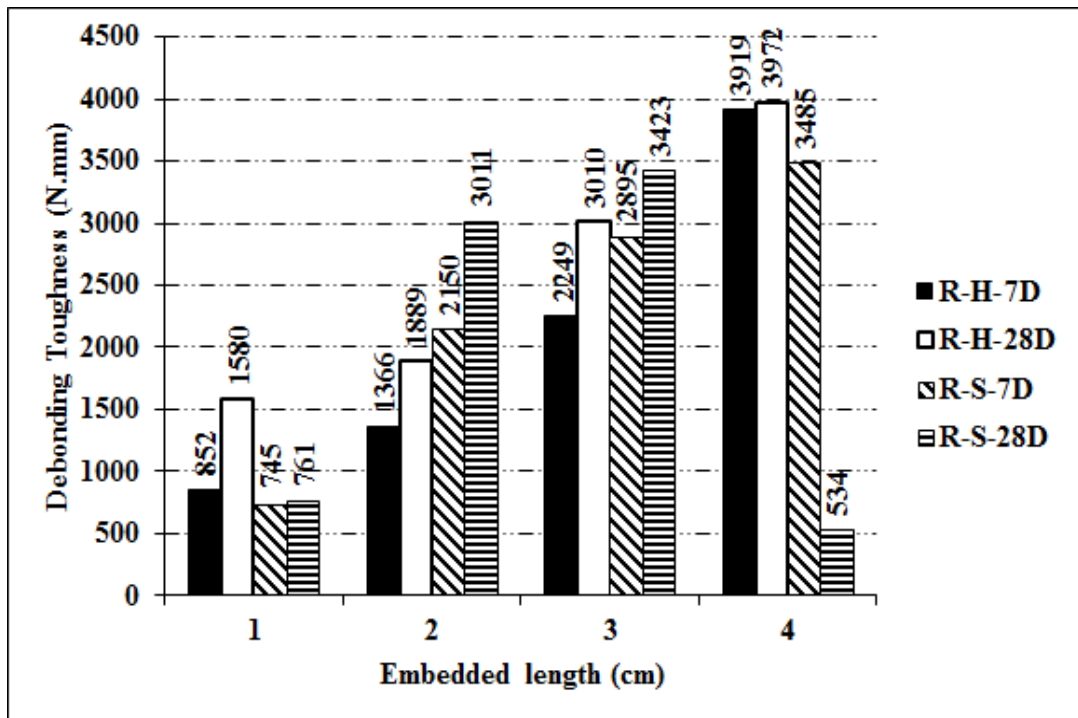


Figure 4.29 Pull-out debonding toughness values of RPC mixture.

The pull-out load – displacement curves of paste phase of RPC mixture without any aggregate for hooked-end fiber in various embedment lengths after 7 and 28 days water curing are presented in Figures 4.30 and 4.31, respectively. As can be seen from Figures 4.30 and 4.31 the pull-out peak load values of all fibers with different embedment lengths is not much different especially at 28 days. However, the peak load was increased as embedment increased. Generally, the pull-out performance of hooked-end fibers in paste phase of RPC is lower than RPC once. Existence of micro cracks due to the high cement content and lack of aggregate leads to lower pull-out peak load in case of paste phase of RPC mixture. Furthermore, the slipping of fiber is smoother compared to the RPC and other mixtures. As mentioned earlier the additional peak points were observed after second peak point in the load-displacement graphs of mixtures. This behavior may be related to the effect of aggregate (especially coarser aggregate 1-5 mm) on frictional resistance of fiber-matrix. Forasmuch as the paste mixture doesn't include any aggregate, this was an expected behavior. This behavior was also observed in SIFCON matrix which has aggregate smaller than 1 mm (Tuyan & Yazıcı, 2012).

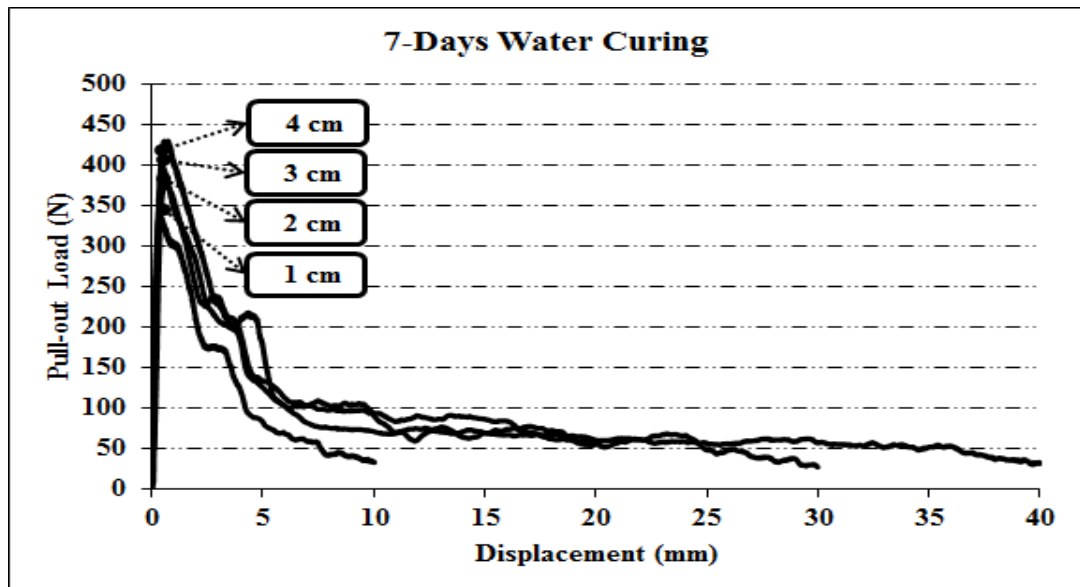


Figure 4.30 Pull-out load–displacement relationship of paste phase RPC for hooked-end fibers according to the embedment length (7 days).

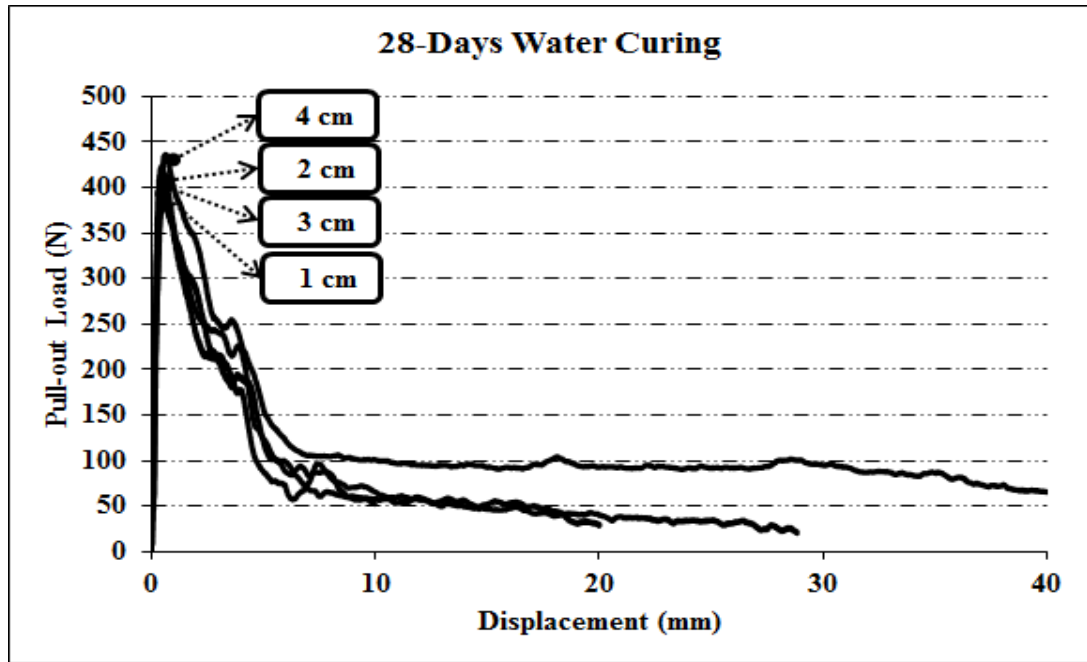


Figure 4.31 Pull-out load–displacement relationship of paste phase RPC for hooked-end fibers according to the embedment length (28 days).

The pull-out test load – displacement curves of RPC paste mixture for smooth fiber in various embedment lengths after 7 and 28 days water curing are presented in Figures 4.32 and 4.33, respectively. As can be seen from Figure 4.32 and 4.33 pull-out behavior of smooth fiber in paste mixture is similar to RPC, but the peak load was lower than RPC mixture. Furthermore, the peak load of smooth fiber was increased as the embedment length increased. Additionally, the weak pull-out behavior of smooth fiber in 1 cm embedment length is more visible in paste mixture.

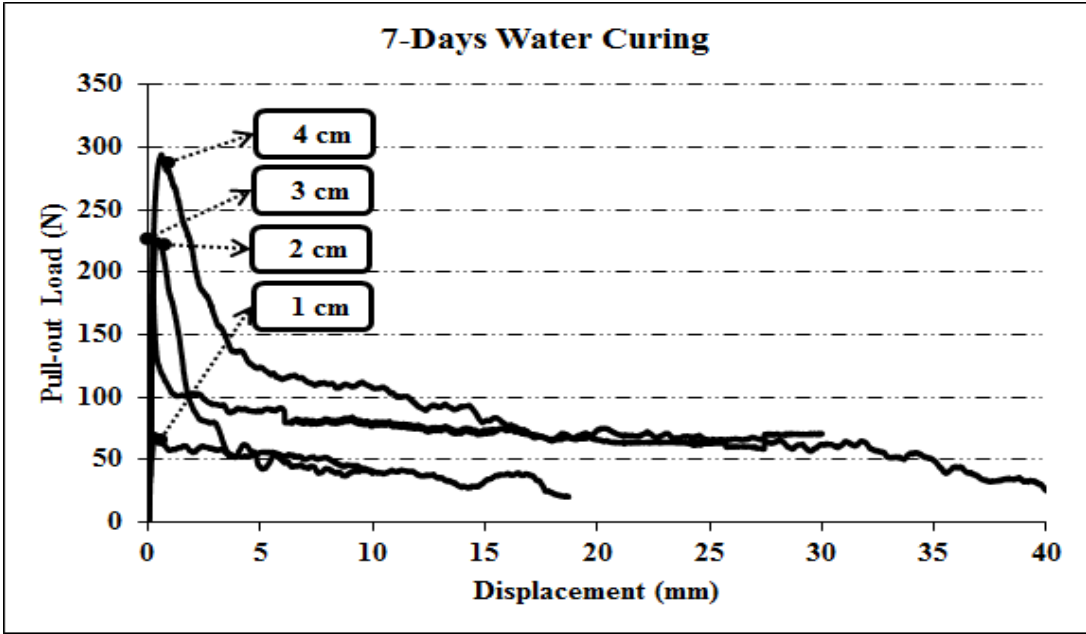


Figure 4.32 Pull-out load–displacement relationship of paste phase RPC for smooth fibers according to the embedment length (7 days).

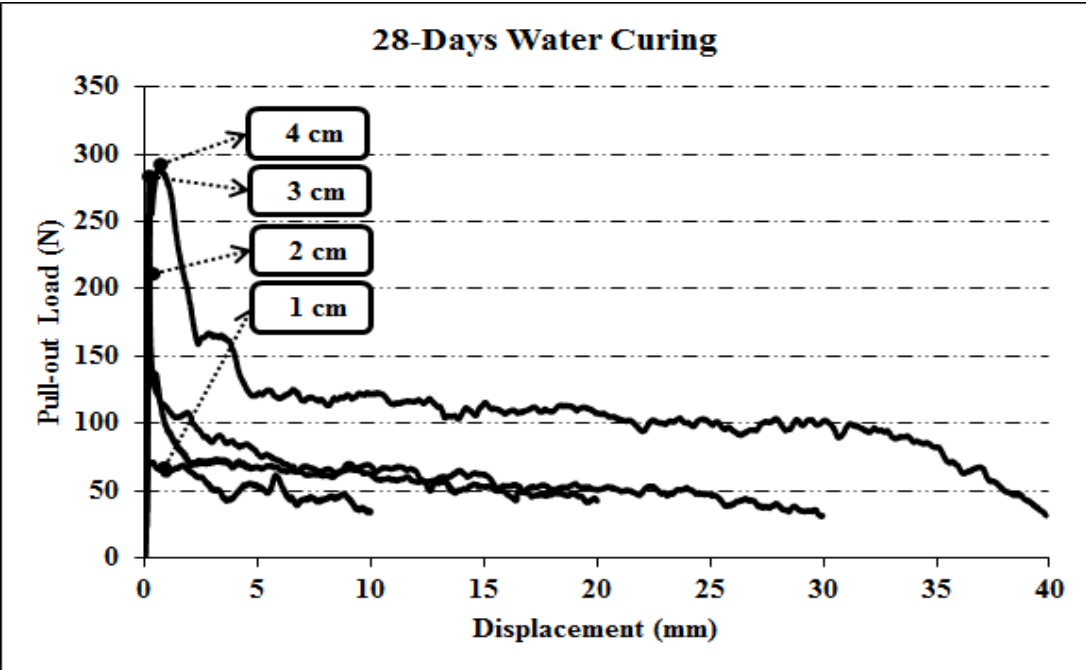


Figure 4.33 Pull-out load–displacement relationship of paste phase RPC for smooth fibers according to the embedment length (28 days).

Average peak load and debonding toughness in different embedment lengths for hooked-end and smooth steel fibers of RPC mixture are presented in Figures 4.34 and 4.35. As can be seen in Figures 4.34 and 4.35 both the pull-out peak load and debonding toughness of hooked-end fiber is much higher than smooth once. However, this difference has been decreased by increasing the embedded length. The pull-out load values of hooked-end fibers is 390 %, 65 %, 51 %, and 38 % higher than smooth once for 1, 2, 3, and 4 cm embedment lengths, respectively.

Lack of aggregate leads to more homogeneous mixture. However, the peak load and debonding toughness values of both hooked-end and smooth fiber are lower than RPC mixture containing aggregate.

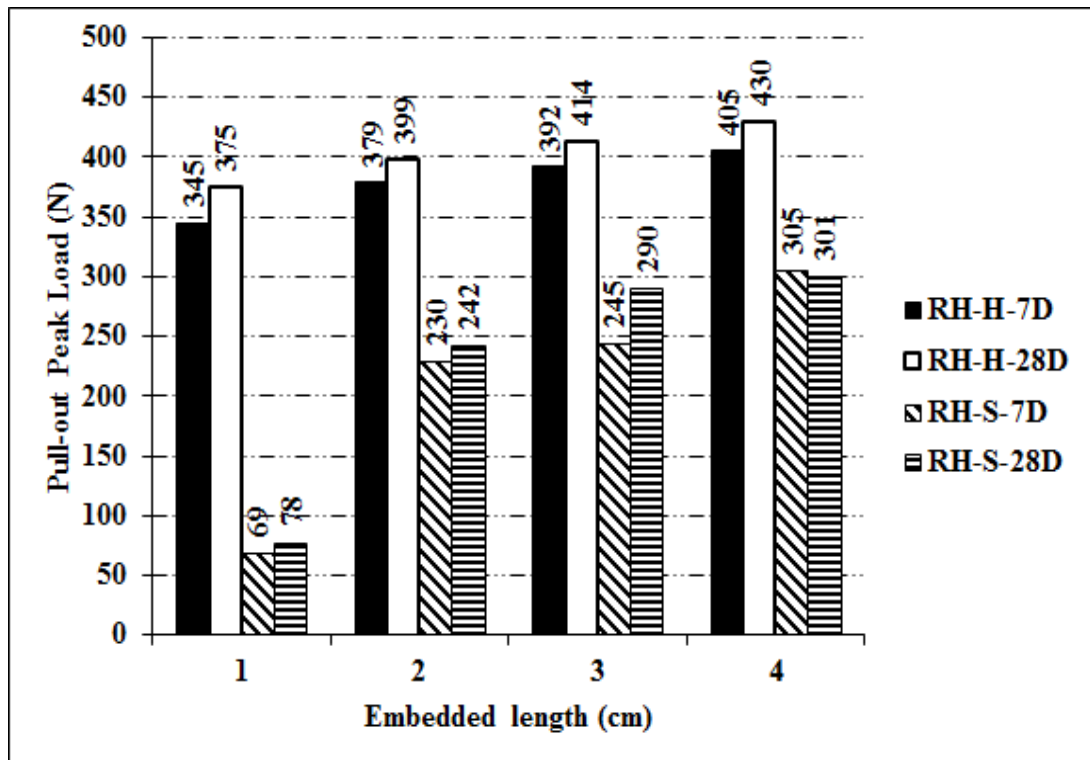


Figure 4.34 Pull-out peak load values of paste phase of RPC mixture.

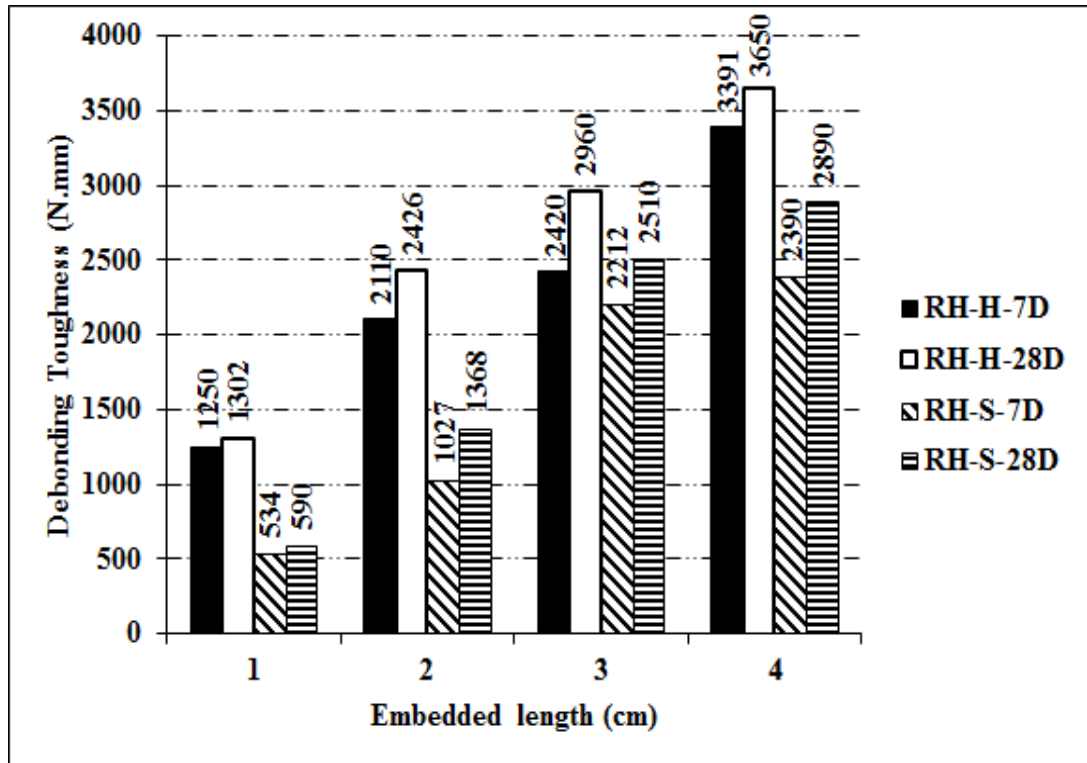


Figure 4.35 Pull-out debonding toughness values of paste phase of RPC mixture.

4.1.3 The Effect of Water/Binder Ratio on Pull-out Behavior

In order to investigate the effect of W/B ratio on pull-out behavior, the OM mixture with 0.5 W/C ratio was redesigned. The W/C ratio increased to 0.6 and decreased to 0.4 and 0.3. Furthermore, the RPC matrix with 0.2 W/B ratio was redesigned. The W/B ratio increased to 0.3, 0.4, 0.5, and 0.6 ratios. It must be noted that cement dosage of the redesigned RPC mixtures was decreased as W/B ratio increased. Hooked-end fibers with 3 cm embedment length were used.

The Pull-out load–displacement curves of OM mixtures with various W/C ratios for 7 and 28 days water curing are presented in Figures 4.36 and 4.37, respectively. As can be seen from figures the pull-out maximum loads were increased as W/C ratio decreased. It is well known that decreasing the W/C ratio improves all characteristics of cement based composites positively. The denser microstructure of fiber-matrix interface as a result of decreasing W/C ratio leads to better bond

characteristics. However there is no remarkable difference between 0.5 and 0.6 W/C ratios, while a more visible increment was occurred by decreasing the W/C ratio from 0.5 to 0.4. Furthermore, the pull-out behavior of mixture with 0.3 W/C ratio is approximately similar to the 0.4 once. The relationships which discussed above are valid in both 7 and 28 days water curing condition. As can be seen from Figures 4.36 and 4.37 the pull-out behavior of all mixtures was improved at 28 days compared to 7 days.

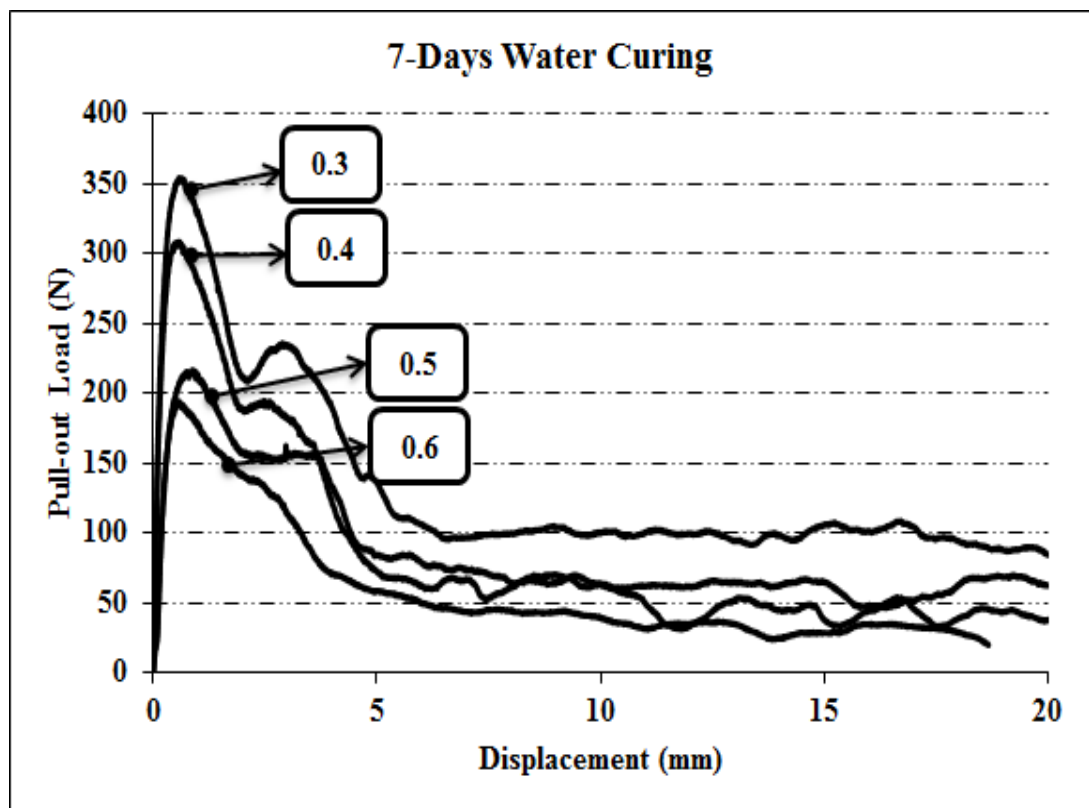


Figure 4.36 Pull-out load–displacement relationships of redesigned OM mixtures with various W/C ratios (7 days water curing).

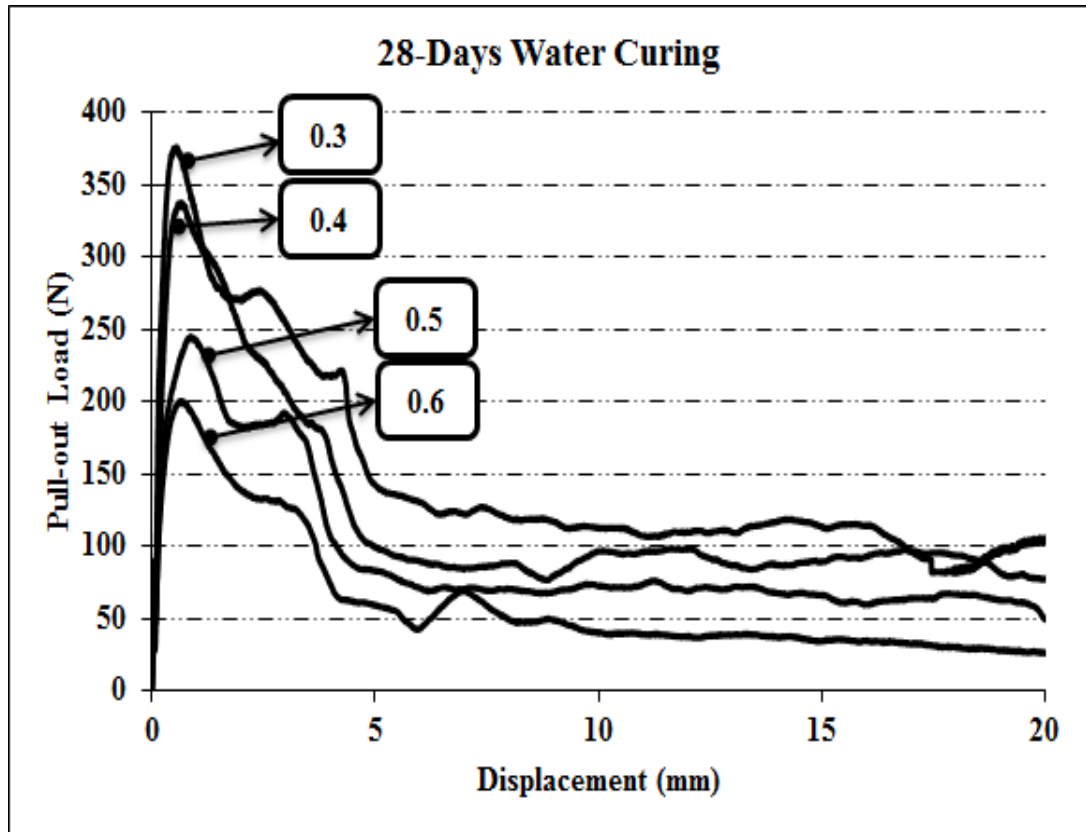


Figure 4.37 Pull-out load–displacement relationships of redesigned OM mixtures with various W/C ratios (28 days water curing).

The Pull-out load–displacement curves of OM mixtures with various W/C ratios for steam curing are presented in Figure 4.38. Similar strength loss which was observed in mechanical strength of OM mixtures was also occurred in pull-out performance. The pull-out behavior was improved by decreasing the W/C ratio just like the water cured once. Steam curing caused some strength loss especially at high W/C ratio compared to the 28-day water curing.

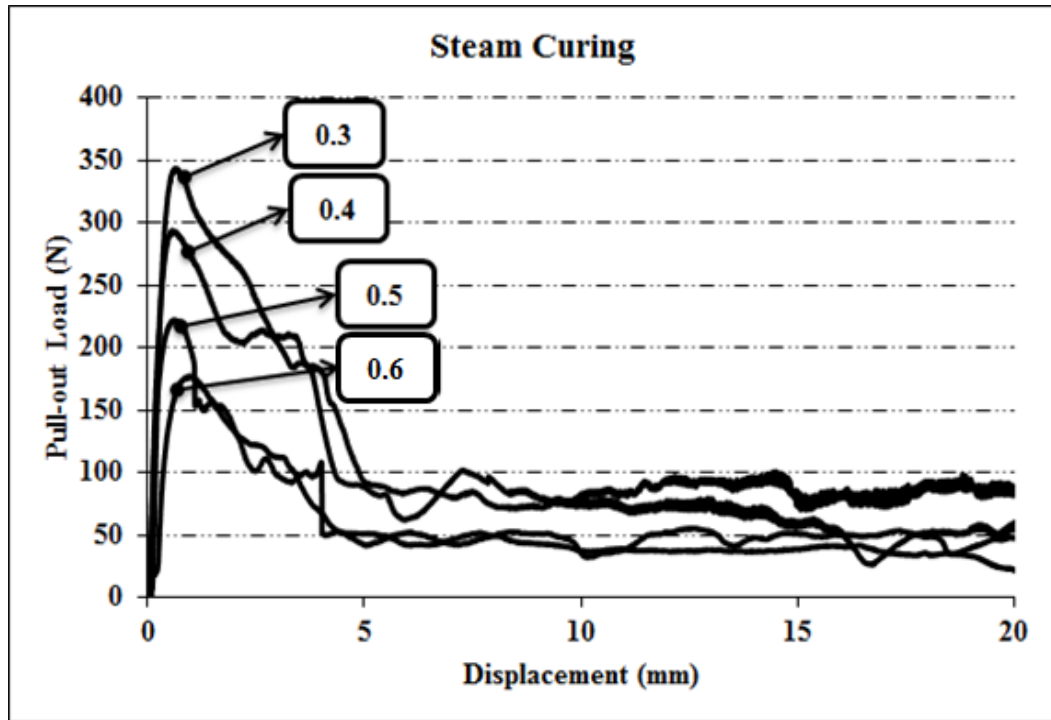


Figure 4.38 Pull-out load–displacement relationships of redesigned OM mixtures with various W/C ratios (steam curing).

The Pull-out load–displacement curves of OM mixtures with various W/C ratios for autoclave curing are presented in Figure 4.39. As can be seen from curves both pull-out peak load and debonding toughness of all mixtures were increased remarkably. However, the mechanical strength of these mixtures was decreased in autoclave curing compared to the 28-day water curing as a result of absence of SiO_2 components; the pull-out behavior was increased oppositely (except OM mixture with 0.6 W/C ratio). This behavior is a result of congestion of products which was created during the autoclave curing (Please see the microstructure investigation section). This superior effect of autoclave has been reported by Tuyan & Yazıcı, 2012. It must be noted that this increment in autoclave curing was become more visible by decreasing the W/C ratio. Increments in pull-out peak load compared to the 28-day water curing were 14 %, 20 %, and 32 % for OM mixtures with 0.5, 0.4, and 0.3 W/C ratios, respectively. In case of debonding toughness these values were 39 %, 84 %, and 124 %.

Additionally, because of the porous matrix of the mixture with 0.6 W/C ratio as a result of autoclave curing, the mechanical anchorage (interlock) of hooked-end of fiber has not occurred completely. This phenomenon leads to higher debonding toughness value (72%) compared to the 28-day water curing. However, pull-out peak load was not affected.

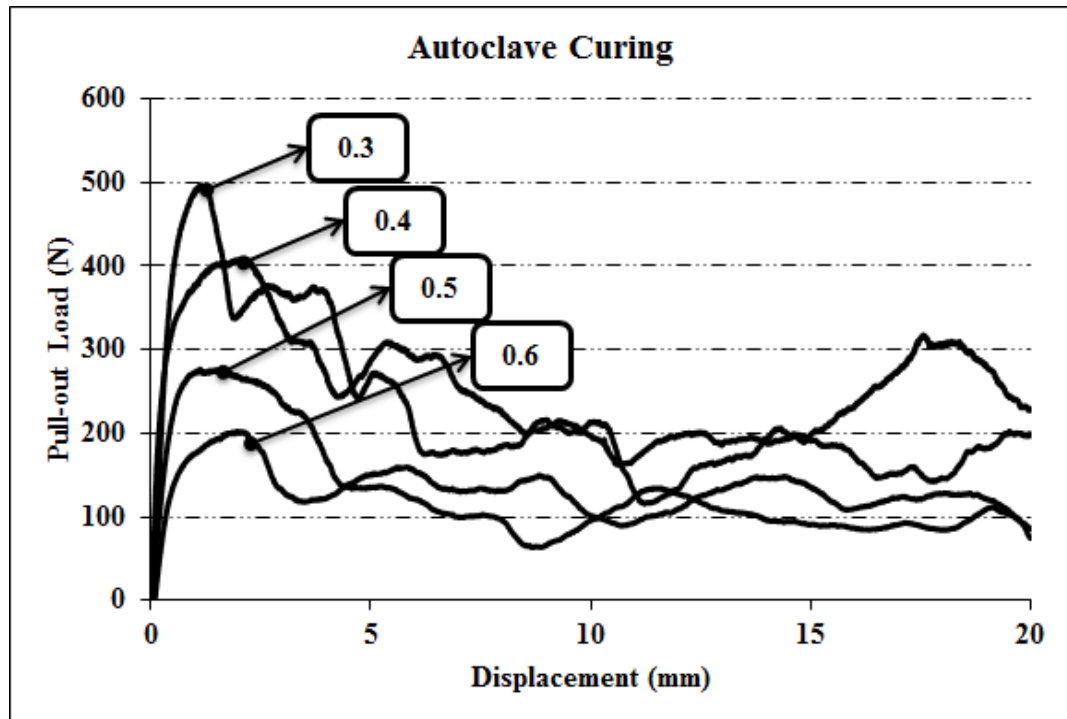


Figure 4.39 Pull-out load–displacement relationships of redesigned OM mixtures with various W/C ratios (autoclave curing).

Average pull-out peak load and debonding toughness of OM mixtures with various W/C ratios in different curing conditions are presented in Figures 4.40 and 4.41. Generally, it can be concluded that a bond characteristics of cement based composites with any W/C ratio is affected by curing conditions significantly.

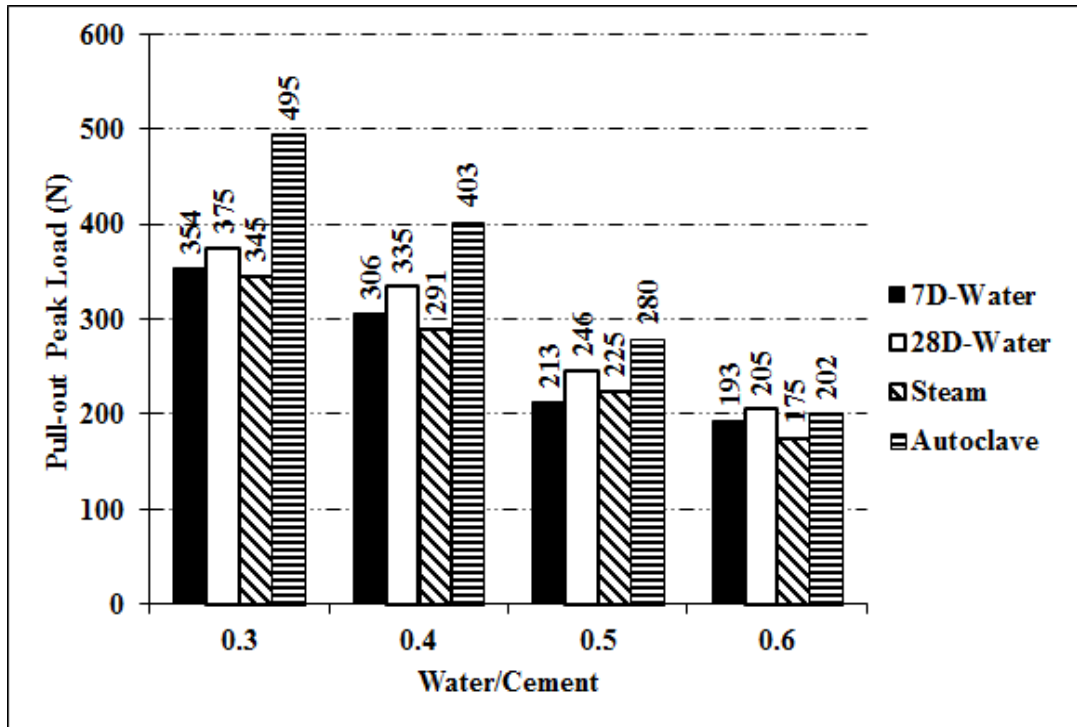


Figure 4.40 Pull-out peak load values of redesigned OM mixtures with various W/C ratios.

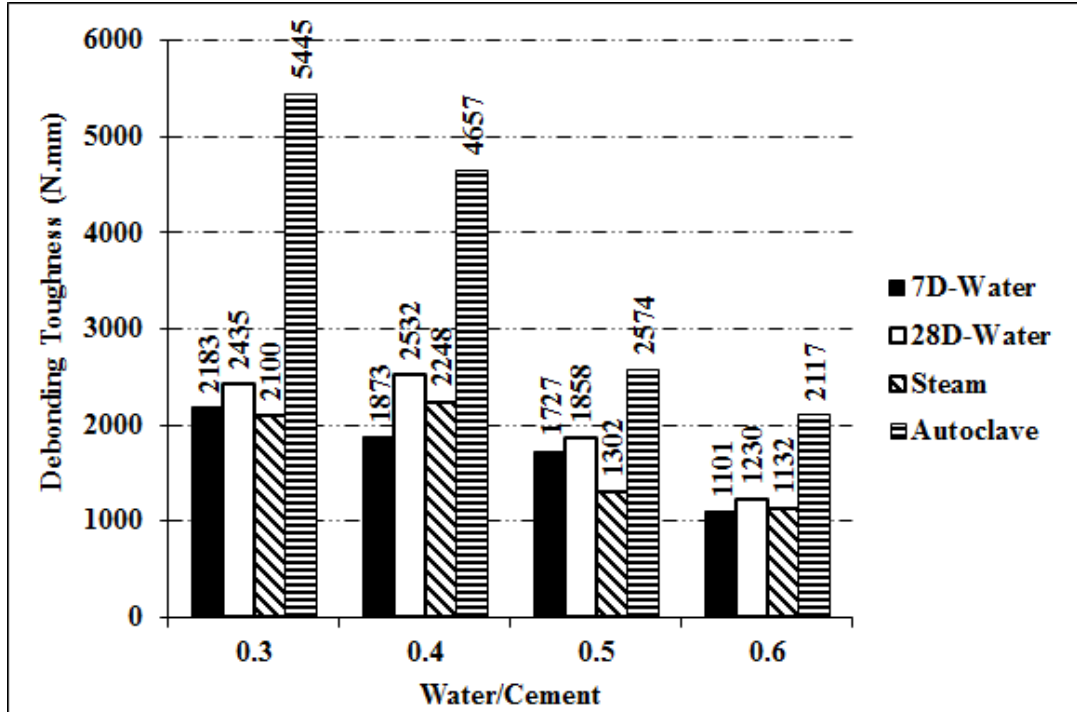


Figure 4.41 Debonding toughness values of redesigned OM mixtures with various W/C ratios.

The Pull-out load–displacement curves of redesigned RPC mixtures with various W/C ratios for 7 and 28 days water curing are presented in Figures 4.42 and 4.43, respectively. It can be concluded from curves that the pull-out behavior of mixtures with 0.6 and 0.5 W/B ratios are approximately similar at both 7 and 28 days water curing. In the other hand the pull-out behavior of mixtures with 0.3 and 0.2 W/B ratios are almost similar to each other especially in 28 days water curing. Similar to the previous mixtures (OM mixtures), the pull-out behavior was improved as the W/B ratio decreased. The effect of cement content of these mixtures must not be ignored. However, the effect of W/B ratio is definitely predominant.

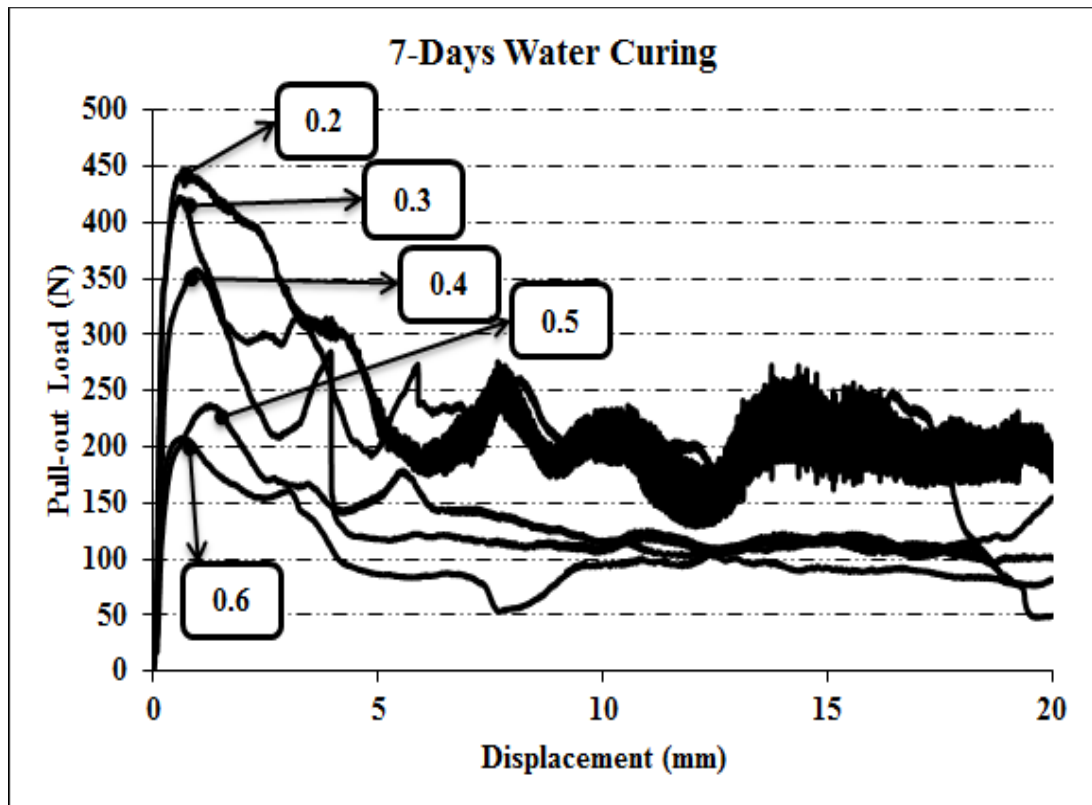


Figure 4.42 Pull-out load–displacement relationships of redesigned RPC mixtures with various W/C ratios (7 days water curing).

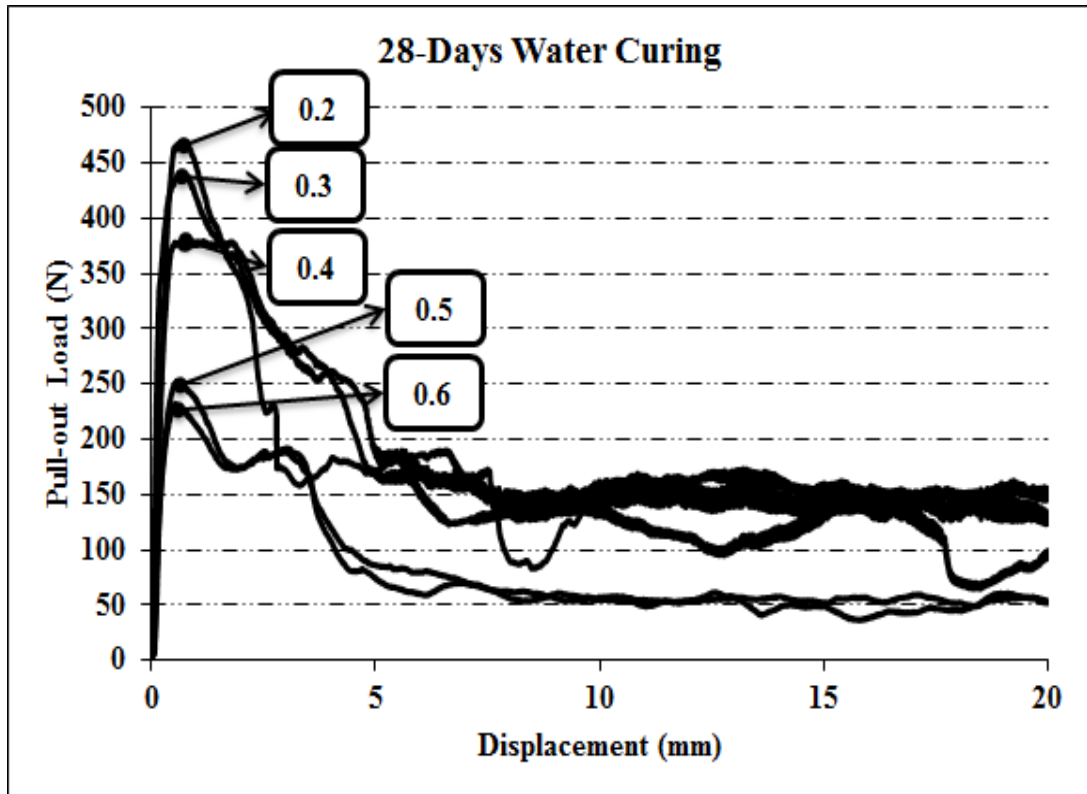


Figure 4.43 Pull-out load–displacement relationships of redesigned RPC mixtures with various W/C ratios (28 days water curing).

The Pull-out load–displacement curves of redesigned RPC mixtures with various W/B ratios for steam curing are presented in Figures 4.44. As can be seen from Figure 4.44 the pull-out behavior was improved by decreasing the W/B ratio. However, similar to the OM mixtures the peak load peak load and debonding toughness of mixtures in steam curing is lower than 28 days water curing.

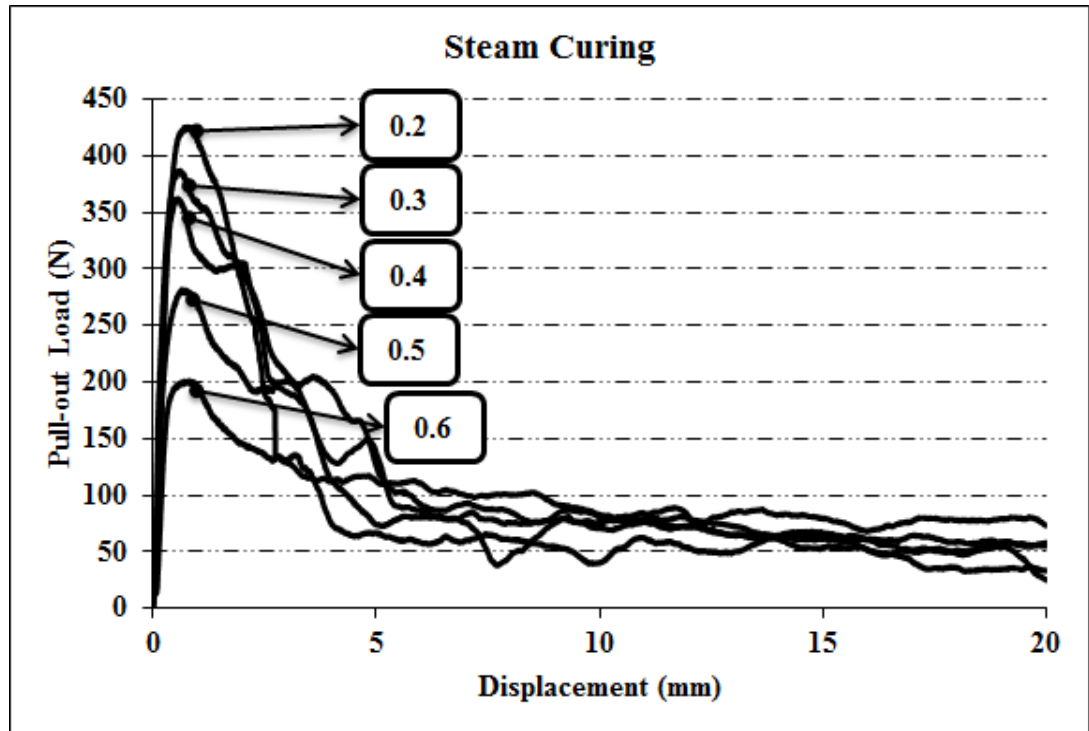


Figure 4.44 Pull-out load–displacement relationship of redesigned RPC mixture in various W/C ratios (steam curing).

The Pull-out load–displacement curves of redesigned RPC mixtures with various W/C ratios in autoclave curing are presented in Figures 4.45. As can be seen from Figure 4.44 the pull-out peak load and debonding toughness of all mixtures was increased remarkably after autoclave curing. Fiber rupture was occurred in case of 0.3 and 0.2 which means the pull-out peak load is higher than tensile strength of the steel fiber. As shown in Figure 4.45 the fiber was ruptured with low debonding. It must be noted that this behavior is different from that fiber rupture which was observed in 4 cm embedment length of smooth fiber in RPC mixture. In other words, this rupture of fiber occurred after autoclave curing is the result of congestion of tobermorite gel in fiber-matrix interface and low W/B ratio which increased the bond strength strongly, while the rupture of smooth fiber with 4 cm embedded length in 28-day water curing was occurred after debonding of the fiber as a result of excellent fraction resistance of RPC.

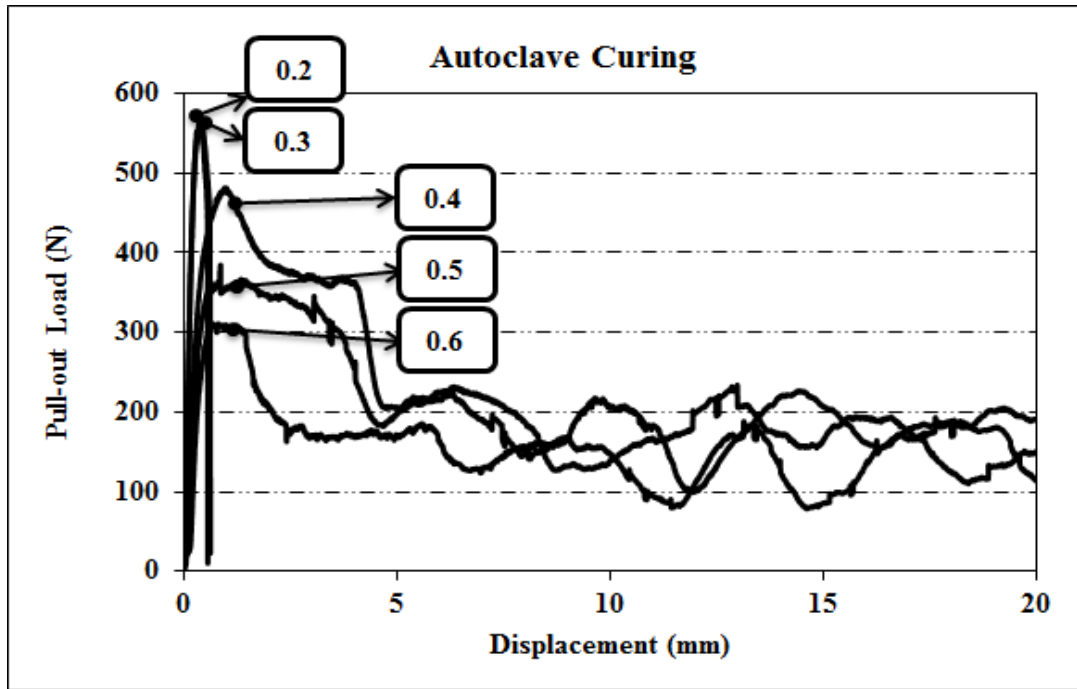


Figure 4.45 Pull-out load–displacement relationships of redesigned RPC mixtures with various W/B ratios (autoclave curing).

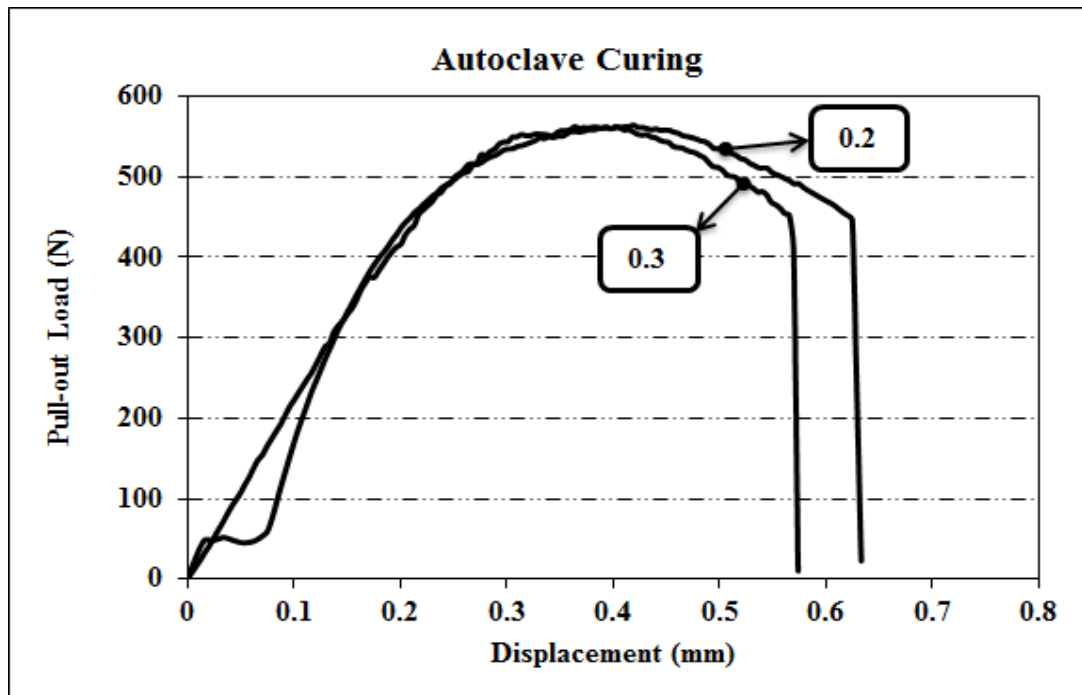


Figure 4.46 Pull-out load–displacement relationship of RPC with 0.3 and 0.2 W/B ratios (autoclave curing).

Average pull-out peak load and debonding toughness of OM mixtures with various W/C ratios in different curing conditions are presented in Figures 4.47 and 4.48. It can be concluded from test results that pull-out behavior of all mixtures is depend on curing condition. The pull-out peak load values of 0.2 and 0.3 mixture is same as a result of fiber rupture in load which exceeds the tensile strength of the fiber after autoclave curing. Additionally, the debonding toughness values of those mixtures are very low as a result of fiber rupture without considerable debonding. It must be noted that the mixture with 0.4 W/B ratio in autoclave curing has an excellent bond characteristics compared to 28 water cured once. This remarkable increment after autoclave curing is also valid in case of 0.5 and 0.6 mixtures. Generally, it can be concluded that the pull-behavior of specimens cured in steam is similar to the 7-day water cured once, while both pull-out peak load and debonding toughness was improved at 28 days water curing.

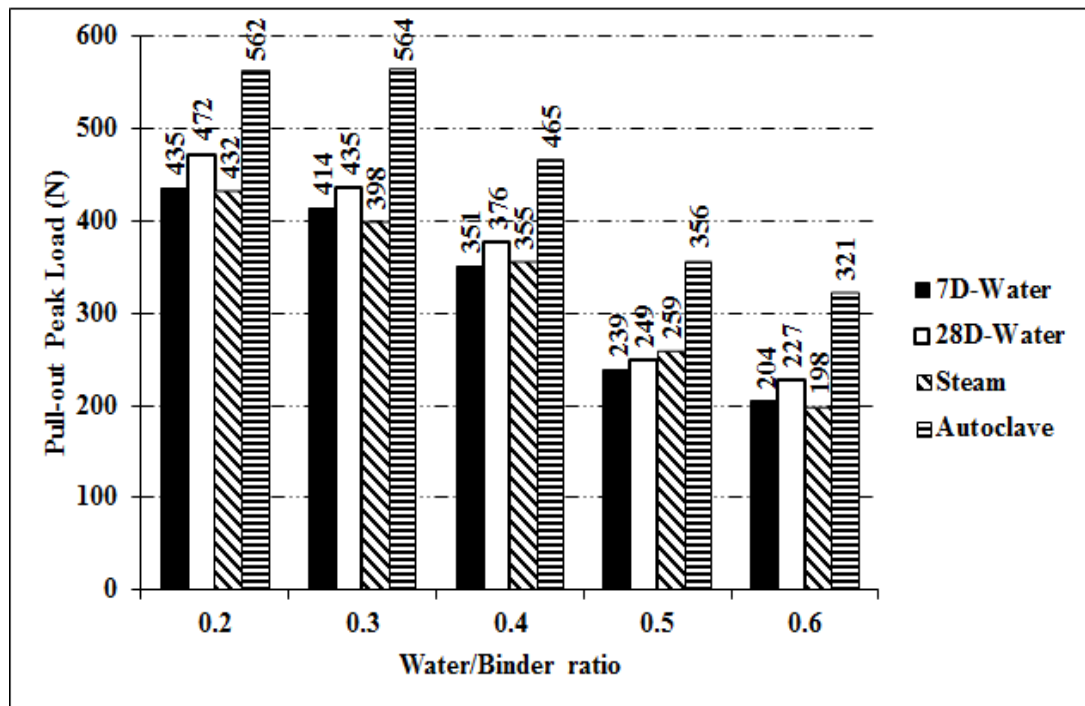


Figure 4.47 Pull-out peak load values of redesigned RPC mixtures in various W/B ratios.

Increments in pull-out peak load of redesigned RPC mixtures after autoclave curing compared to the 28-day water curing were 41 %, 43 %, 30 %, and 19 % for mixtures with 0.6, 0.5, 0.4, 0.3, and 0.2 W/B ratios.

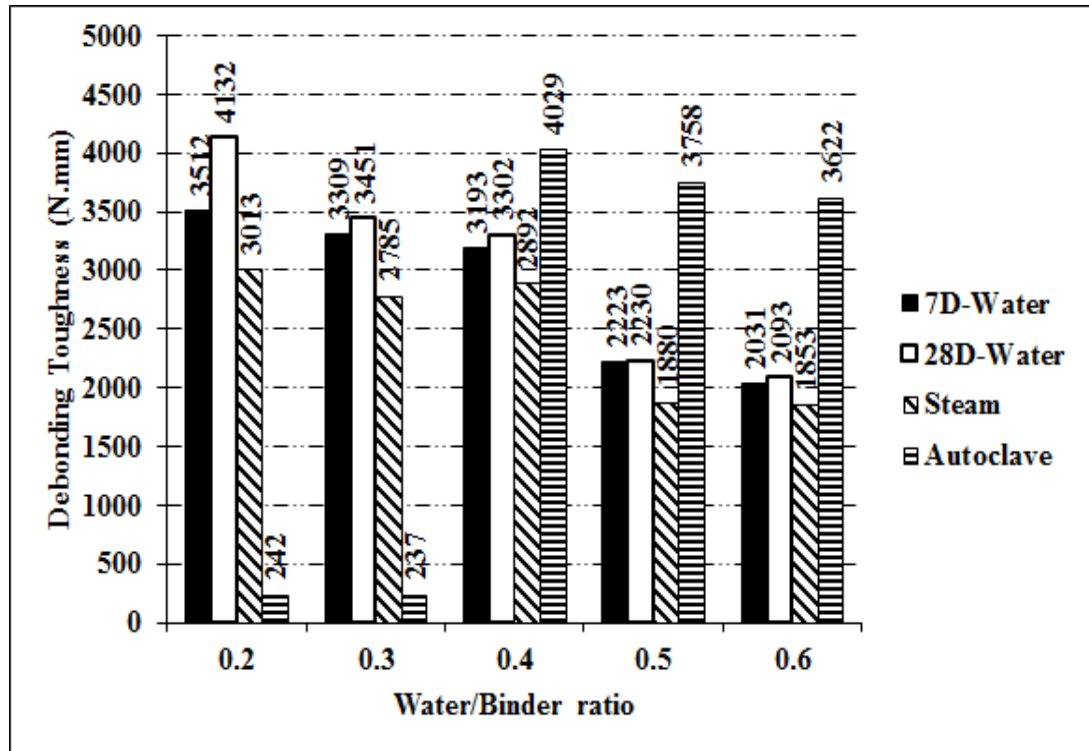


Figure 4.48 Debonding toughness values of redesigned RPC mixtures in various W/B ratios.

The Pull-out load–displacement curves of redesigned RPC mixtures reinforced by 2% micro fiber (RF) for 7 and 28 days water curing are presented in Figures 4.49 and 4.50, respectively. As shown in figures the pull-out behavior of RF mixture is similar to RPC mixture. The pull-out peak load and debonding toughness were increased as W/B ratio decreased. On the other hand, the pull-out behavior of specimens was improved at 28-day water curing compared to the 7-day cured once.

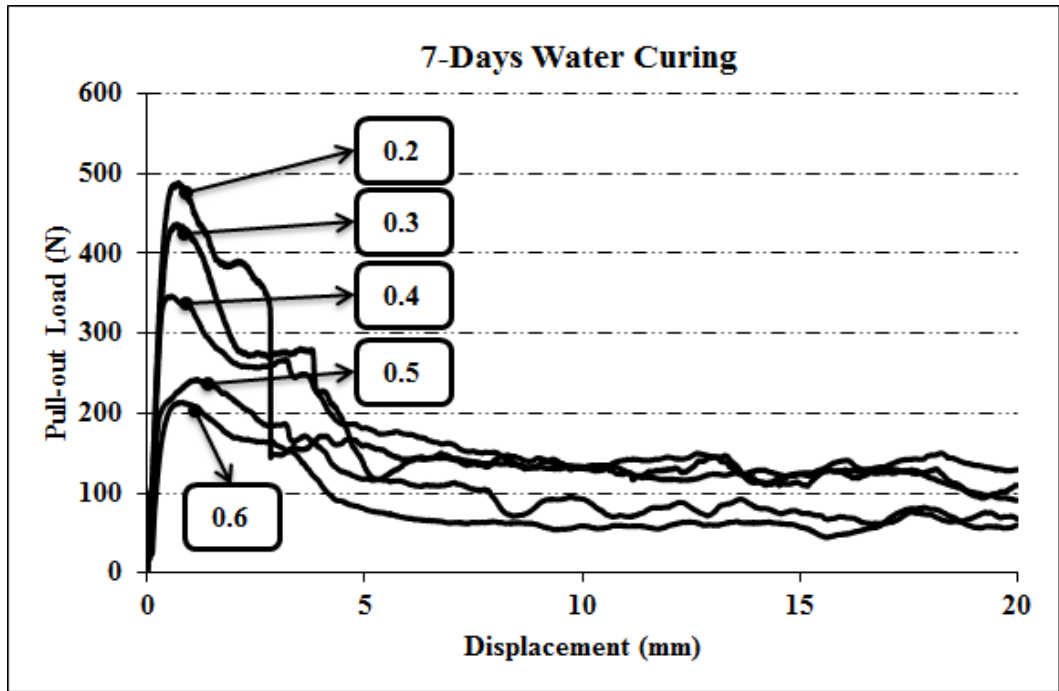


Figure 4.49 Pull-out load–displacement relationships of fiber reinforced redesigned RPC mixtures in various W/B ratios (7 days water curing).

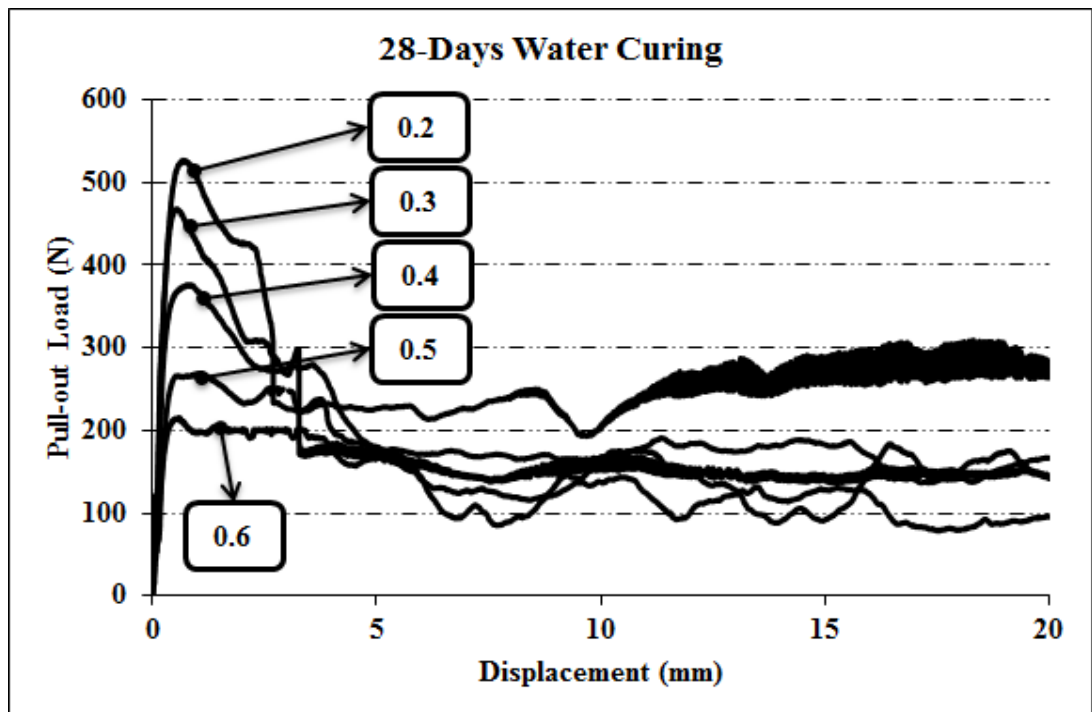


Figure 4.50 Pull-out load–displacement relationship of fiber reinforced redesigned RPC mixtures in various W/B ratios (28 days water curing).

The pull-out peak load and debonding toughness of RPC mixtures (R) and fiber reinforced RPC mixtures (RF) at 7 and 28 days water curing are illustrated in Figures 4.51 and 4.52. As can be seen from figures there is not major difference between pull-out behavior of R and RF mixtures. However it seems that reinforcement of matrix by steel micro fiber has improved somewhat both peak load and debonding toughness. It seems that the properties of matrix phase (W/B ratio) are more important.

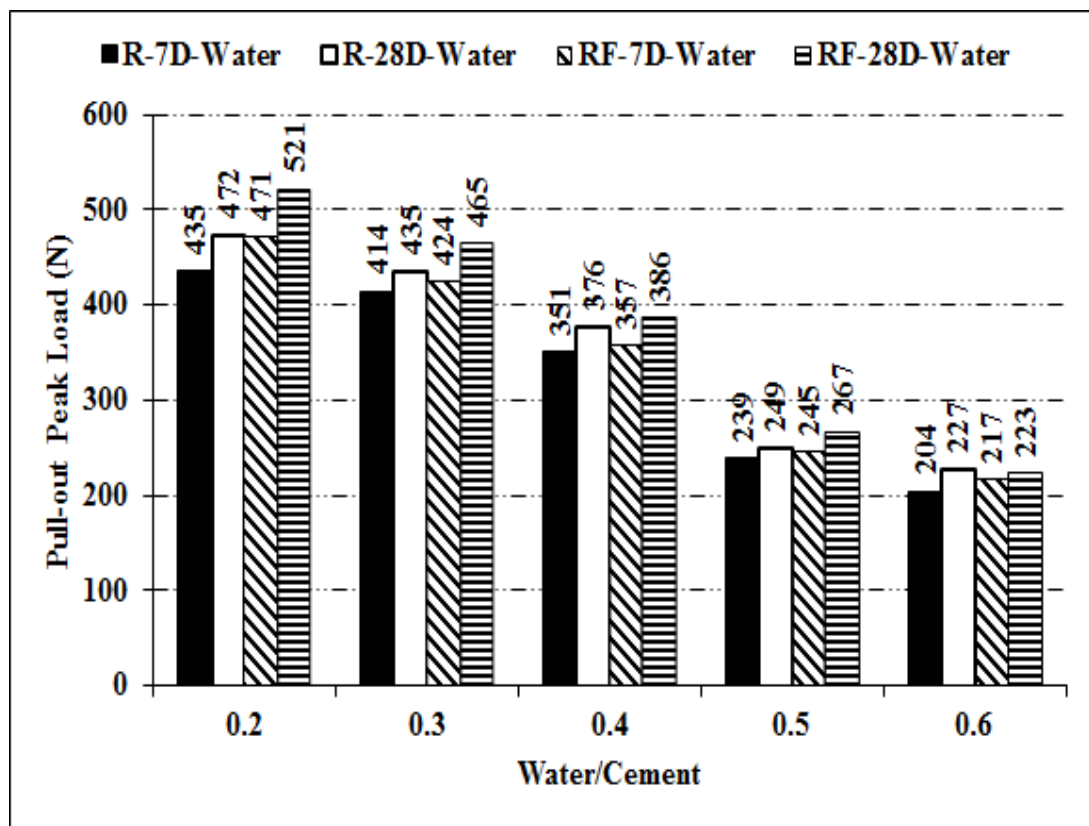


Figure 4.51 Pull-out peak load of RPC mixtures (R) and fiber reinforced RPC mixtures (RF) at 7 and 28 days water curing.

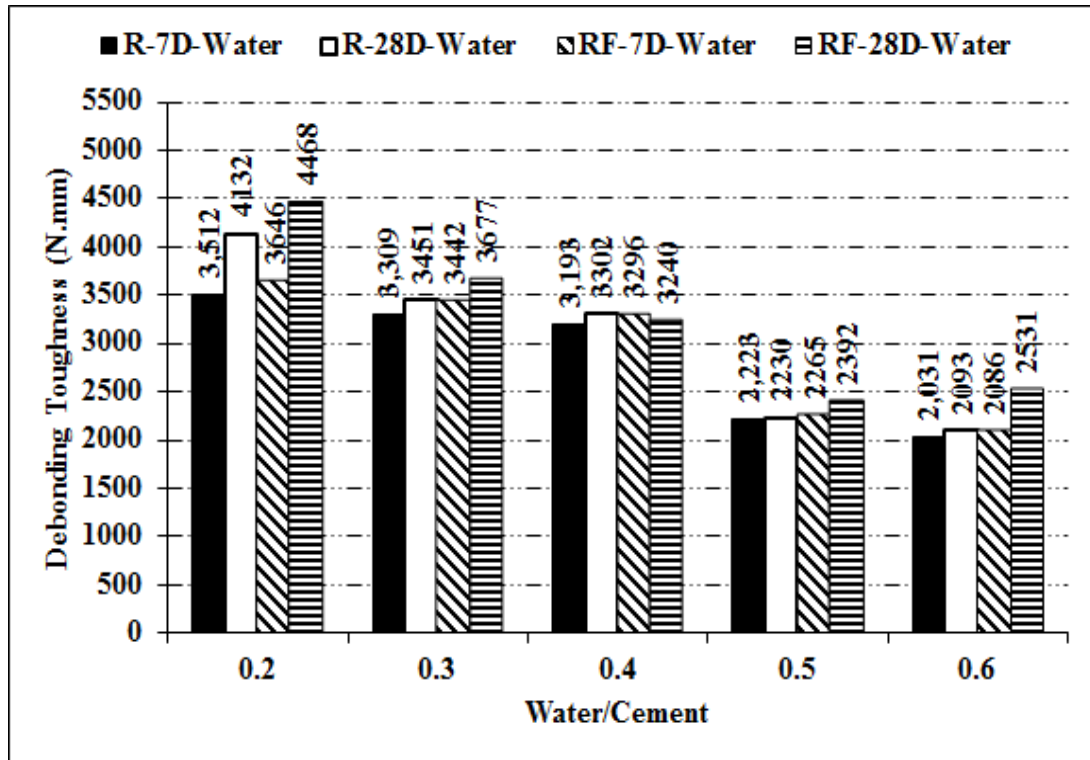


Figure 4.52 Pull-out debonding toughness of RPC mixtures (R) and fiber reinforced RPC mixtures (RF) at 7 and 28 days water curing.

4.1.4 Microstructure Investigation

The microstructural investigation was carried out on some selected mixtures by using a JEOL JSM 6060 electron microscope (SEM) at 10 kV.

Reaching to the 28-day strength in a short time is possible by autoclave curing as a result of high temperatures which increases the rate of reactions of ingredients. On the other hand, the chemistry of hydration products is changed by increasing temperature (Neville, 1995). In case of absence of SiO_2 source, crystalline α -dicalcium SiO_2 hydrate, $\text{Ca}_2(\text{HSiO}_4) \cdot (-\text{OH})$ forms instead of a usual amorphous C-S-H phase which cause strength loss in matrix (Odler, 2004). This behavior was observed in ordinary mortar mixtures which their mechanical strength decreased strongly. In the presence SiO_2 components such as finely ground quartz (quartz powder) or silica fume in mix design of mixture, a pozzolanic reaction takes place in

autoclave curing, yielding crystalline 1.1 nm tobermorite (C5S6H5). This behavior leads to increase in mechanical strength and improving the bond strength.

Figures 4.53 and 4.54 show the SEM images of the steel-fiber matrix interface of RPC mixture after autoclave curing. It can be seen from figures that the tobermorite gel filled throughout the fiber-matrix interface after autoclave curing. This congestion of the hydration products in the fiber-matrix interface increased the bond strength of RPC (0.2 W/B ratio) mixture significantly.

To identify the composition of observed tobermorite gel congested throughout the fiber matrix interface, energy dispersive spectrometry (EDS) analyses were also attempted. As can be seen from Figure 4.55 the Ca/SiO₂ ratio of these products is 0.88.

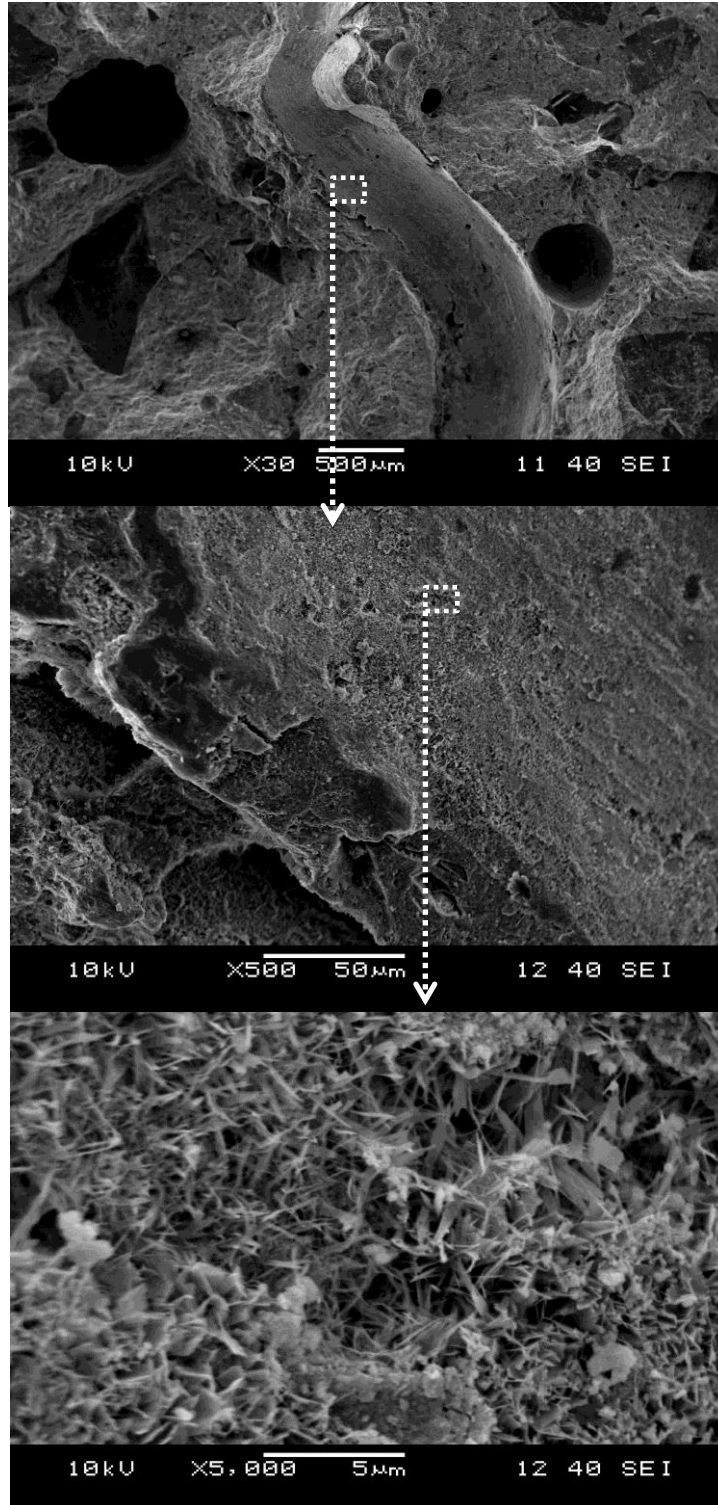


Figure 4.53 SEM images of fiber-matrix interface of RPC (0.2 W/B ratio) mixture after autoclave curing.

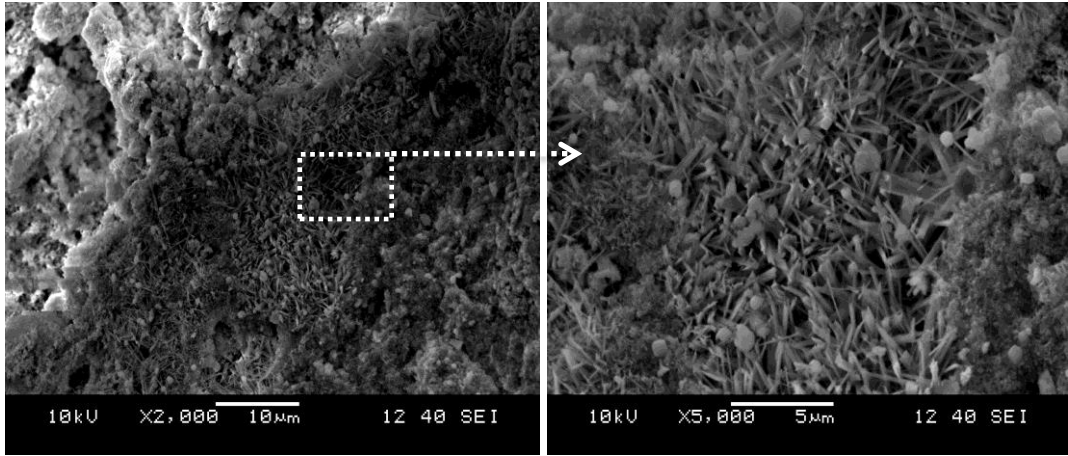


Figure 4.54 SEM images of fiber-matrix interface of RPC (0.2 W/B ratio) mixture after autoclave curing.

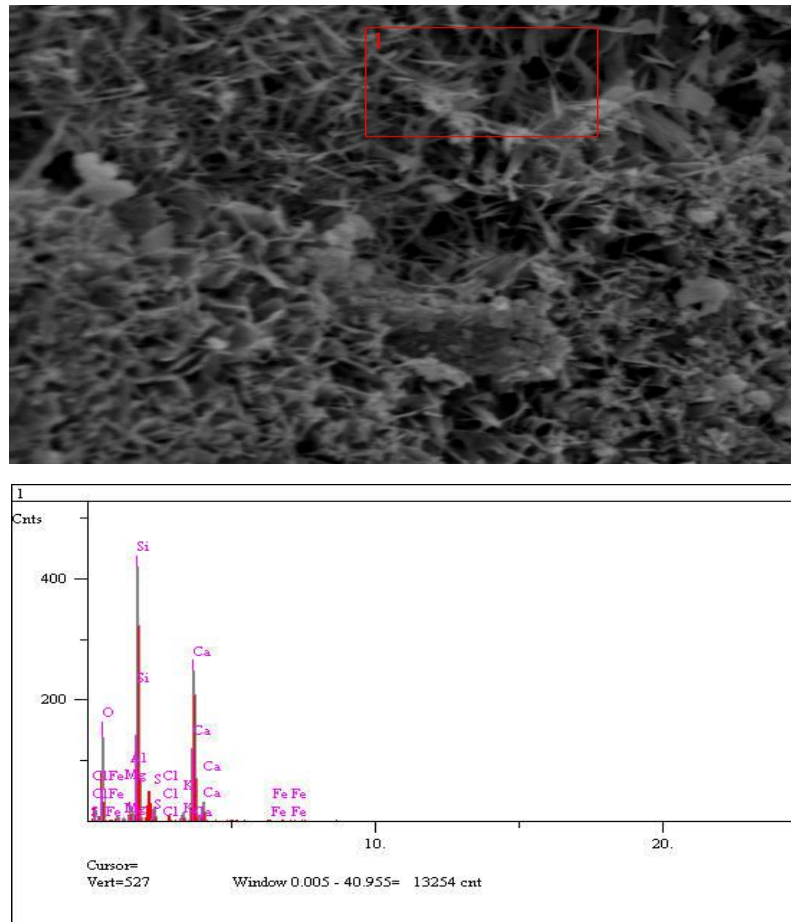


Figure 4.55 EDS analysis of tobermorite gel observed in fiber-matrix interface of RPC (0.2 W/B ratio) mixture after autoclave curing.

The microstructure analysis shows that the hydration product congestion phenomenon is also valid in case of higher W/B ratio. Figures 4.56 and 4.57 show SEM images of fiber-matrix interface of redesigned RPC mixture with 0.3 W/B ratio after autoclave curing. It can be seen from figures that similar to previous mixture the tobermorite gel with fibrous morphology filled throughout the interface. Congestion of these products increased the bond strength significantly similar to the previous mixture. Similar result was also observed in mixtures with 0.4 W/B ratio (Figure 4.58).

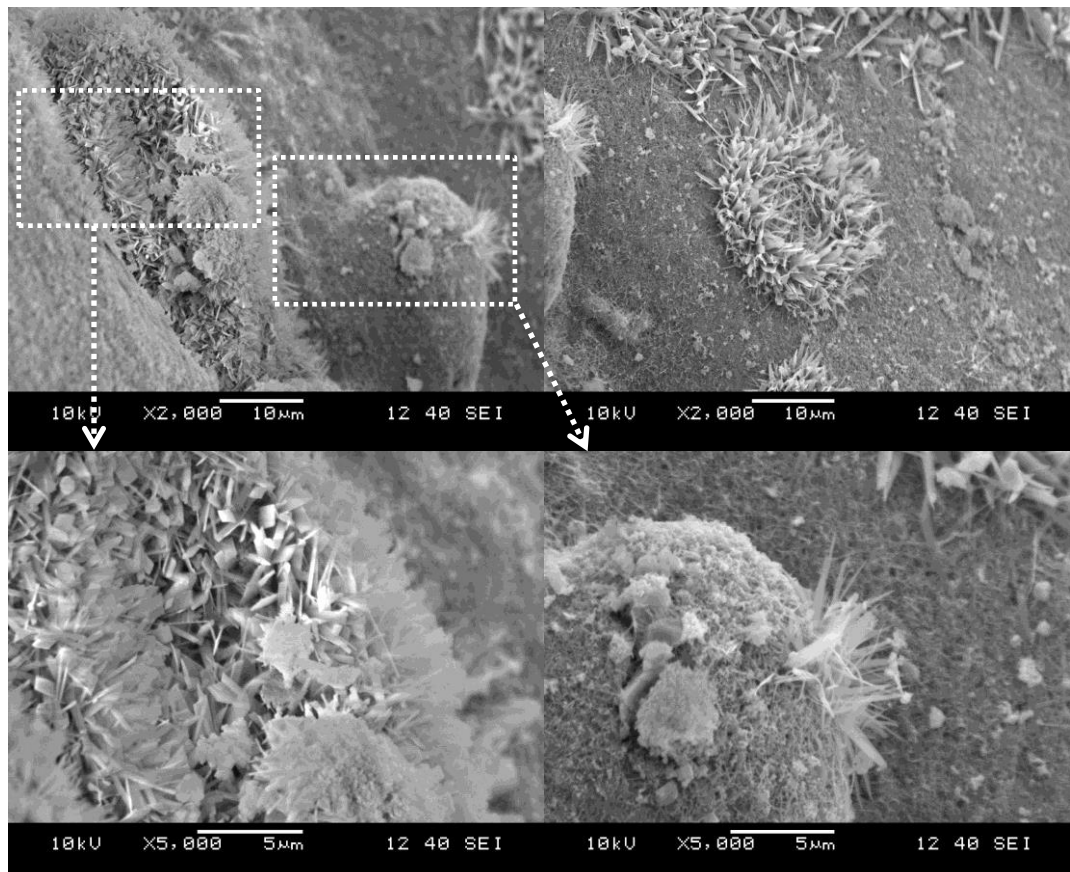


Figure 4.56 SEM images of fiber-matrix interface of redesigned RPC (0.3 W/B ratio) mixture after autoclave curing.

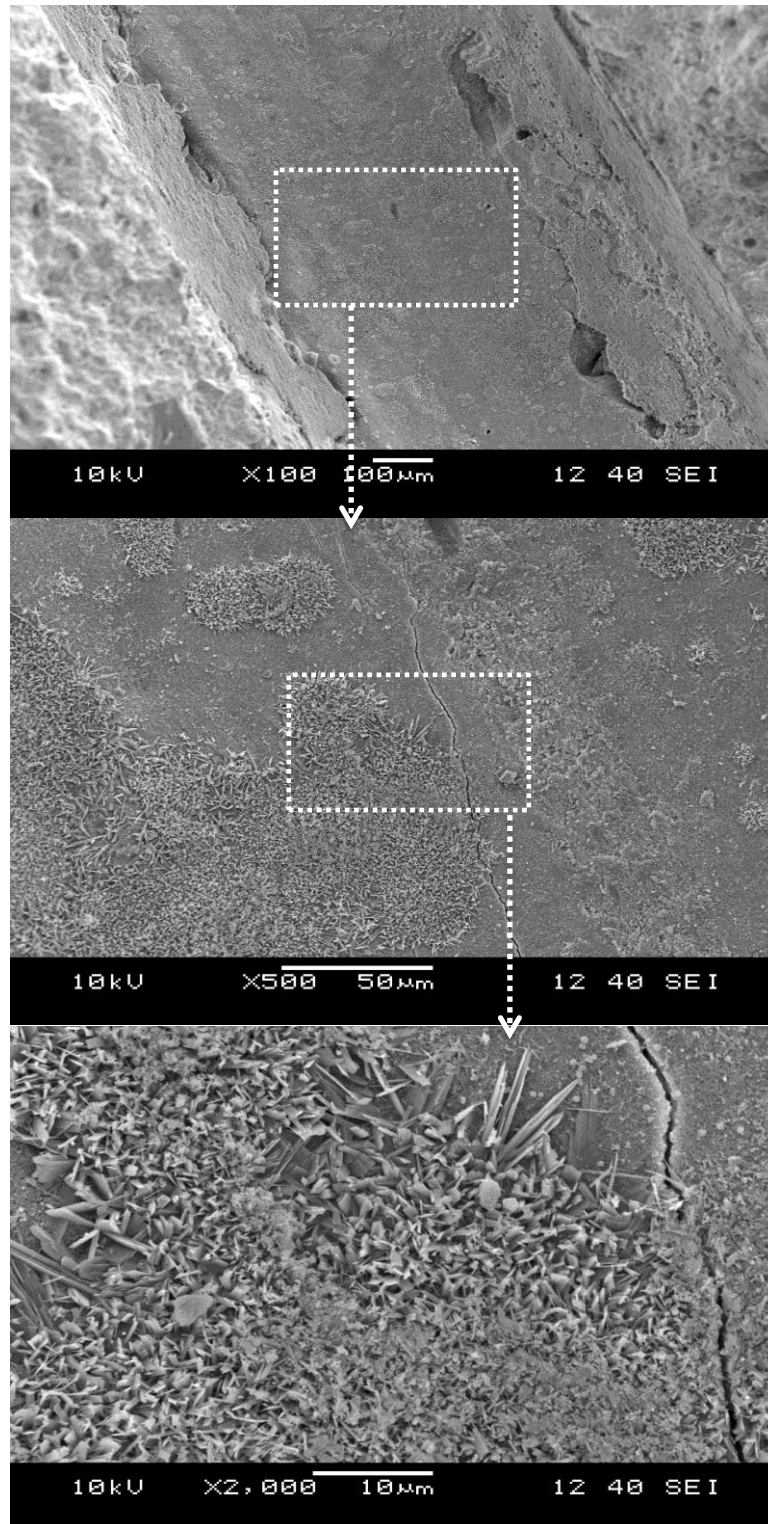


Figure 4.57 SEM images of fiber-matrix interface of redesigned RPC (0.3 W/B ratio) mixture after autoclave curing.

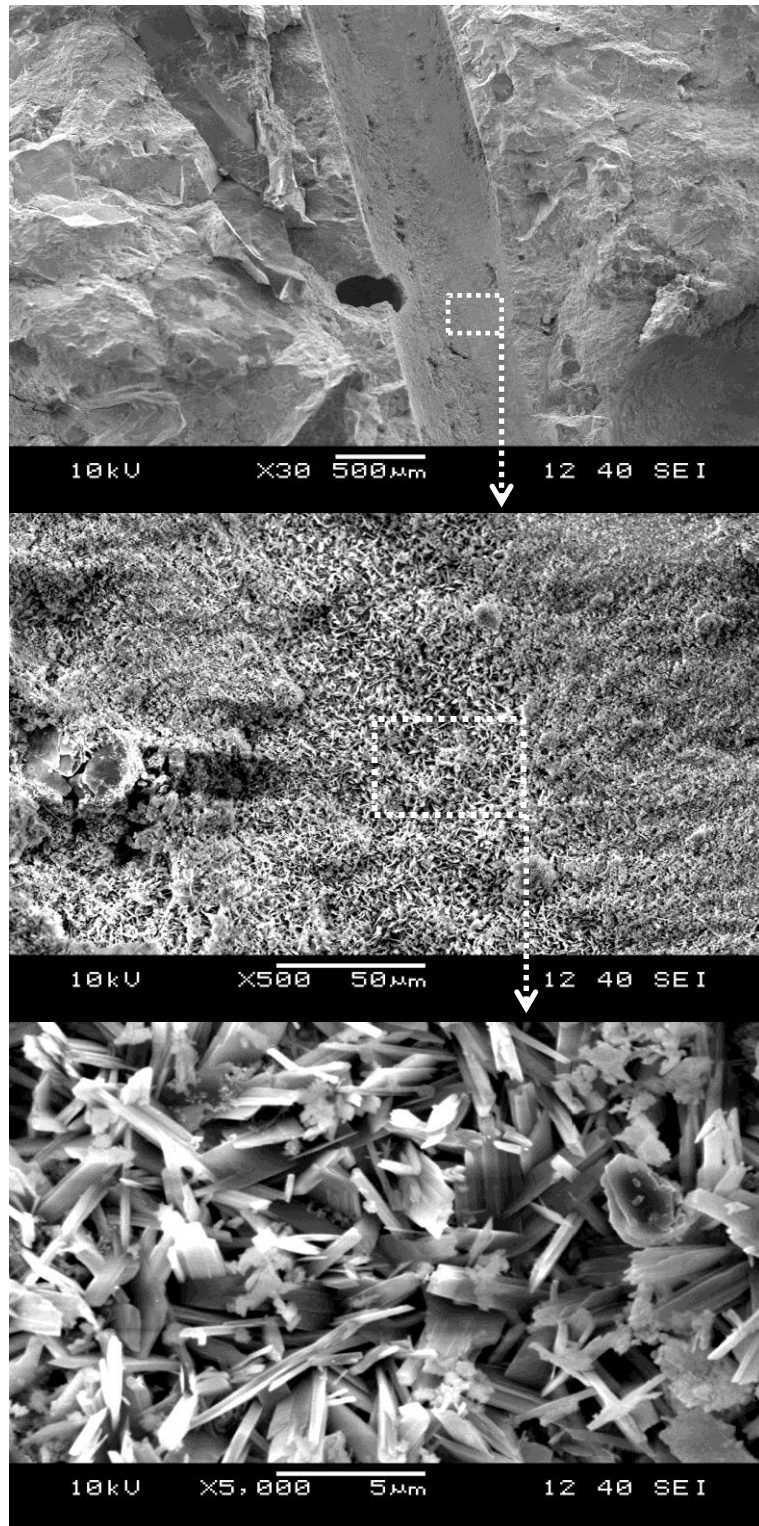


Figure 4.58 SEM images of fiber-matrix interface of redesigned RPC (0.4 W/B ratio) mixture after autoclave curing.

4.2 The Effect of Chemical Admixtures

4.2.1 Fresh State

First of all it would be better to discuss the effect of chemical admixtures used in this study on fresh state of OM and RPC mixtures. The flow table values of all mixtures were fixed in 150 ± 10 mm and 220 ± 10 mm for OM and RPC mixtures, respectively.

Generally, polymer based admixtures improve the workability of the cement based composites as a result of their air entraining and friction reducing effect (Ohama, 1997). As can be seen from Figure 4.59 the polymer latex emulsions group admixtures reduced the superplasticizer dosage between 16 – 34 % depending on polymer/cement dosage, polymer type, and matrix type (OM or RPC). It must be noted that both corrosion inhibitor and waterproofing mixtures didn't affect the superplasticizer dosage. The superplasticizer dosage reduction effect of acrylic based polymers was more than SBR one. This behavior can be explained by more air entraining effect of acrylic based polymers. Additionally, the superplasticizer dosage reduction effect of all polymers was much more visible in OM mixtures than RPC.

The polymer containing mixtures was also very sticky. This behavior is one of the positive effects of polymers in the case of using them in repair works.

As mentioned later the chemical admixtures names and dosages were abbreviated as follow:

- 1- 5% of SBR1 = A1
- 2- 15% of SBR1 = A2
- 3- 5% of SBR2 = B1
- 4- 15% of SBR2 = B2
- 5- 1.5% of ADP1 = R1
- 6- 5% of ADP1 = R2

7- 1.5% of ADP2 = L1

8- 5% of ADP2 = L2

9- 3 % WP = SI

10- CNI = F

Two control mixtures for each OM and RPC were prepared as follow:

KN: Control mixture which was cured for 28 days in $20\pm 2^{\circ}\text{C}$ water (Normal curing). This control mixture was prepared in order to compare with corrosion inhibitor containing mixture.

KM: Control mixture which was cured for 7 days in $20\pm 2^{\circ}\text{C}$ and 21 reminder days in air (Mix curing). This control mixture was prepared in order to compare with polymer and WP containing mixtures.

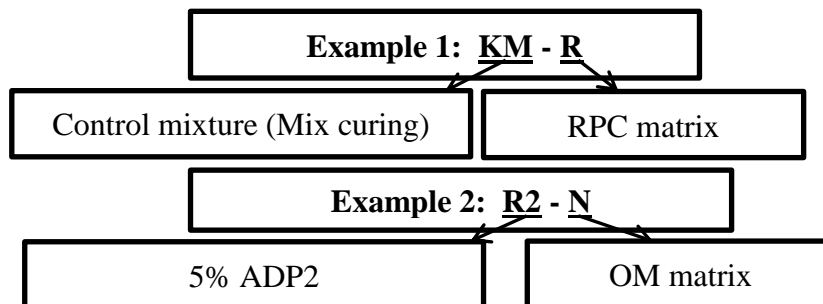
The matrixes were also abbreviated as follow:

1- Ordinary mortar = N

2- RPC = R

The mixtures in second section which were prepared to evaluate the effect of chemical admixtures were also abbreviated as follow:

- Chemical admixtures name and dosage – matrix type (OM or RPC)



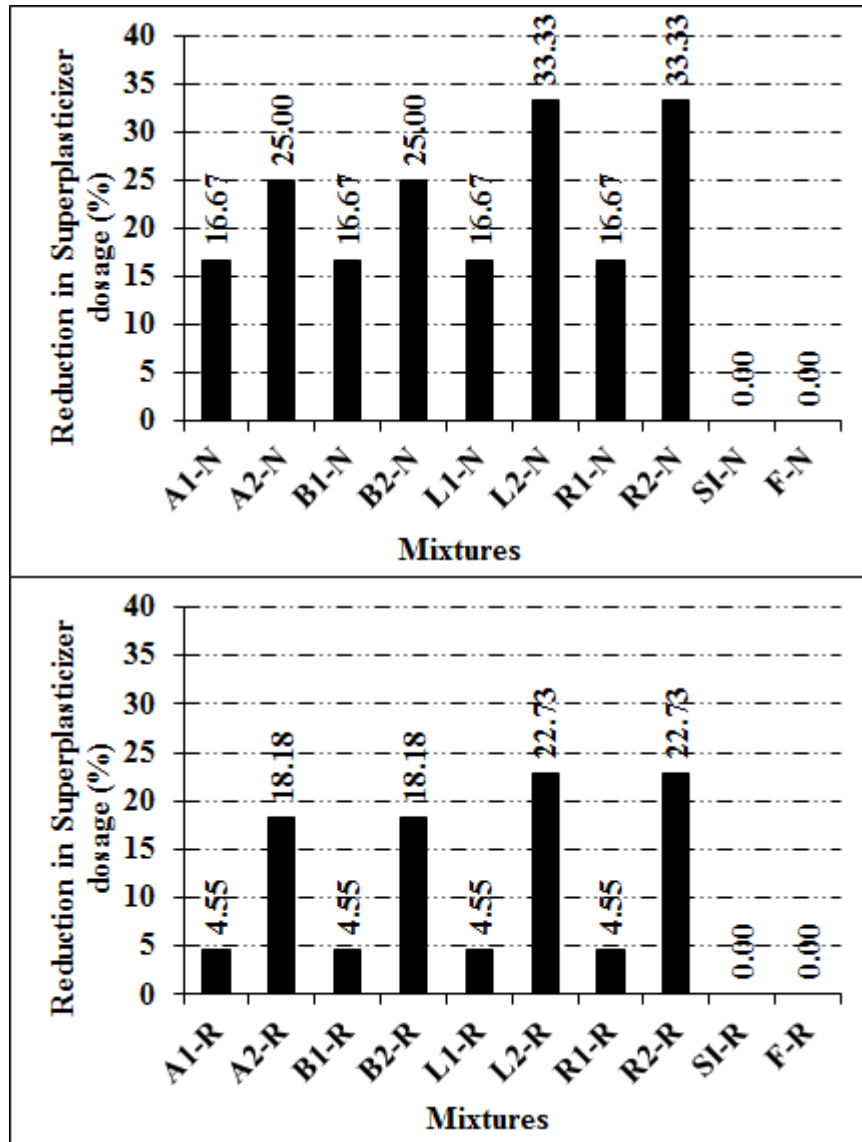


Figure 4.59 The percentage of reduction in superplasticizer dosage for both OM and RPC mixtures.

The unit weight of fresh OM mixtures is presented 4.60. Because of very low air entraining effect of the corrosion inhibitor (F) in this used dosage; its unit weight didn't changed compared to the control mixture. However, as a result of air entraining effect of polymers, all of them have decreased the unit weight of fresh OM mixtures.

The fresh unit weight of OM mixtures with 5% SBR based polymers (A1 and B1) was much more than 15% SBR containing mixtures (A2 and B2). However, ADP

based polymers reduced the unit weight in both dosages (1.5% and 5% of cement content). Also, the SI waterproofing admixture reduced 163 kg/m^3 of the unit weight.

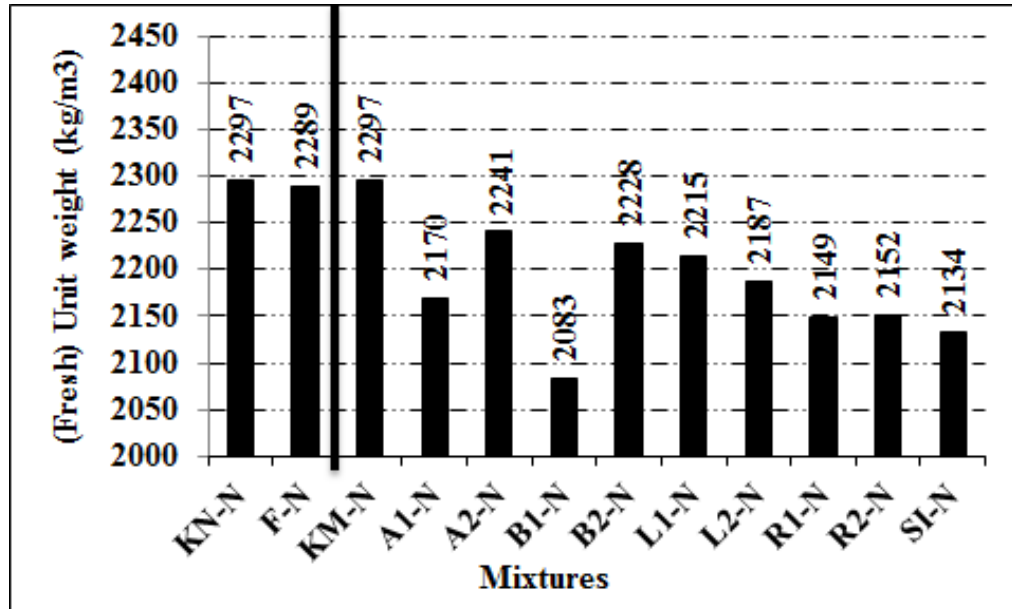


Figure 4.60 Unit weight of fresh OM mixtures.

The unit weight of fresh RPC mixtures is presented 4.61. As can be seen from figure the fresh unit weight of SBR polymer containing mixtures was reduced, while it is just opposite in case of ADP polymers and corrosion inhibitor containing mixtures. These behaviors are not valid for SI mixture and its unit weight didn't change significantly.

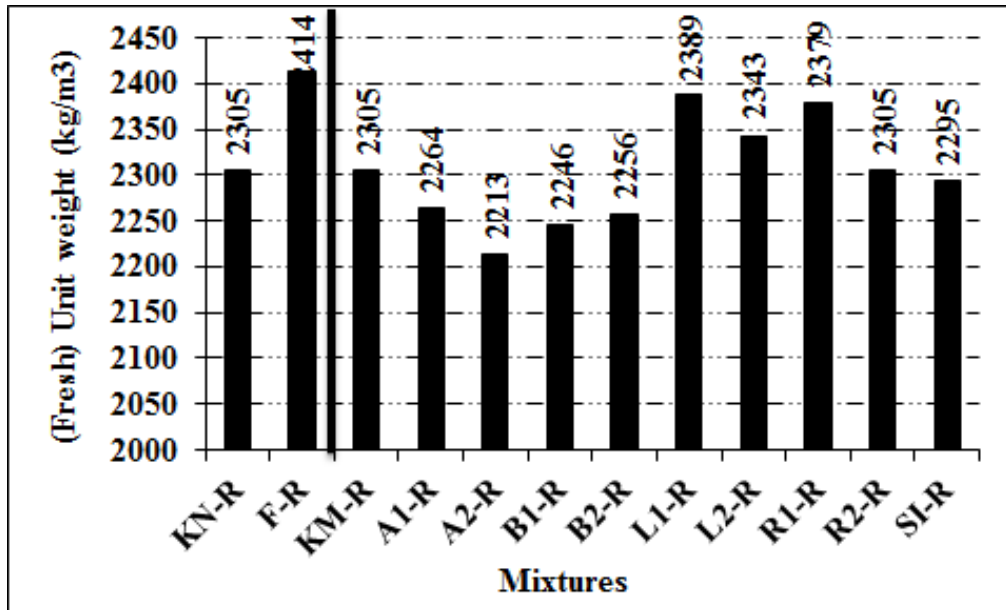


Figure 4.61 Unit weight of fresh RPC mixtures.

4.2.2 Mechanical Properties

The effect of chemical admixtures on compressive and flexural strength of OM mixtures are presented in Figure 4.62. It can be seen from figure that the compressive strength of OM mixture was not affected significantly by using corrosion inhibitor, while its flexural strength decreased by approximately 50% compared to the control (KN) mixture. Furthermore, both compressive and flexural strength of SI mixture was reduced as result of excessive air entraining effect of this waterproofing admixture in OM mixture.

The compressive strength of SBR polymer containing OM mixtures were also decreased as a result of air entraining effect of them, while there is a negligible increment in flexural strength of A mixture in both dosage (5% and 15% of cement content). This behavior is accordance with literature. Generally, the compressive strength of cement based composites can be decreased as a result of air entraining effect of polymer based admixtures (Çolak, 2005; Pascal, Alliche, & Pilvin, 2004; Pei, Hyung, Ango, & Soh, 1998), while they can have a positive effect on flexural strength of concrete and mortar (Ohama, 1998, 1997; Pascal, Alliche, & Pilvin, 2004). This positive effect of polymers on flexural strength is explained in literature

by the better bond strength between aggregate and matrix as a result of film formation.

The compressive strength of acrylic based polymers containing OM mixtures was not affected significantly. However, the flexural strength decreased by using acrylic based polymers.

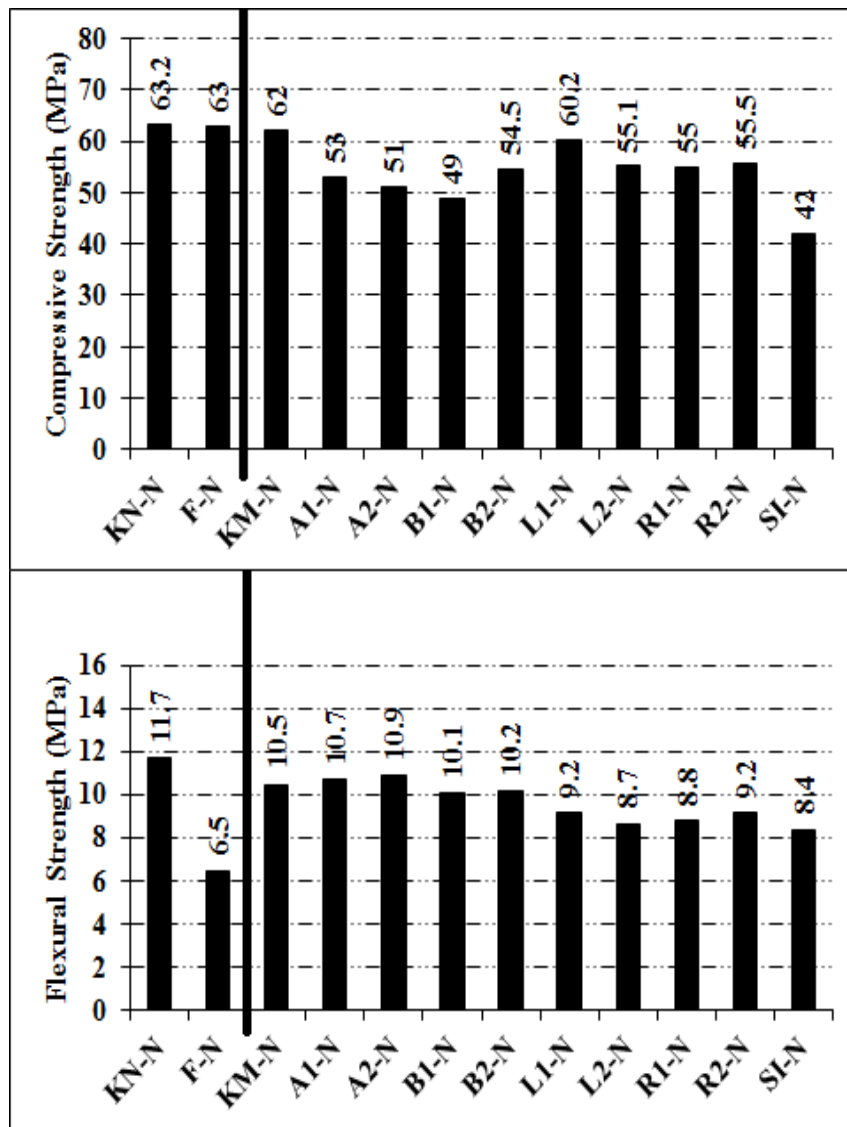


Figure 4.62 Mechanical strength of chemical admixture containing OM mixtures.

As can be seen from Figure 4.63 the mechanical strength of RPC mixture was not affected significantly by using corrosion inhibitor and waterproofing admixtures. On the other hand the mechanical strength of RPC was decreased remarkably in case of using SBR polymer admixtures.

However, incorporating 1.5 % acrylic based polymers increased the compressive strength of RPC, the flexural strength decreased significantly.

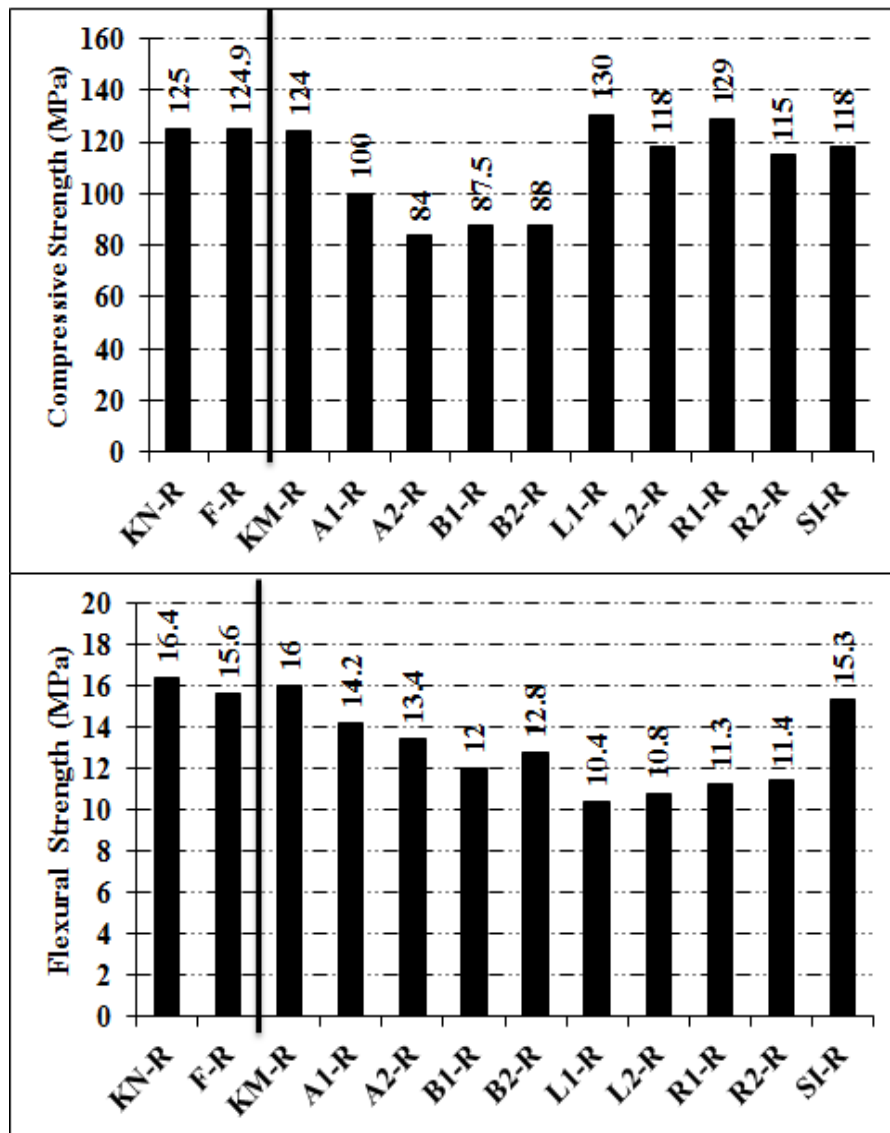


Figure 4.63 Mechanical strength of chemical admixture containing RPC mixtures.

4.2.3 Chloride Penetration

The rapid chloride ion penetration test (ASTM C 1202) results of all mixtures are presented in Figure 4.64. The chloride penetration value of all OM mixtures are above the 4000 coulombs which indicates all OM mixtures have high chloride penetrability. However, it can be indicated from test result the corrosion inhibitor mixture didn't affect the chloride penetration of OM mixture. ASTM C 1202 recommends the use of the qualitative terms (Table 4.1).

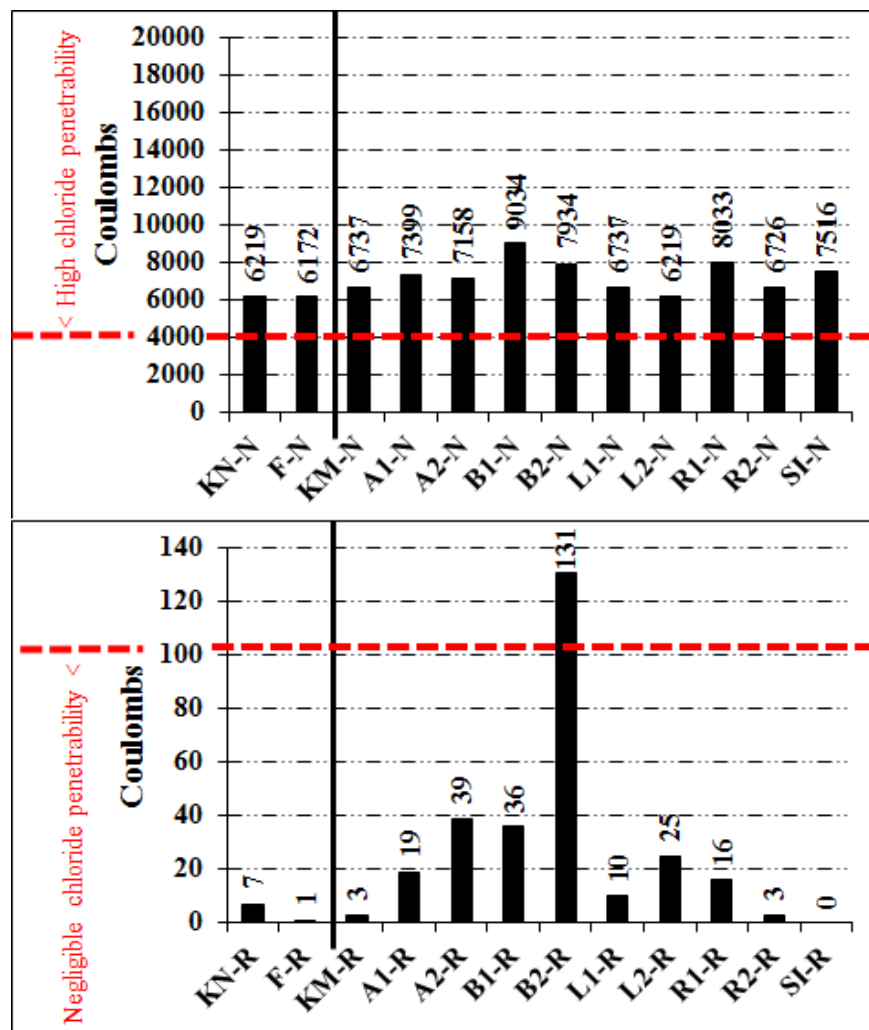


Figure 4.64 Rapid chloride ion penetration test result.

Table 4.1 Chloride ion penetrability based on charge passed (ASTM C 1202).

Charge Passed (coulombs)	Chloride Ion Penetrability
> 4,000	High
2,000 - 4,000	Moderate
1,000 - 2,000	Low
100 - 1,000	Very Low
< 100	Negligible

Furthermore, chloride penetration value of both SBR polymers containing mixtures is more than OM control mixture, while this behavior is opposite in case of acrylic based polymers. The chloride penetration value of SI mixture was also 779 coulombs higher than OM control mixture. However, these decrement or increments values cannot be a reasonable finding in order to comparing chloride penetrability of OM mixtures.

SBR1 admixture with 15% of cement content dosage increased the chloride penetrability of RPC mixture remarkably. Also, the other SBR admixture increased the chloride penetration value of RPC mixture. However, except the B2 mixture, the chloride penetrability of RPC mixtures is negligible. Although, the chloride penetration values of F and SI mixtures are 1 and 0, but it can't be concluded that they increased or decreased the chloride penetrability of the RPC mixture.

4.2.4 Physical Properties of the Mixtures

Dry bulk density, porosity, water absorption, and capillary water absorption of the mixtures were determined. The dry bulk density values of all mixtures are presented in Figure 4.65.

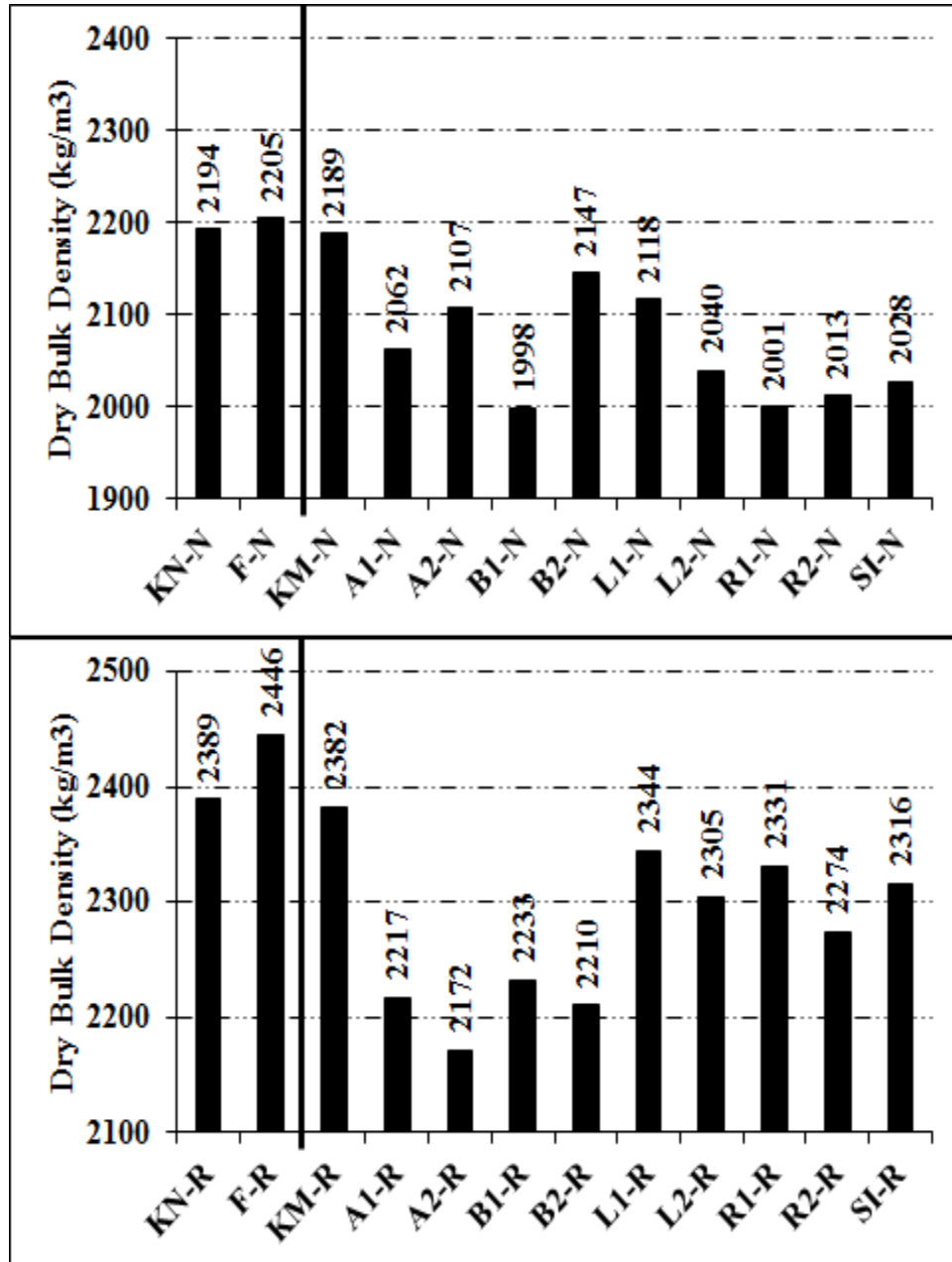


Figure 4.65 Dry bulk density values.

As can be seen from Figure 4.65 the dry bulk density of OM mixture was decreased by using polymers and waterproofing admixtures as a result of air entraining effect and low specific gravity of the solid content of admixtures, while the corrosion inhibitor admixture didn't affect significantly. This decrement in bulk density was also valid in case of RPC matrix. However, corrosion inhibitor admixture increased somewhat the bulk density of RPC.

The porosity of OM mixtures are presented in Figure 4.66. It can be seen from figure that corrosion inhibitor admixture didn't affect the porosity of OM mixture. Furthermore, except B2 mixture the porosity of all mixture is higher than OM control mixture especially acrylic based polymers containing mixtures.

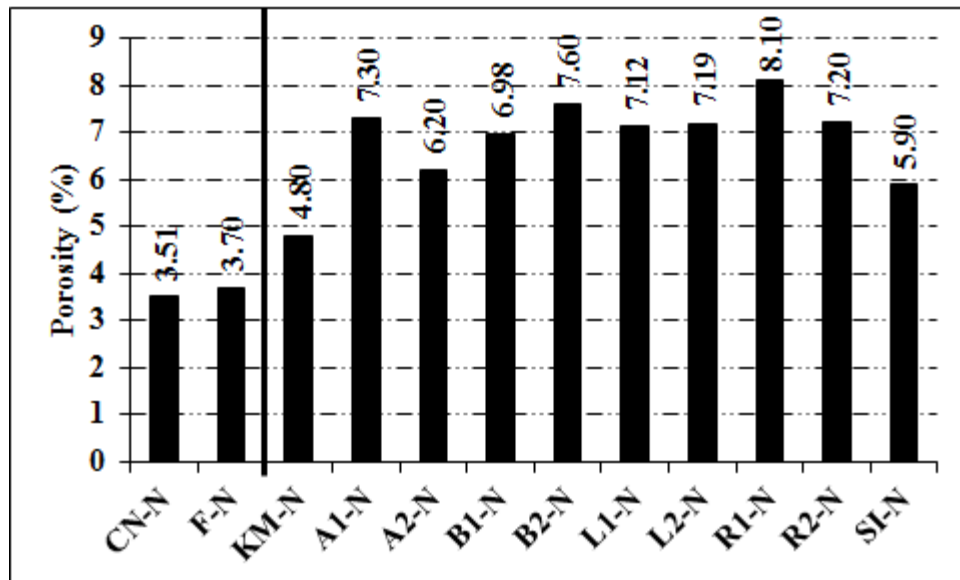


Figure 4.66 Porosity of OM mixtures.

The porosity of RPC mixtures are shown in Figure 4.67. The porosity of F, SI, B1, and L2 is lower than RPC control mixture. However, the porosity of other mixtures is higher than control mixture especially R1, B2, and A1.

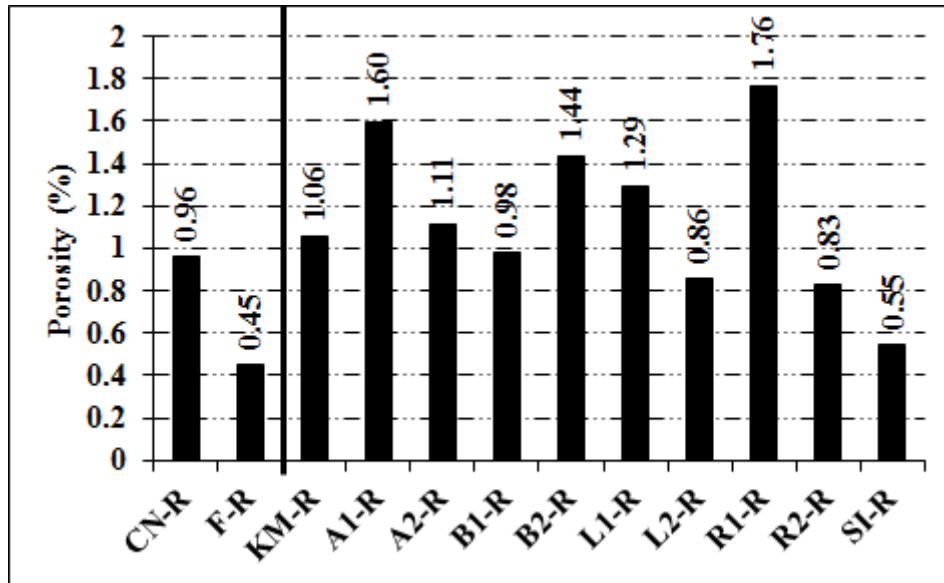


Figure 4.67 Porosity of RPC mixtures.

The water absorption percentage of mixtures is illustrated in Figures 4.68 and 4.69 for OM and RPC mixtures, respectively. As can be seen from figures except corrosion inhibitor, all of admixtures increased the water absorption of OM mixture. However, except A1, A2 (SBR1-5 and 15%), B2 (SBR2-15%), and R1 (ADP2-1.5%) mixtures, water absorption percentage of all mixtures are lower than RPC control mixture.

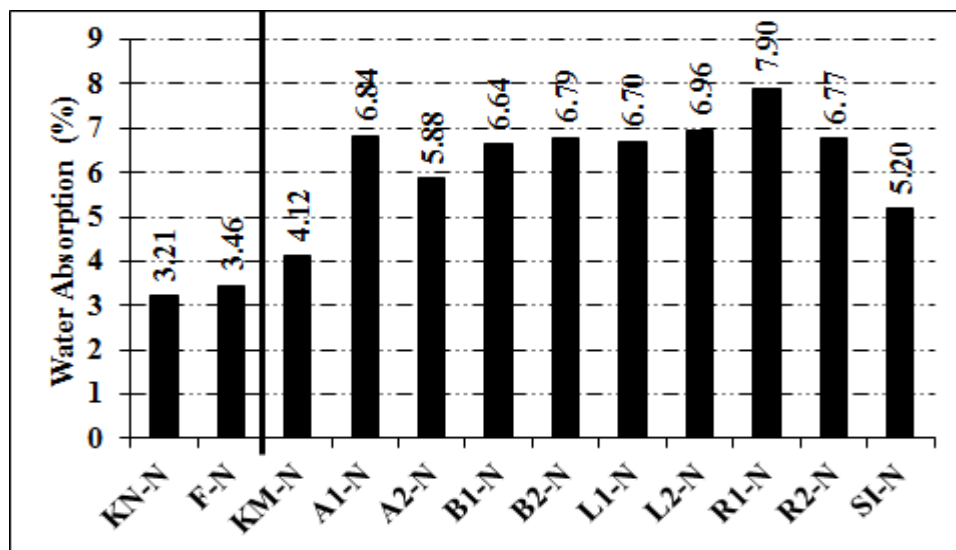


Figure 4.68 Water absorption of OM mixtures.

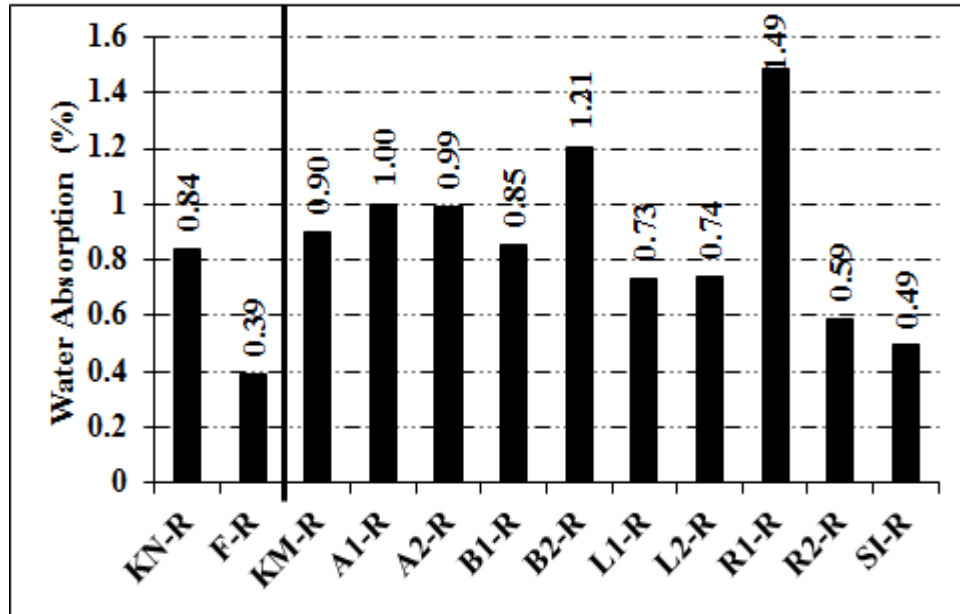


Figure 4.69 Water absorption of RPC mixtures.

Figure 4.70 shows the effect of corrosion inhibitor admixture on capillary water absorption behavior of OM mixture. As can be seen from figure capillary suction of F mixture was higher than OM control mixture. It must be noted that this behavior was opposite at the beginning of the test.

Figure 4.71 and shows the effect of corrosion inhibitor admixture on capillary water absorption behavior of RPC mixture. It can be seen that the corrosion inhibitor admixture reduced remarkably the capillary water absorption of the RPC mixture. Additionally, the capillary suction of the F mixture is zero after first hour of the test until 72 h.

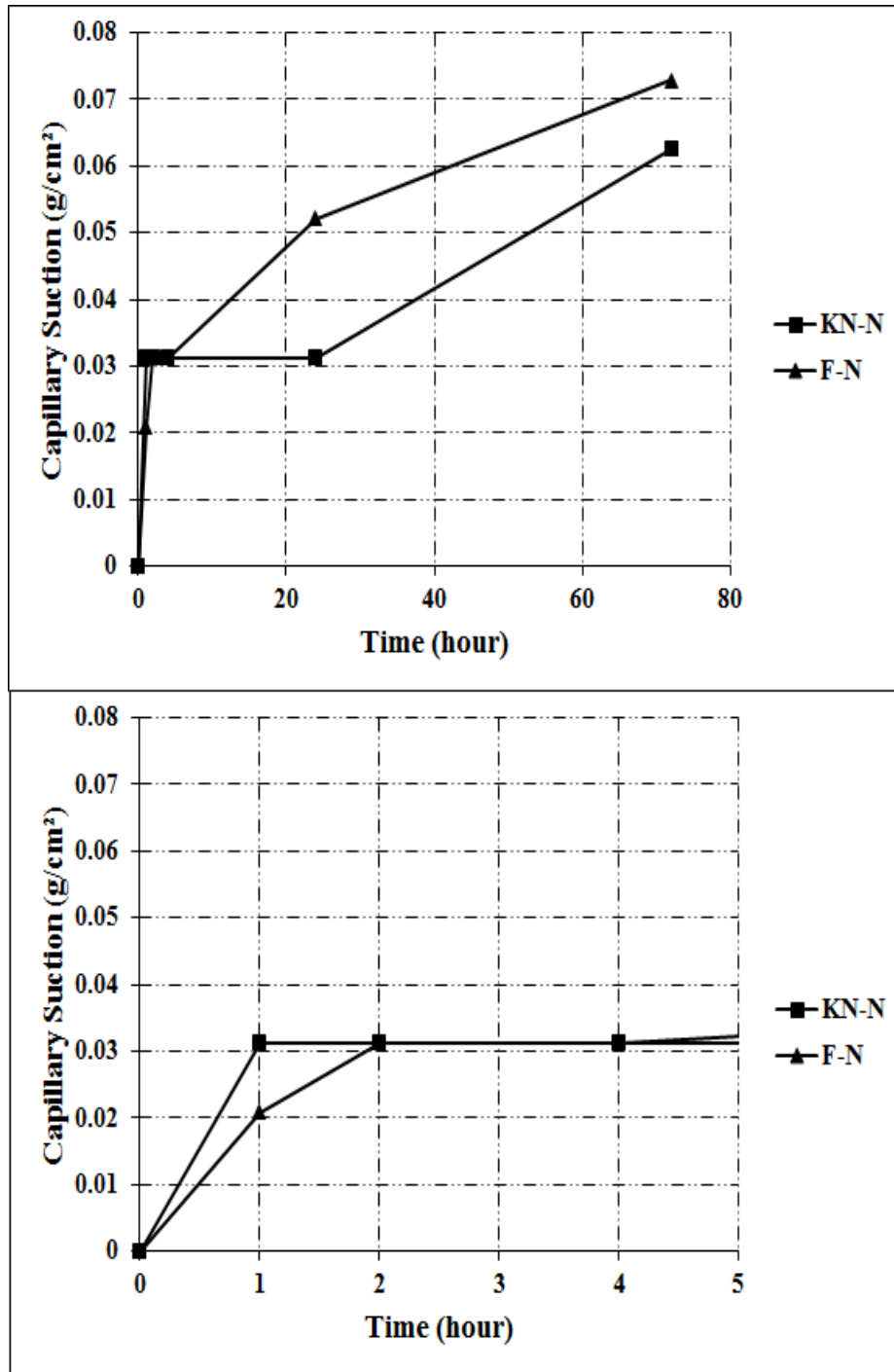


Figure 4.70 Capillary water absorption of F and OM control mixtures.

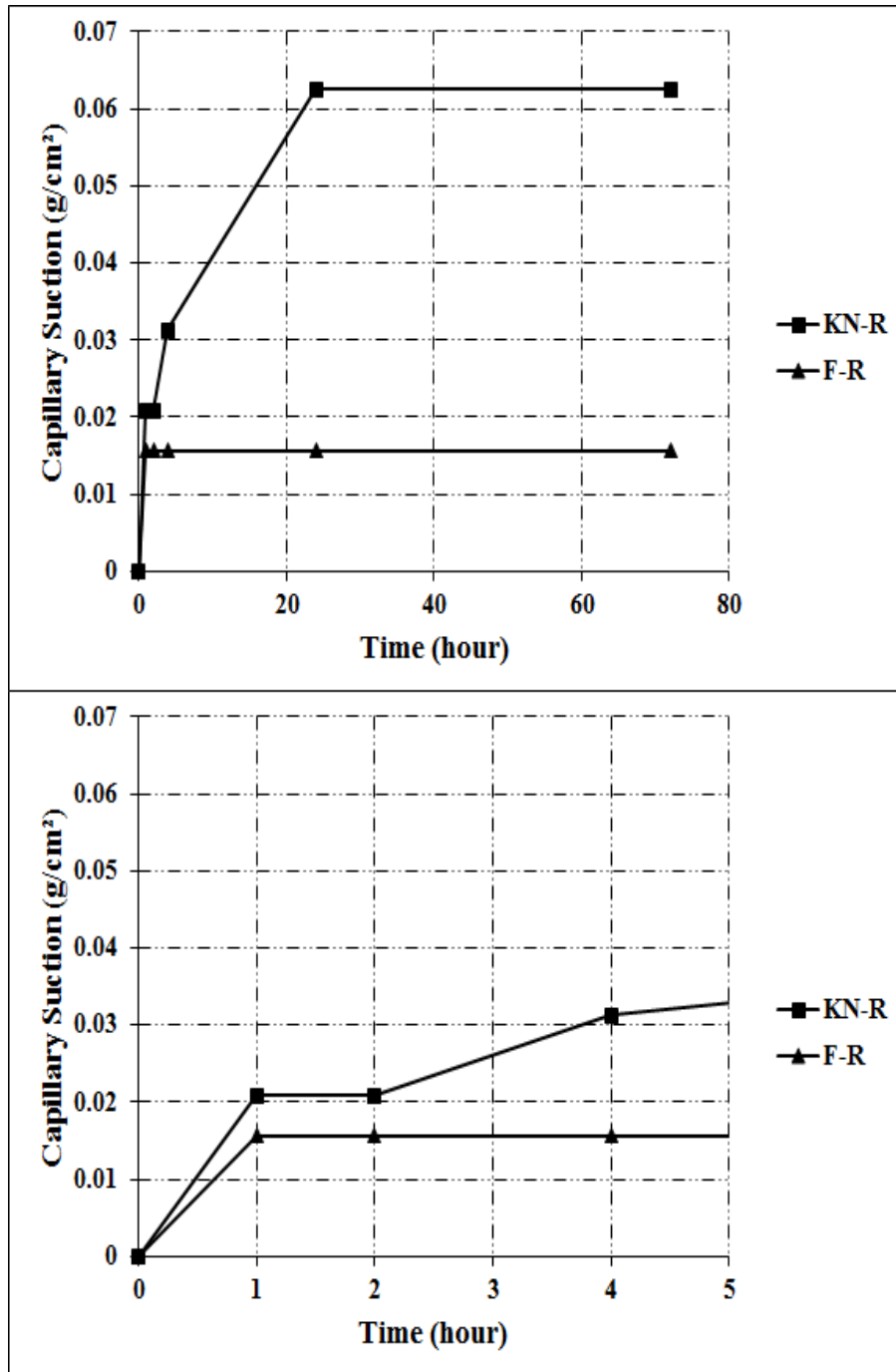


Figure 4.71 Capillary water absorption of F and RPC control mixtures.

As can be seen from Figure 4.72 the waterproofing admixture didn't affect the capillary water absorption behavior of OM mixture in first 5 h, while this behavior is not valid at 24 and 72 hours. The waterproofing admixture increased the capillary water absorption of OM mixture.

As shown in Figure 4.73 waterproofing admixture has a positive effect on capillary water absorption behavior of RPC.

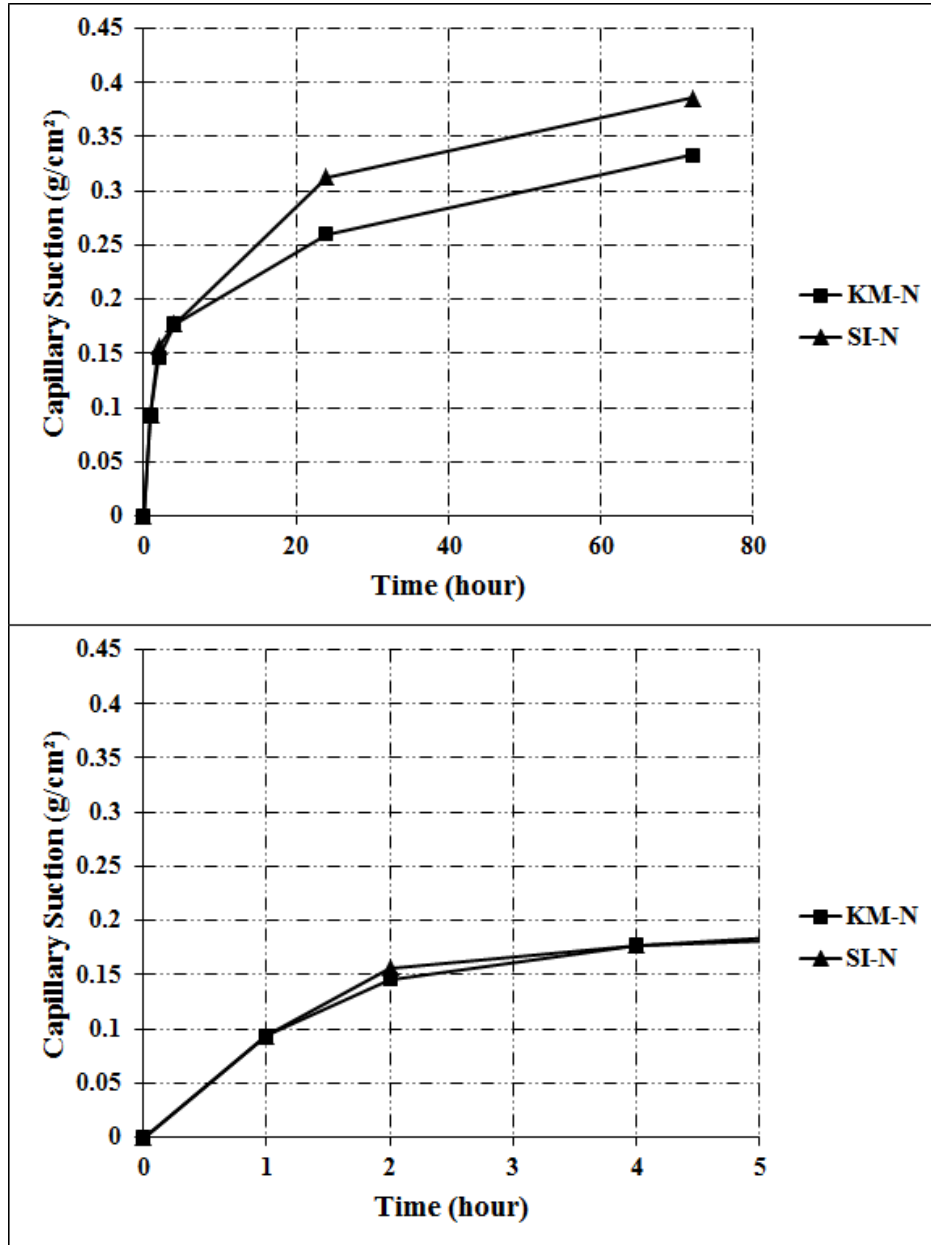


Figure 4.72 Capillary water absorption of SI and OM control mixtures.

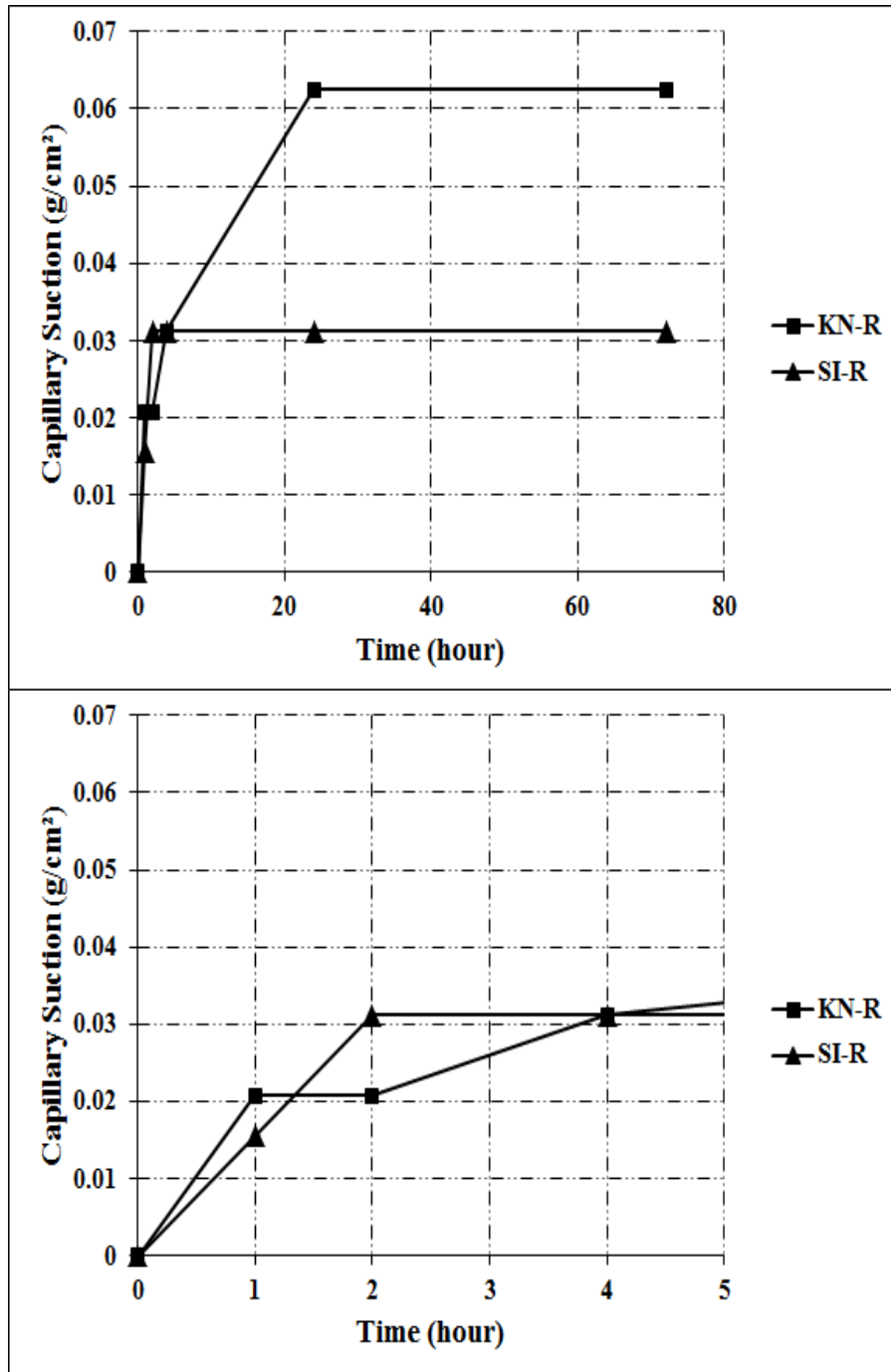


Figure 4.73 Capillary water absorption of SI and RPC control mixtures.

As can be seen from Figure 4.74 the SBR1 admixture with 15% dosage (15% of cement content) reduced the capillary water absorption of OM mixture. However, this behavior is just opposite in case of other mixtures.

It can be seen from Figure 4.75 that the capillary suction of A2 and B1 mixture is lower than RPC mixture at 72 h. However, the SBR1 and SBR2 admixtures which used in A1 (5%) and B2 (15%) increased the capillary water absorption of RPC mixture.

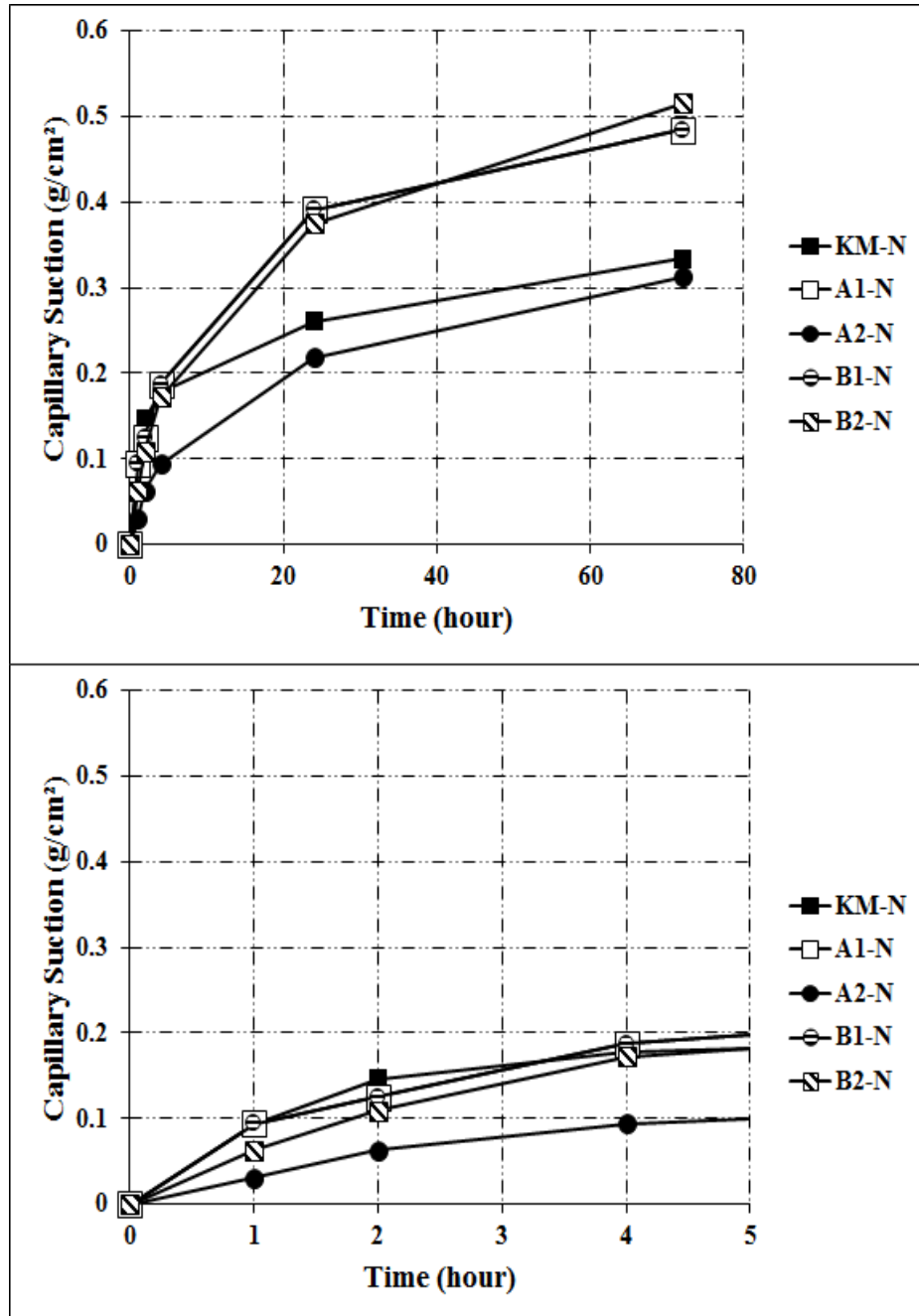


Figure 4.74 Capillary water absorption of SBR containing and OM control mixtures.

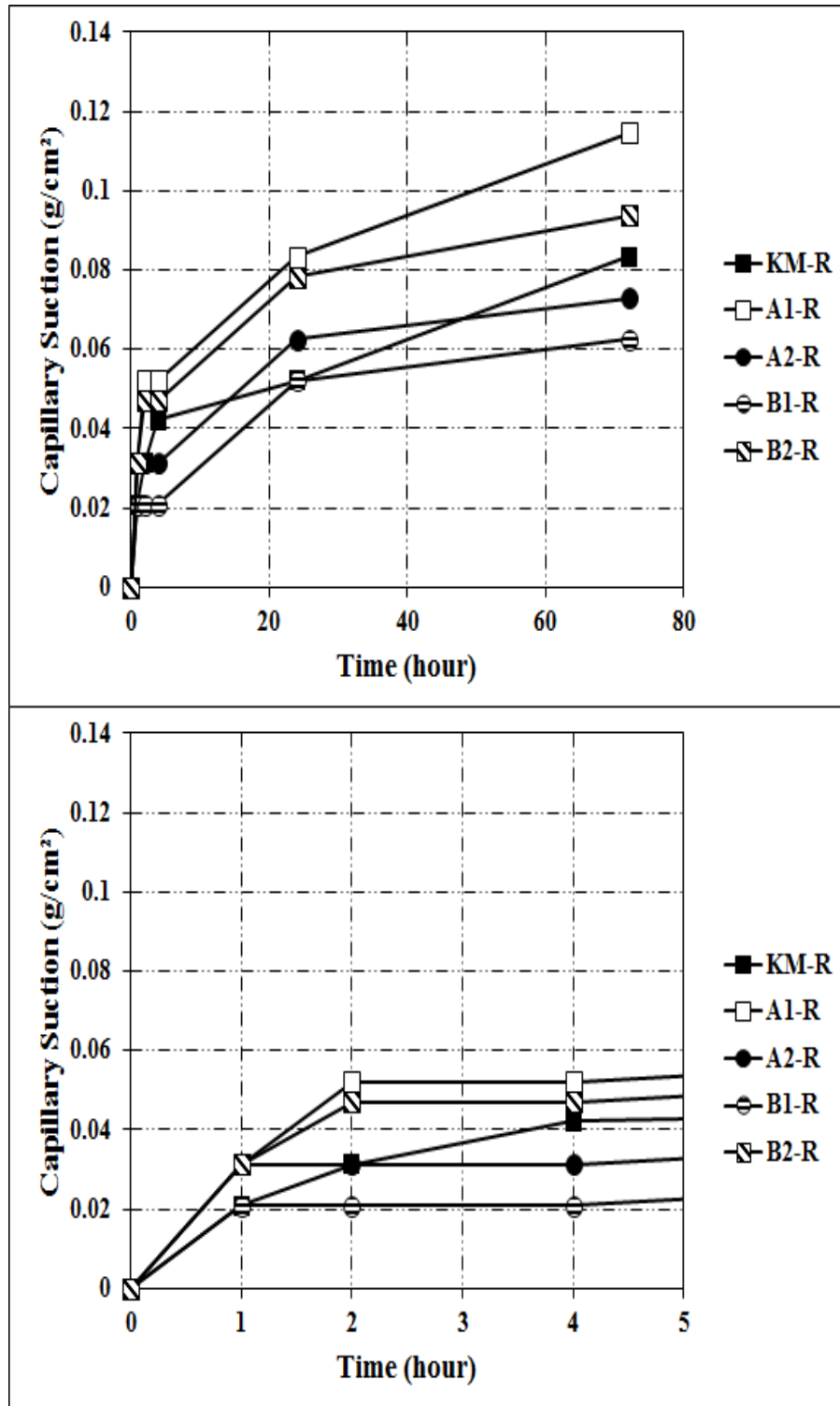


Figure 4.75 Capillary water absorption of SBR containing and RPC control mixtures.

Both acrylic polymers have increased the capillary water absorption of OM mixture (Figure 4.76). While as can be seen from Figure 4.77 these admixtures reduced the capillary suction ratio of RPC mixture. However, it must be noted that

the capillary water absorption behavior of L1 mixture is approximately similar to the RPC mixture.

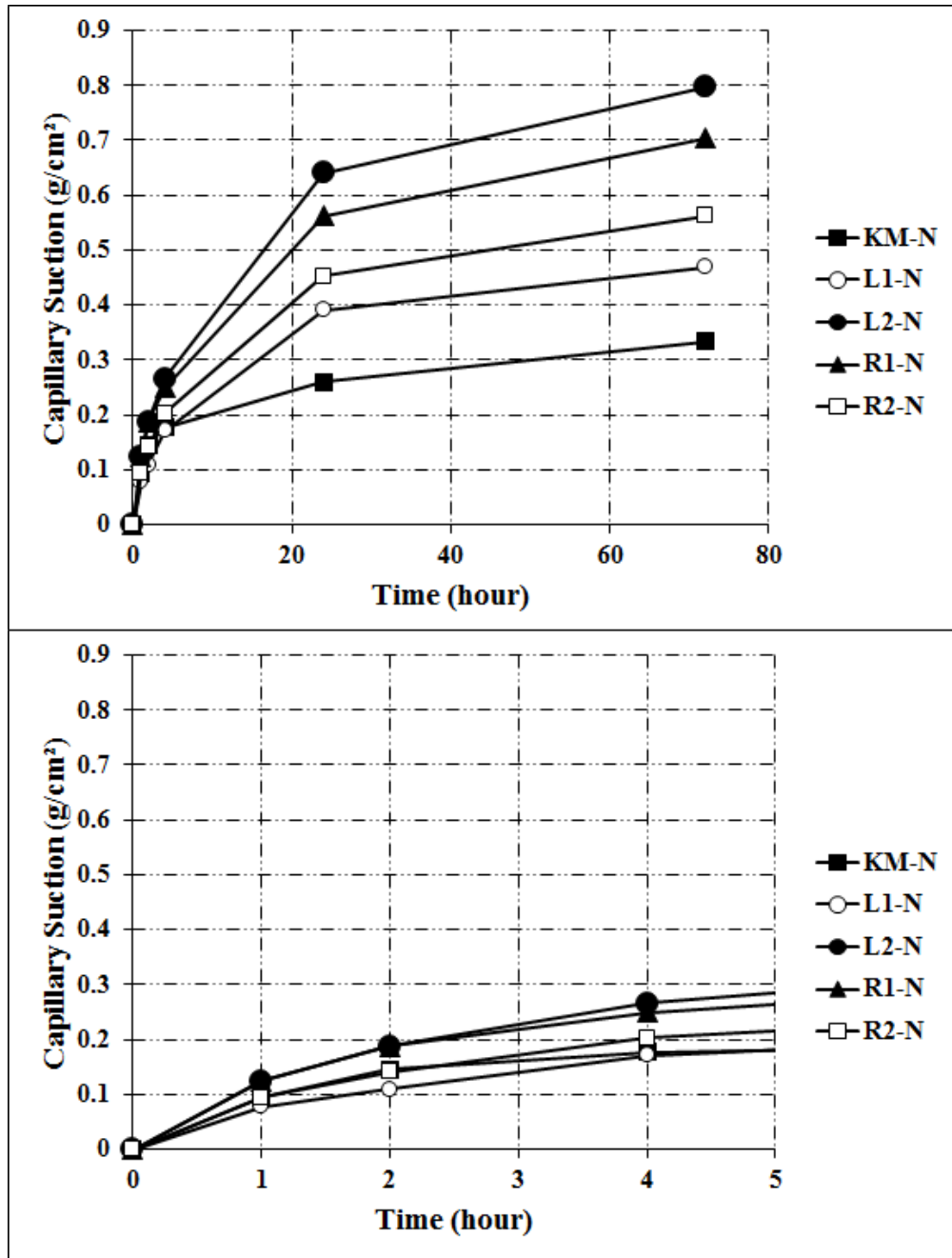


Figure 4.76 Capillary water absorption of ADP containing and OM control mixtures.

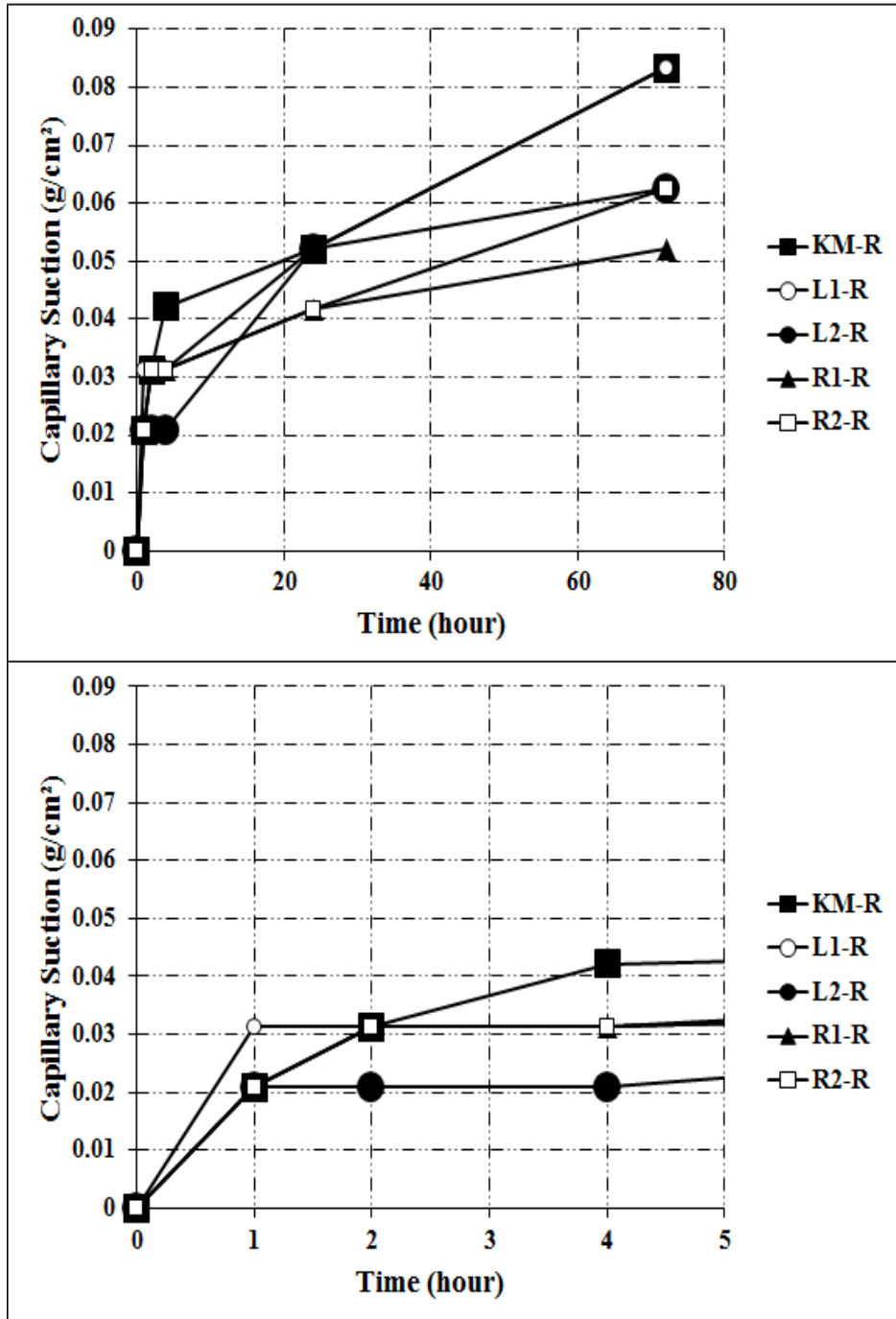


Figure 4.77 Capillary water absorption of ADP containing and RPC control mixtures.

4.2.5 Effect of Chemical Admixtures on Fiber-matrix Pull-out Behavior

As mentioned earlier in Experimental Program section, the effect of chemical admixtures used in this thesis on steel fiber-matrix bond characteristics was determined. Because of using the 48.50 fiber in this section, both pull-out peak load and deboning toughness of OM and RPC mixtures was increased approximately by 100%. This behavior can be explained by the higher diameter of the 48.50 fiber than 80.60 one which causes a greater bond area between fiber and matrix.

The pull-out test load – displacement curves of corrosion inhibitor (CNI) containing and OM control mixtures are presented in Figure 4.78. As can be seen from curves the CNI admixture didn't affect the pull-out behavior of the OM mixture.

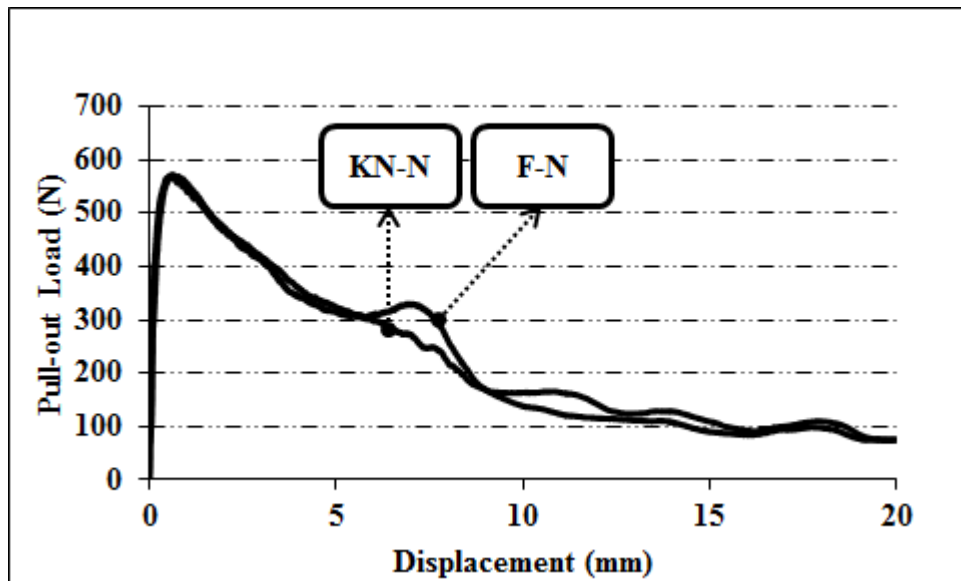


Figure 4.78 Pull-out load–displacement relationships of F and OM control mixtures.

As can be seen from Figure 4.79 both peak load and deboning toughness of RPC mixture is a bit higher than F mixture. However, there is no major difference in pull-out behavior of them.

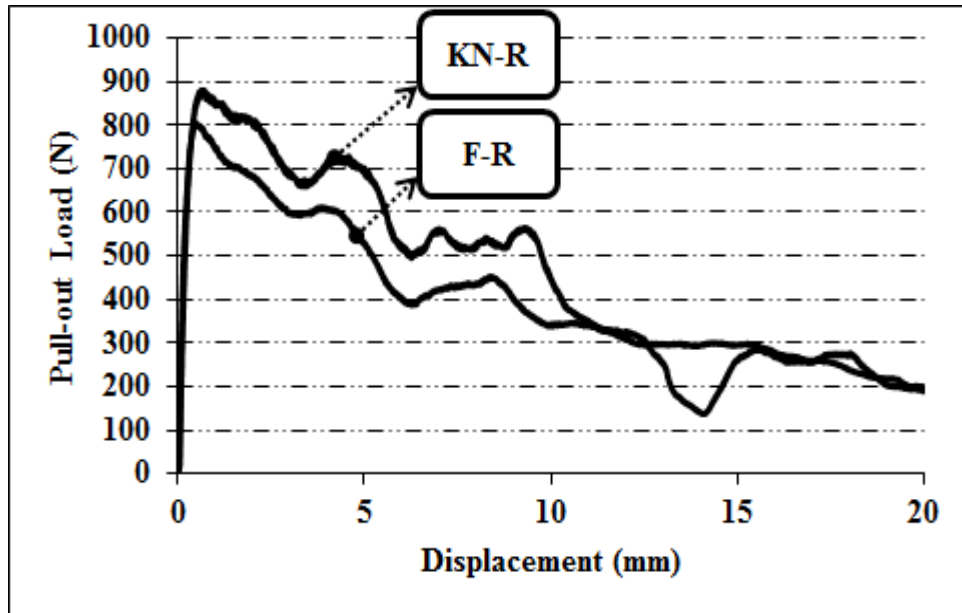


Figure 4.79 Pull-out load–displacement relationships of F and RPC control mixtures.

The waterproofing admixture affects negatively the pull-out behavior of the OM mixture. Both pull-out peak load and deboning toughness was decreased significantly (Figure 4.80). It was observed in microstructure investigation that fiber-matrix interface of SI-N mixture has a high porosity microstructure. Similar result is valid in case of RPC mixture (Figure 4.81).

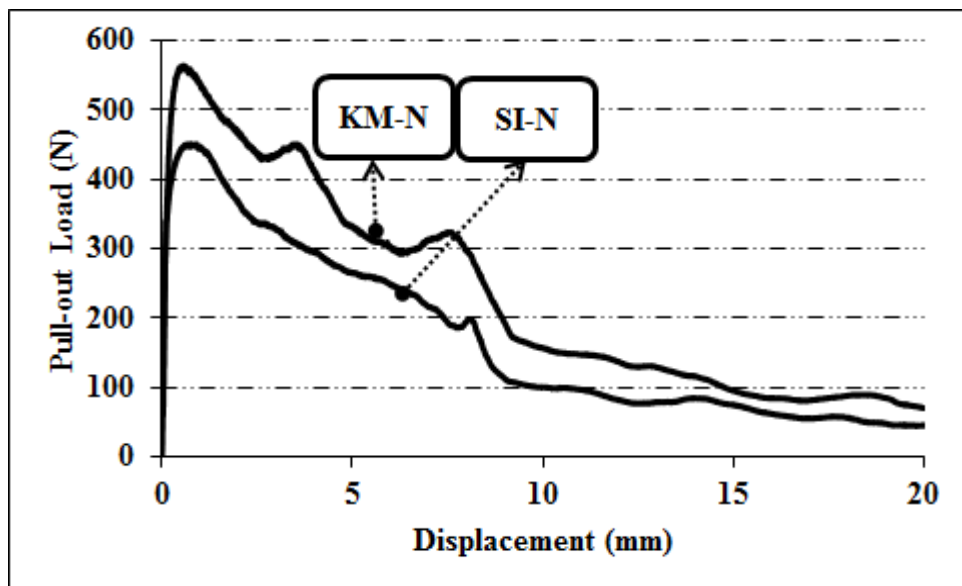


Figure 4.80 Pull-out load–displacement relationships of SI and OM control mixtures.

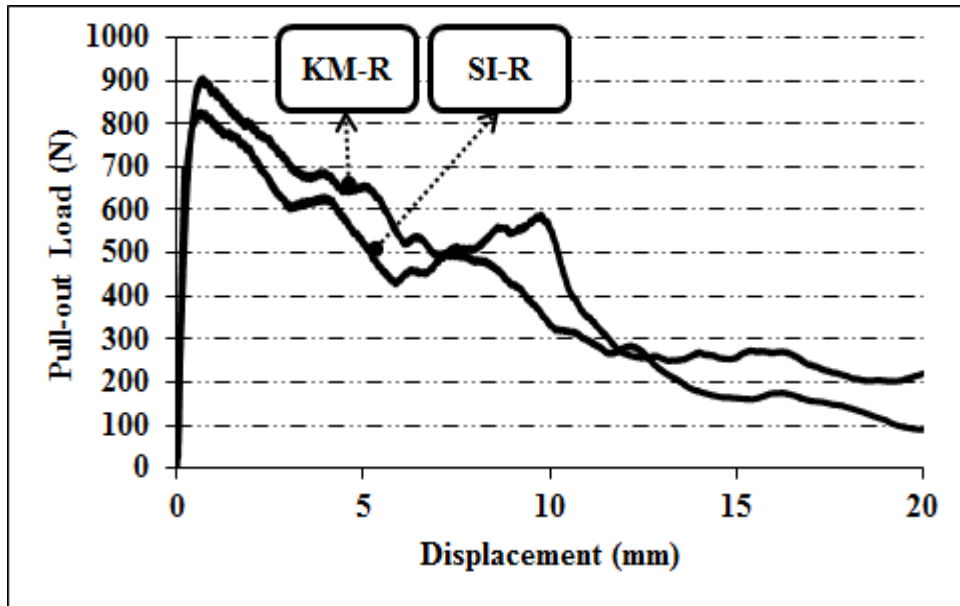


Figure 4.81 Pull-out load–displacement relationships of SI and RPC control mixtures.

The pull-out test load – displacement curves of SBR polymers containing and OM control mixtures are presented in Figure 4.82. The SBR1 admixture with both 5 and 15% dosages (5 and 15% of cement content) improved the pull-out behavior of OM mixture. This behavior can be explained by increasing of bond strength as a result of film formation in fiber-matrix interface. On the other hand, 5% of SBR2 admixture was also improved the pull-out behavior of OM mixture, while 15% of that didn't affect the pull-out behavior.

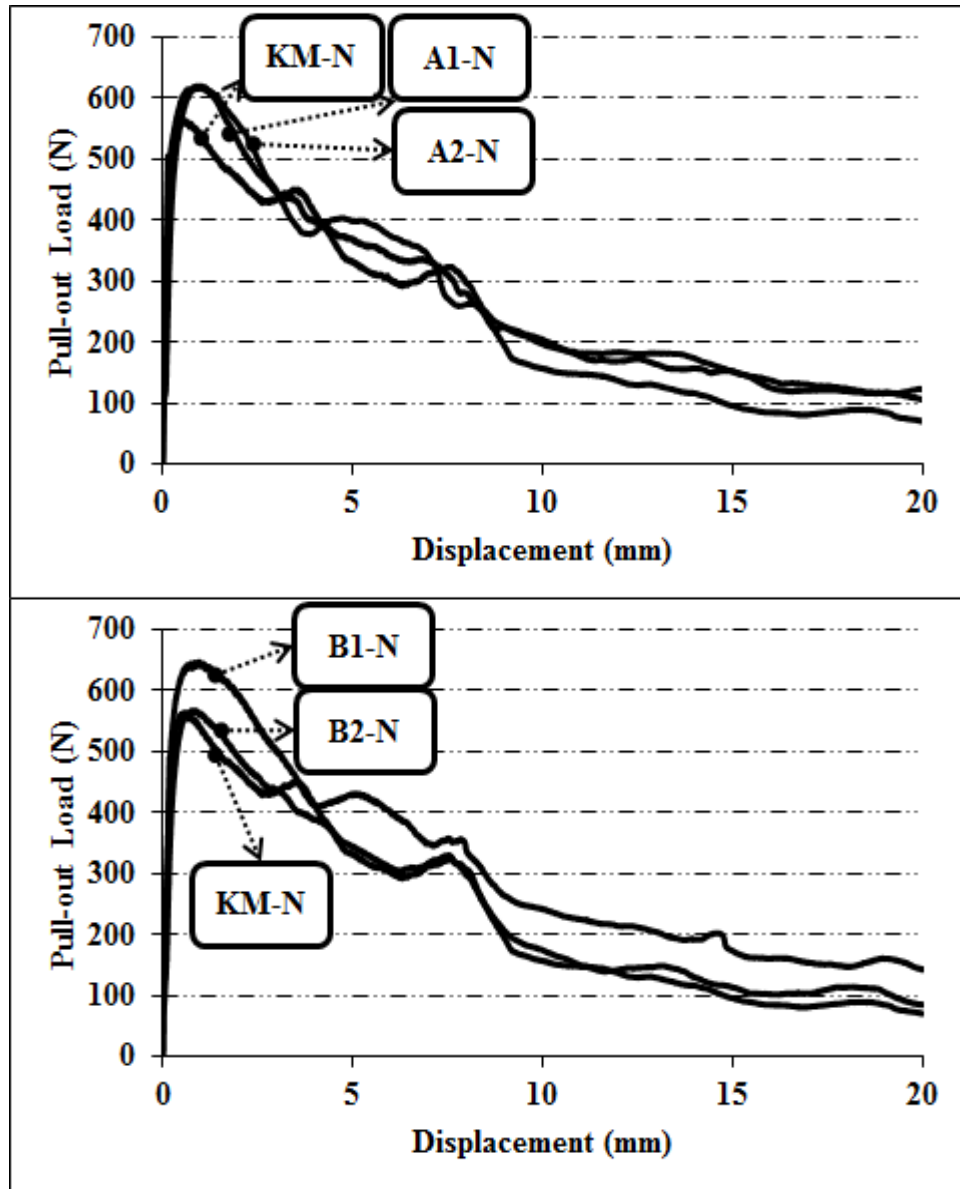


Figure 4.82 Pull-out load–displacement relationships of SBR containing and OM control mixtures.

As can be seen from Figure 4.83 both pull-out peak load and debonding toughness of RPC mixture was reduced by using SBR based polymers. It seems that the dense microstructure of fiber-matrix has been affected negatively by SBR polymers and the film formation was not effective like OM mixture.

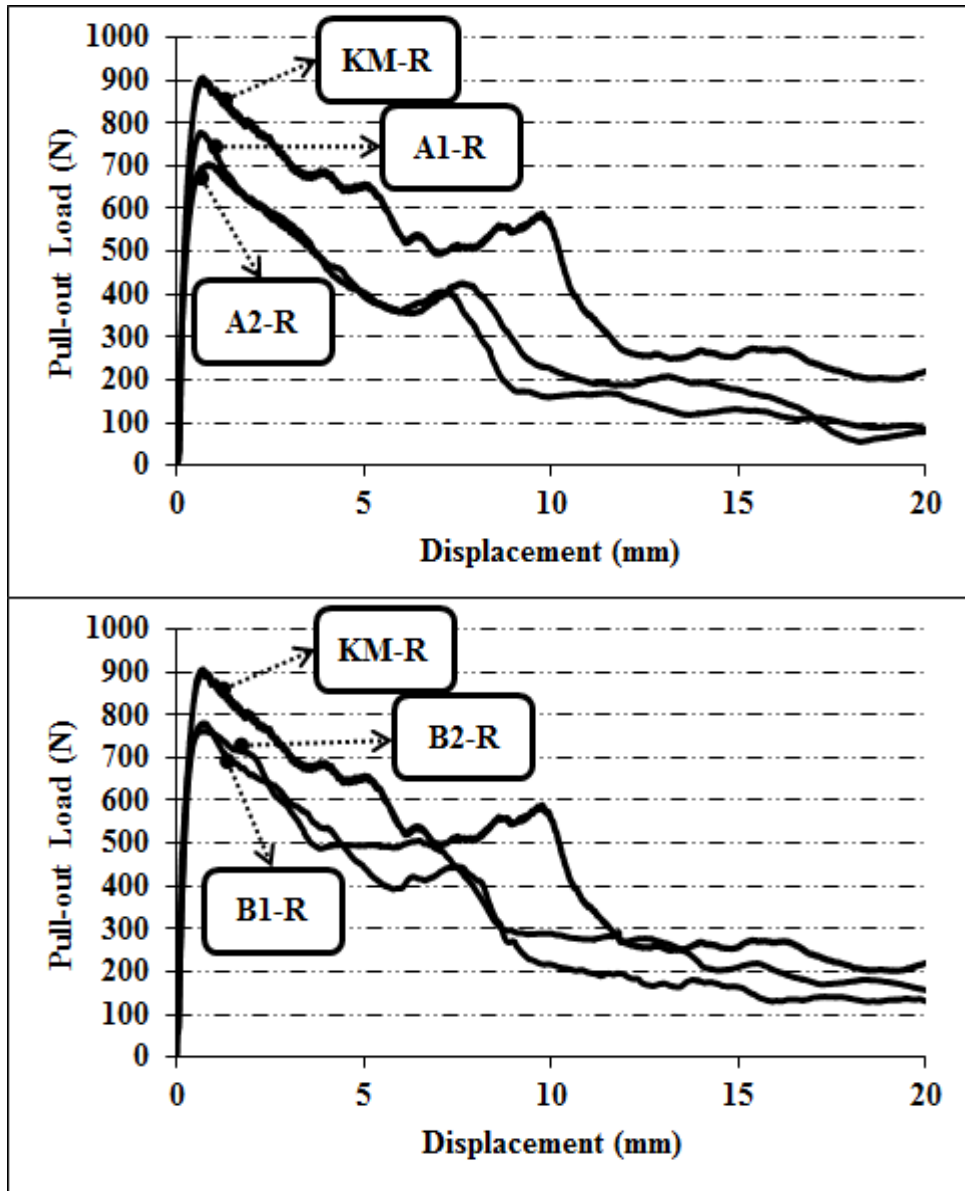


Figure 4.83 Pull-out load–displacement relationships of SBR containing and RPC control mixtures.

It can be said that the pull-out behavior of OM mixture was not affected by using acrylic based polymers. However, a minor positive effect of admixture can be seen in Figure 4.84.

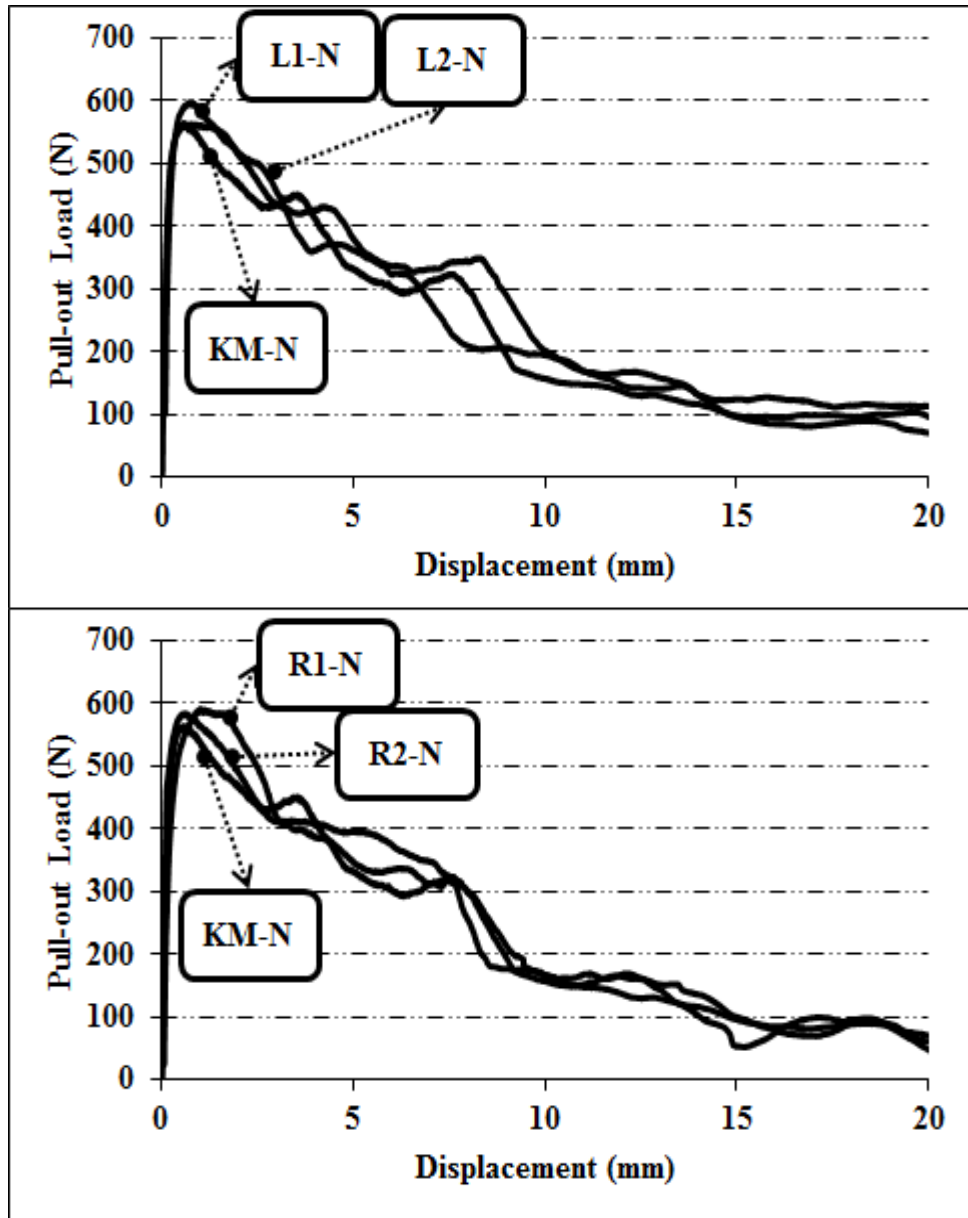


Figure 4.84 Pull-out load–displacement relationships of ADP containing and RPC control mixtures.

Similar to the SBR based admixtures, ADP based admixtures affect negatively the pull-out behavior of RPC mixture (Figure 4.85).

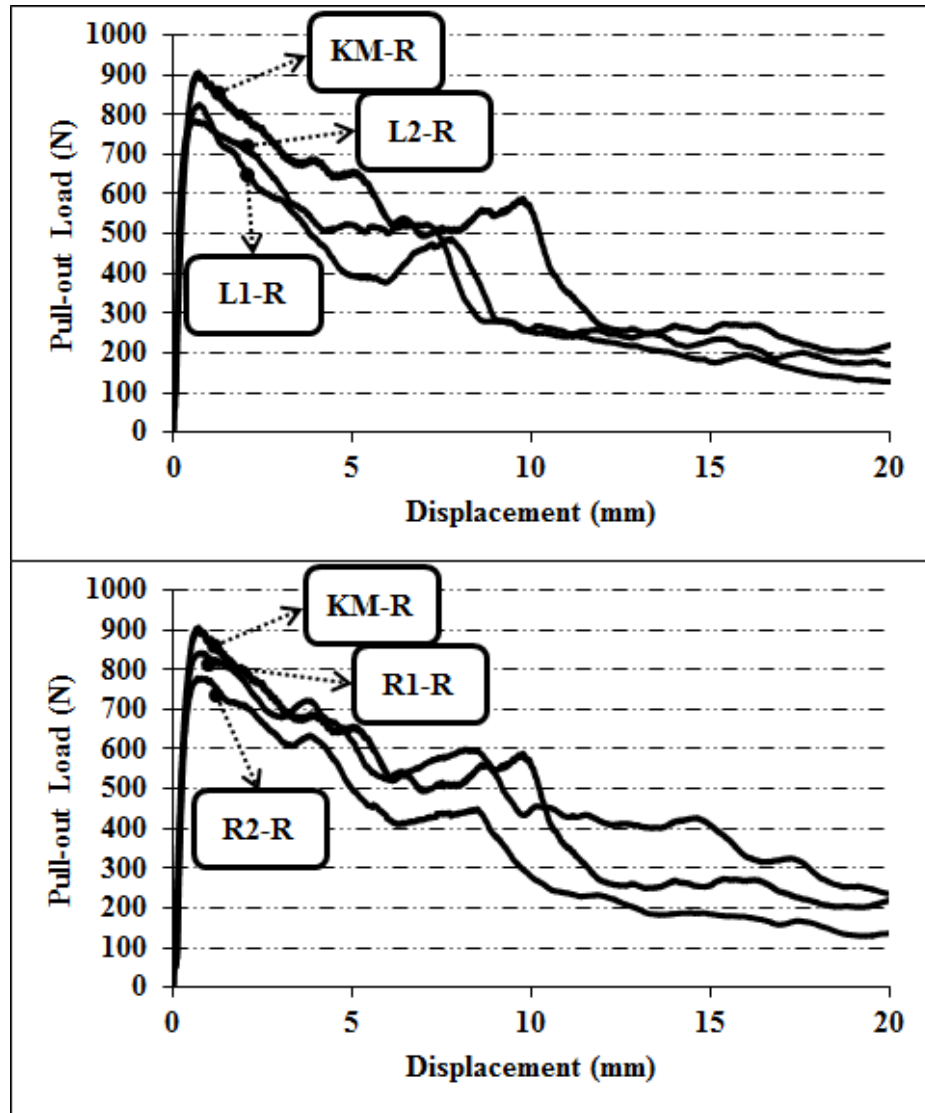


Figure 4.85 Pull-out load–displacement relationships of ADP containing and RPC control mixtures.

Average peak load and debonding toughness values of all mixtures are presented in Figure 4.86. It can be seen from Figure 4.86 that the CNI didn't affect the pull-out behavior significantly. Additionally, the positive effect of polymers in OM mixture is more obvious in debonding toughness values.

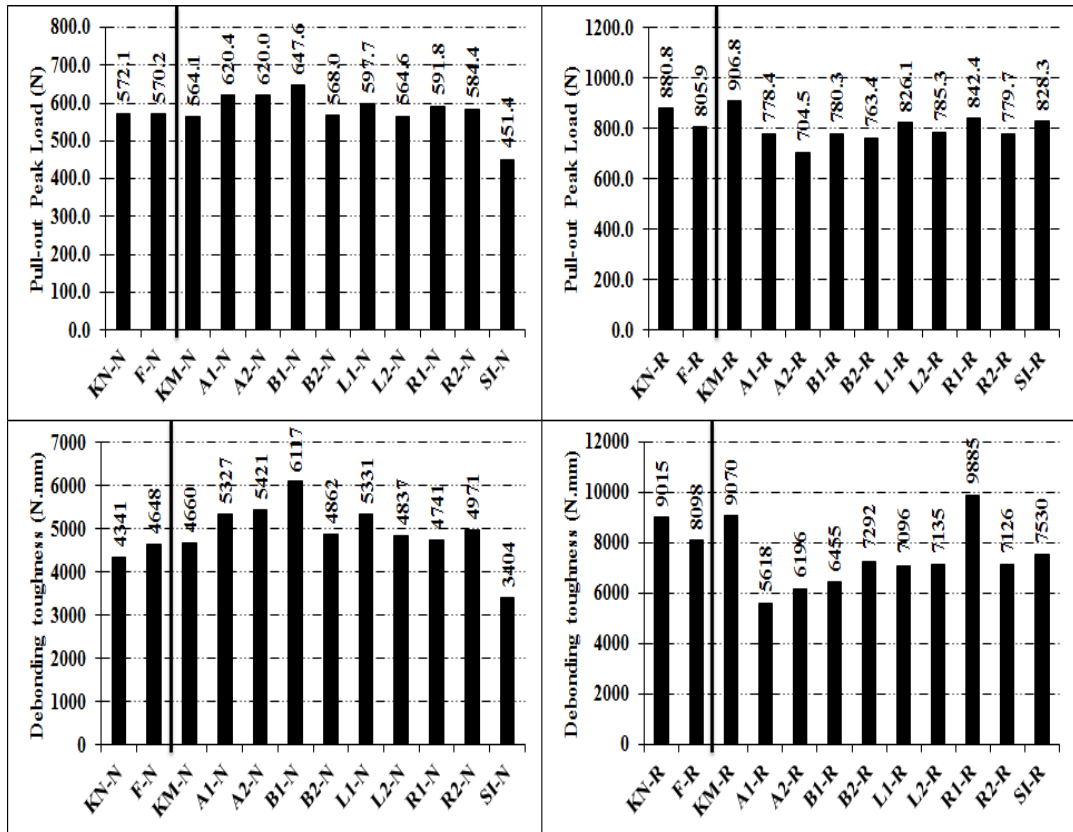


Figure 4.86 Pull-out peak load and debonding toughness of chemical admixture containing mixtures.

4.2.6 Microstructure Investigation

The general and fiber-matrix interface microstructure of some of chemical admixture containing mixtures were investigated by using JEOL JSM 6060 electron microscope (SEM).

Figure 4.87 shows a SEM image of OM mixture incorporating 15% SBR2 admixture. As can be seen from figure all of air voids filled by Ca rich products (4.88).

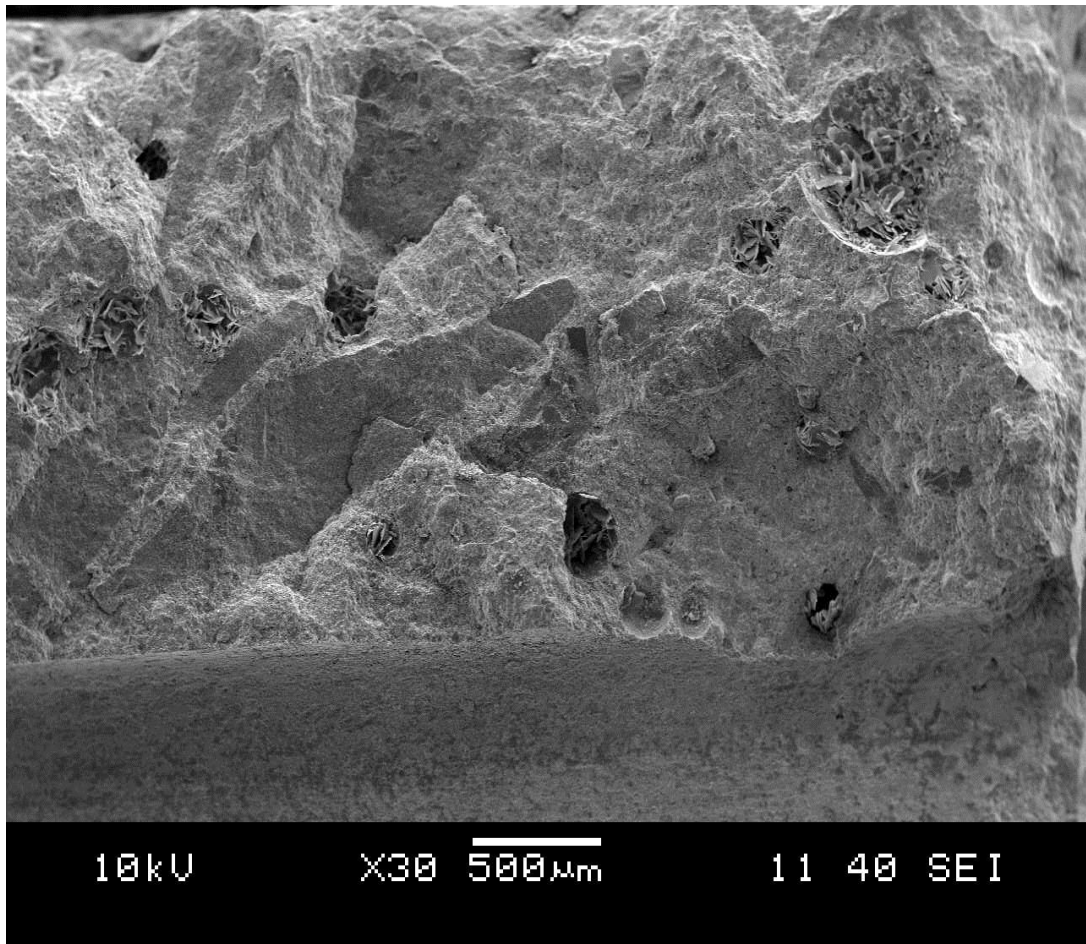


Figure 4.87 SEM image of B2-N mixture.

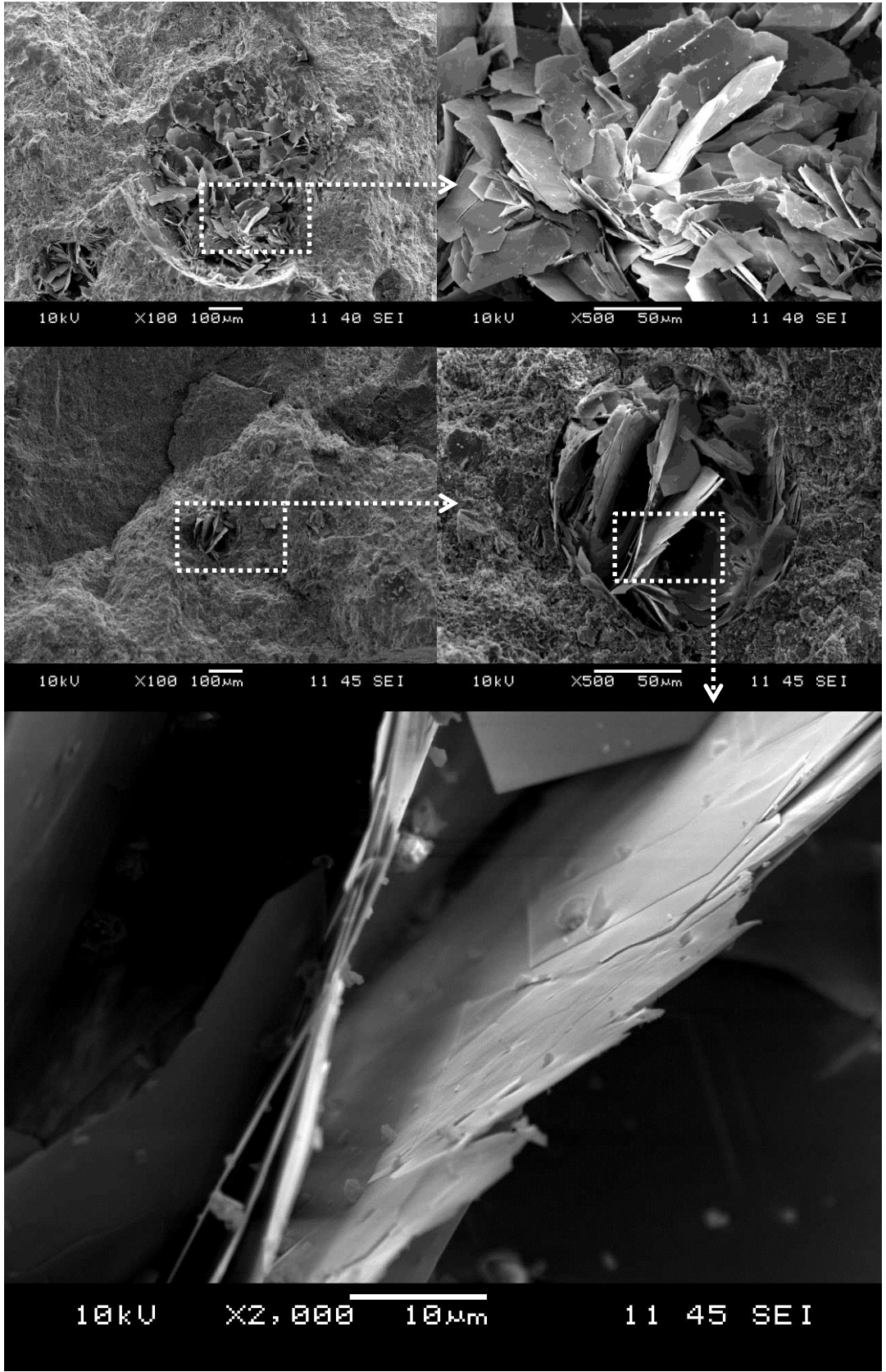


Figure 4.88 SEM image of Ca rich product observed in B2-N mixture.

As can be seen from Figure 4.89 EDS analysis shows the product which observed in air voids of B2-N mixture consist great amount of Ca. Additionally, Ca rich products were also detected in fiber-matrix interface (Figure 4.90).

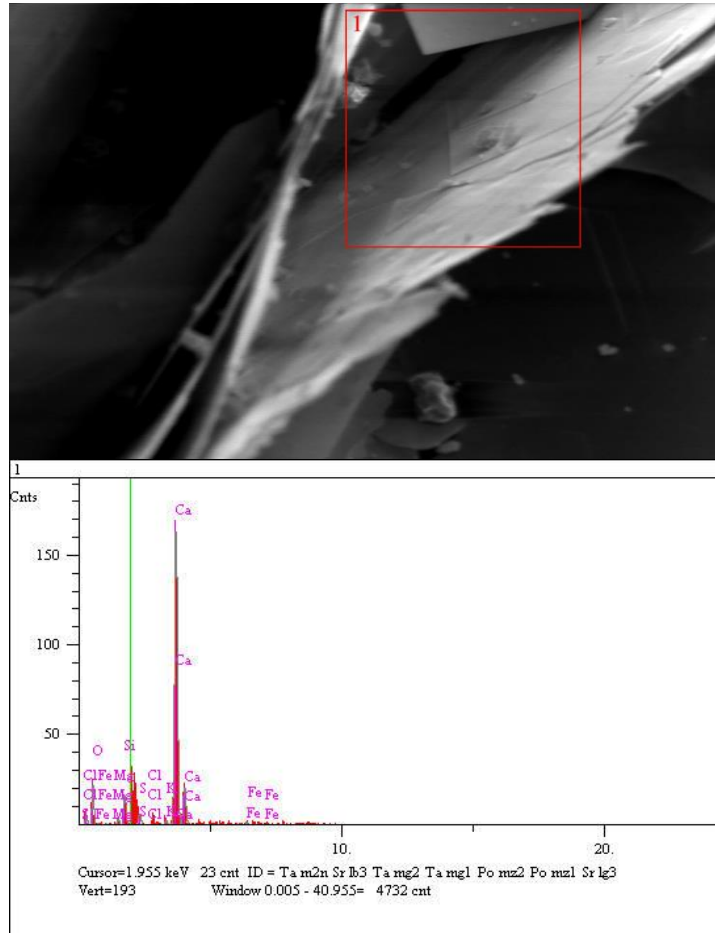


Figure 4.89 EDS analysis of the product which observed in air voids of B2-N mixture.

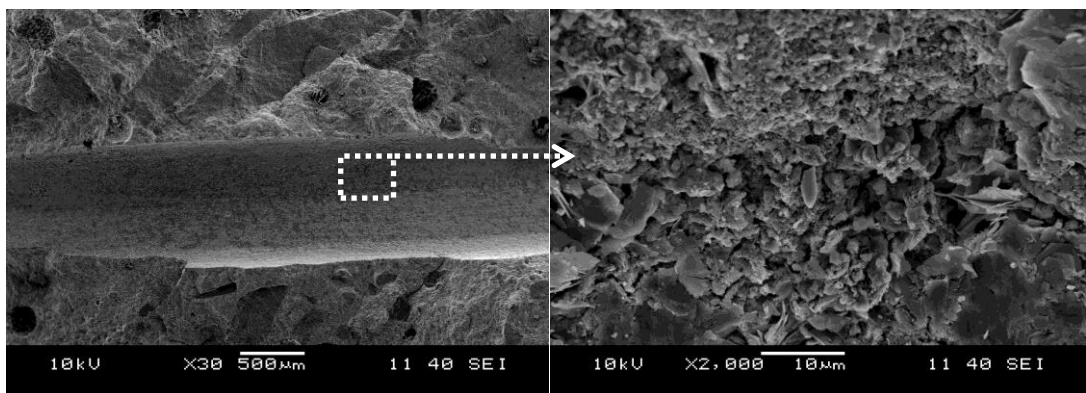


Figure 4.90 SEM image of fiber-matrix interface of B2-N mixture.

It can be seen from EDS analysis of the fiber-matrix interface of A2-N that this zone have a considerable concentration of C which can be related to the film formation of the SBR polymer (Figure 4.91). Furthermore, similar to the B2-N mixture, all of air voids of the OM mixture incorporating 15% SBR1 admixture filled by Ca rich products (4.92).

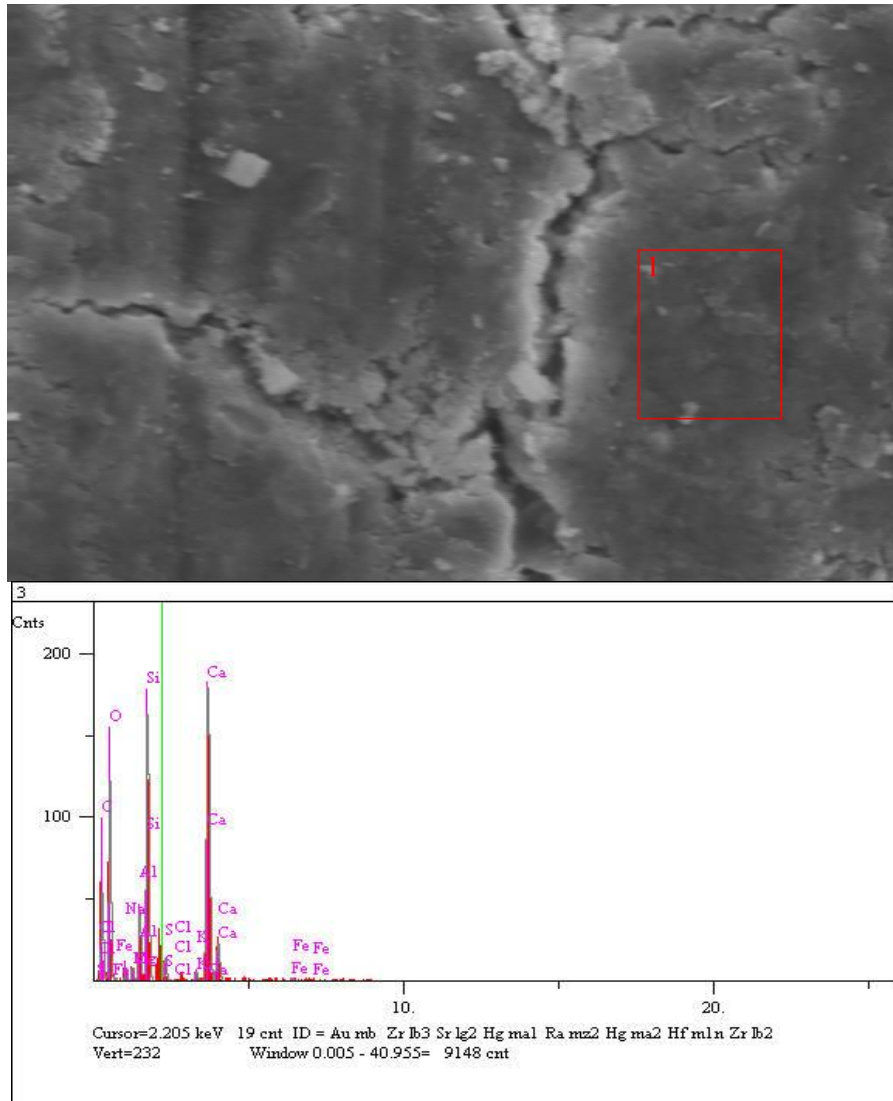


Figure 4.91 EDS analysis of the fiber-matrix interface of A2-N.

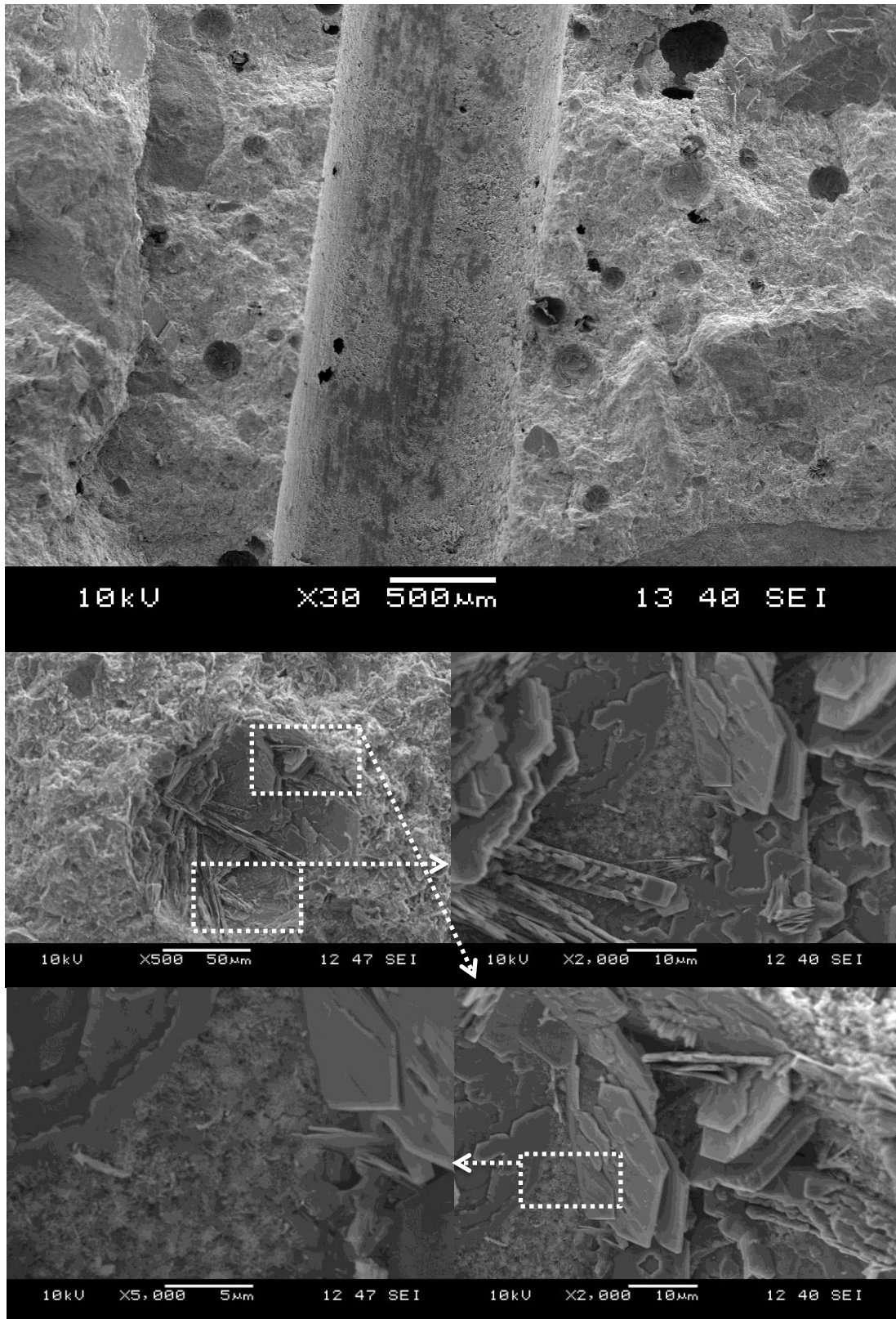


Figure 4.92 SEM image of A2-N mixture.

Figure 4.93 shows the air entraining effect of SBR2 (SBR - 15%) on RPC mixture. These air voids decreased the mechanical strength of the RPC.

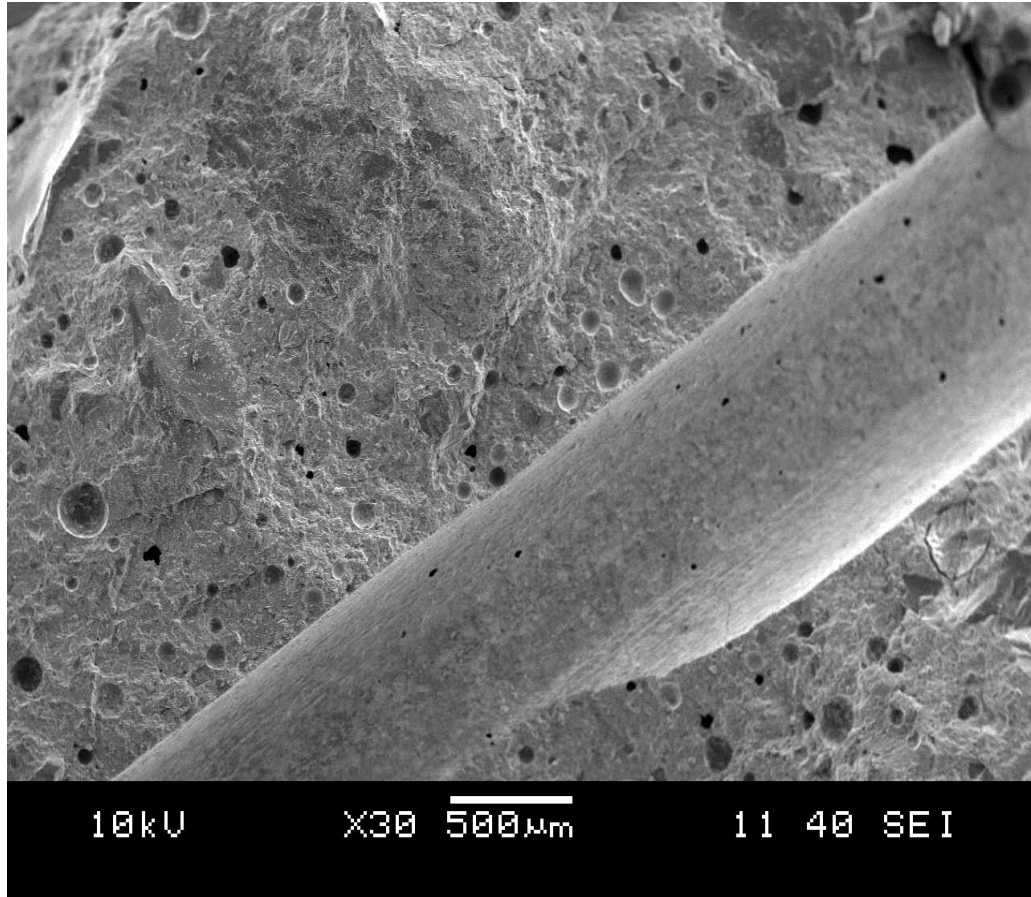


Figure 4.93 SEM image of A2-R mixture.

As can be seen from Figure 4.94 acrylic based admixture (ADP2) has also air entraining effect. The R2-R mixture consists of many air voids. The SEM image of RPC control mixture was also presented in Figure 4.94.

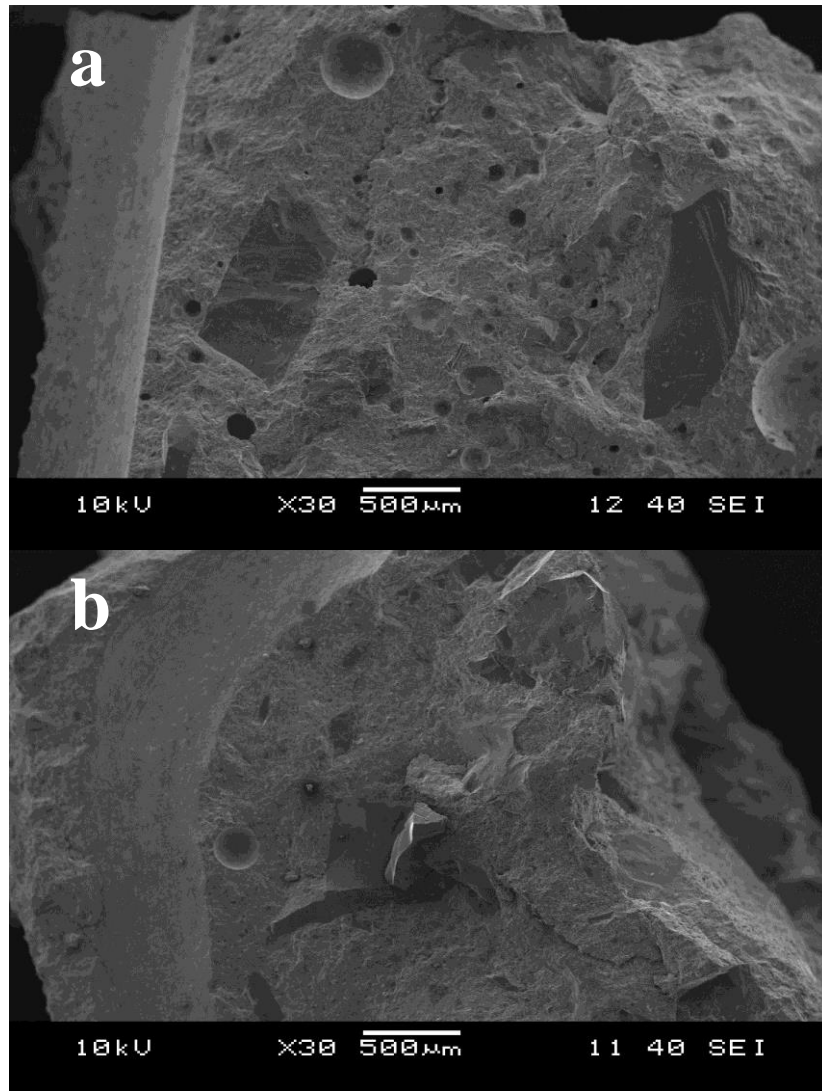


Figure 4.94 SEM images of a) R2-R b) KM-R.

Ca rich products with a minor different morphology also exist in all air voids of SI-N mixture (Figure 4.95).

The porous microstructure of fiber-matrix interface of SI-N mixture can be seen from Figure 4.96. As mention earlier the waterproofing admixture affect negatively the pull-out behavior of OM mixture.

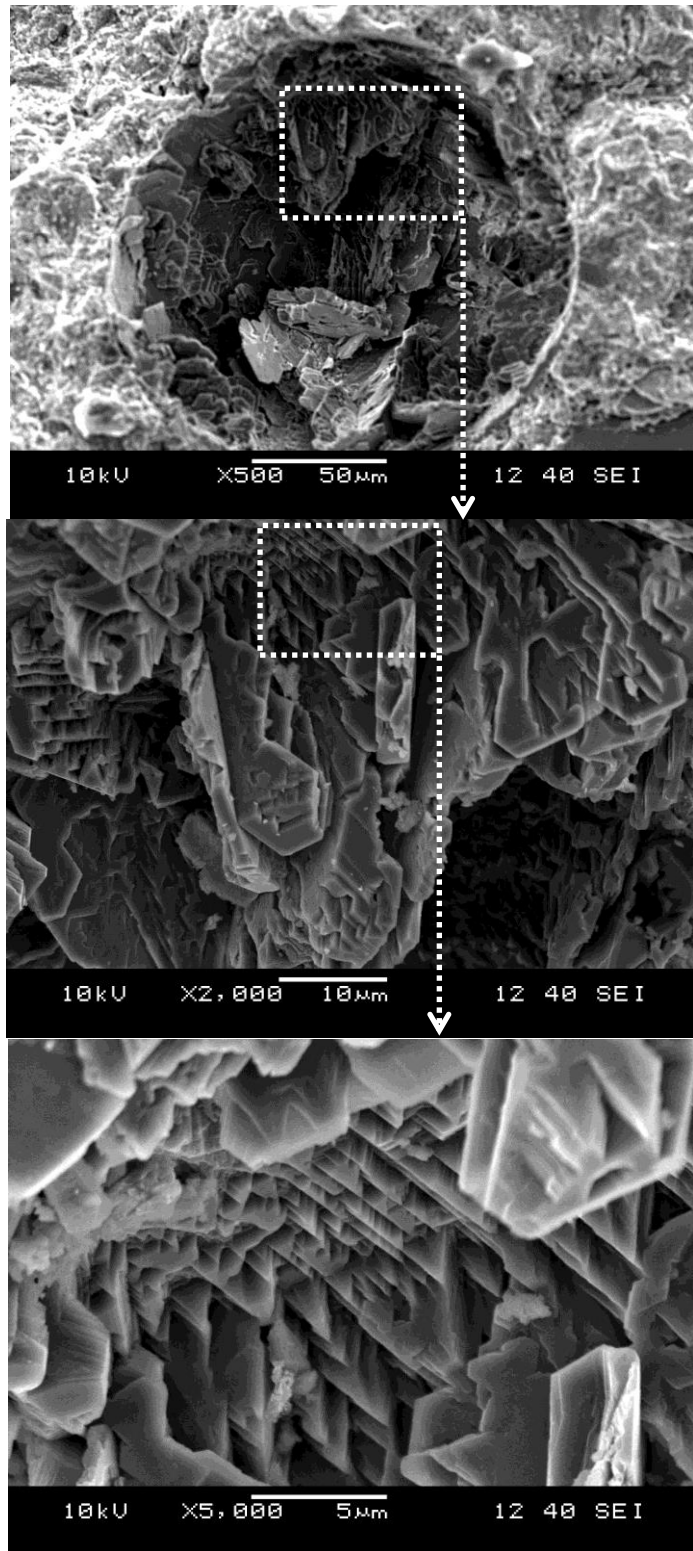


Figure 4.95 SEM images of SI-N mixture.

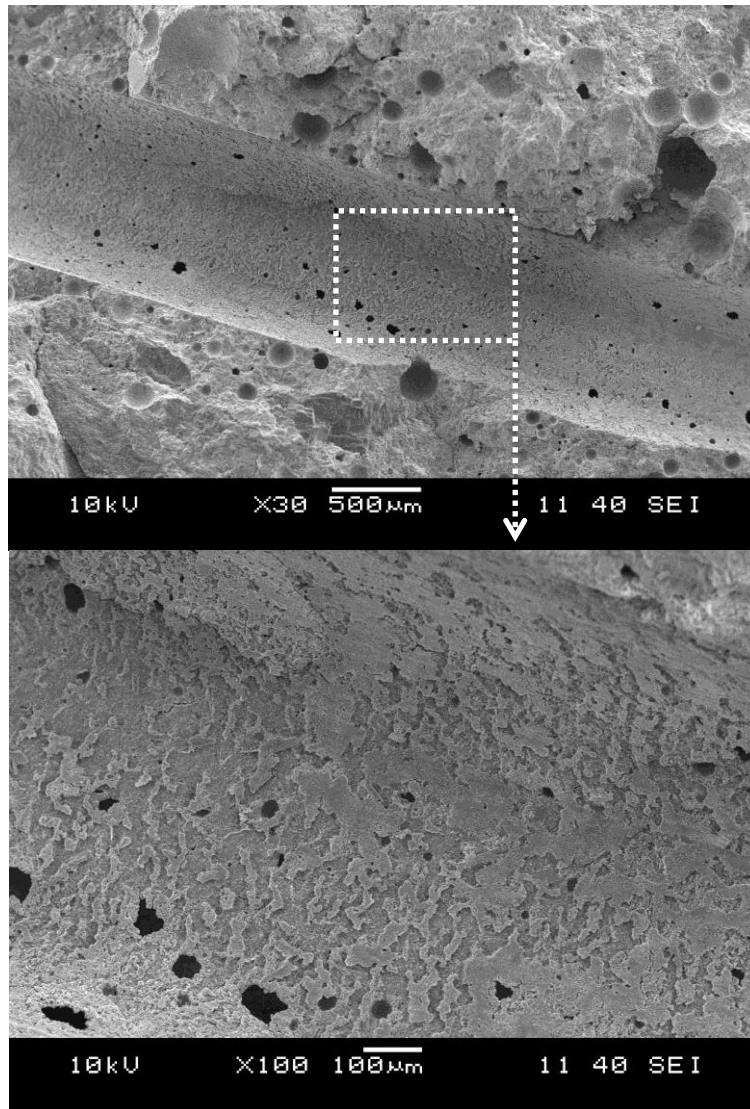


Figure 4.96 SEM images of SI-N mixture.

4.2.7 Corrosion Measurement

The specimens which were subjected to wetting-dyeing cycle were measured after 200 and 400 cycles. However, both corrosion potential and corrosion current density values of all specimens were very low which shows that the corrosion of the fibers was not begun.

The specimens were put the cabin to continue the cycles. The corrosion measurements and pull-out test of them will be carried out in future.

CHAPTER FIVE

CONCLUSIONS

In scope of this thesis, the effect of four (1, 2, 3, 4 cm) different embedment lengths and end condition (Hooked-end and smooth) of steel fiber on pull-out behavior in both OM and RPC mixtures were investigated. Furthermore, paste phase (binder + water) of RPC was examined. The effect water/cement ratio in three groups of matrices was also evaluated. The W/C ratio of mix design of OM was redesigned from 0.5 to 0.6, 0.4, and 0.3 and also the W/B ratio of mix design of RPC has been increased to 0.3, 0.4, 0.5, and 0.6 with and without steel micro fiber. Additionally, the study was carried out under four curing condition (7 and 28 water curing, steam, and autoclave curing). It should be noted that the mechanical properties of all matrices were determined. Additionally, the corrosion rate of steel fiber exposed to corrosive environment was also determined.

The result obtained by experimental program can be summarized as follow:

- The hooked-end fiber has a better performance in pull-out test than smooth once. This behavior is valid in all embedment lengths and mixtures.
- Both pull-out peak load and deboning toughness increases as the embedded length of fiber increased. This behavior is more obvious in case of smooth fiber.
- 1 cm embedment length is strongly insufficient in case of smooth fiber in all mixtures. This behavior is not valid in case of hooked-end fiber.
- Pull-out peak load and deboning toughness value of smooth and hooked-end fiber increased with increasing matrix strength.
- The pull-out behavior of both smooth and hooked-end fiber in all embedment lengths of fibers improves in 28 days water curing compared

to 7 days water curing. The strength development of hooked-end fiber is better than smooth once in case of OM mixture.

- Mechanical strength of OM mixture with low W/C ratio decreased in steam curing.
- Mechanical strength of mixtures decreased in autoclave curing due to absence of SiO₂ components. This behavior becomes stronger with increasing the W/B ratio. However, the pull-out behavior develops significantly in autoclave curing. The bond strength development in autoclave curing is more obvious in RPC mixtures. The tobermorite gel congestion in fiber-matrix interface is the reason for this excellent bond strength in autoclave curing.
- Both pull-out peak load and debonding toughness increased with decreasing the W/B ratio in both OM and RPC mixture in all curing conditions.
- The bond strength of mixtures with any W/B ratio is higher at 28 days water curing compared to the 7 days once.
- Reinforcing the RPC mixture by incorporating steel-micro fiber doesn't affect the pull-out behavior of fiber in all RPC mixtures with various W/B ratios importantly.
- Corrosion inhibitor (CNI) admixture doesn't affect significantly the pull-out behavior of steel fiber in both OM and RPC mixtures. However, the mechanical strength of OM mixture was affected negatively by using CNI, while this behavior is not valid in case of RPC. Additionally, CNI admixture has a positive effect in physical properties of OM and especially RPC mixtures.
- Waterproofing admixture has a negative effect on all properties of OM mixture, while it improved some of characteristics of RPC or didn't affect them.

- SBR polymer based admixtures depends on their type and dosage has positive affect on flexural strength and some physical properties of OM mixture, but this behavior is not valid in case of compressive strength. Furthermore, they improved the pull-out behavior of fiber in OM mixture. The positive effect of SBR admixtures wasn't observed in RPC.
- Acrylic based polymers depend on their type and dosage has positive effect on mechanical strength of RPC and some of physical properties of that such as capillary water absorption and chloride ion penetration. However, this behavior is not valid in case of OM mixture.

This study mainly aimed to evaluate the effect of a few of many factors on bond characteristics of fiber-matrix of cement based composites. It can be concluded from test result that matrix properties, steel fiber characteristics, and curing condition has a remarkable effect on pull-out behavior of steel fiber.

Since the bond characteristics of fiber-matrix are relatively new matter, the future research for these subject include a wide research area. The following suggestions are potentially new research topics:

- Effect of durability problems such as freezing-thawing and high temperature.
- Influence of aggregate size and dosage.
- Effect of mineral additives.

REFERENCES

- Abu-Lebdeh, T., Hamoush, S., Heard, W., & Zornig, B. (2011). Effect of matrix strength on pullout behavior of steel fiber reinforced very-high strength concrete composites. *Construction and Building Materials*, 25(1), 39-46.
- Aiello, M.A., Leuzzi, F., Centonze, G., & Maffezzoli, A. (2009). Use of steel fibres recovered from waste tyres as reinforcement in concrete: Pull-out behavior, compressive and flexural strength. *Waste Management*, 29(6), 1960-1970.
- Armelin, H.S., & Banthia, N. (1997). Predicting the flexural postcracking performance of steel fiber reinforced concrete from the pullout of single fibers. *American Concrete Institute Materials Journal*, 94(1), 18-31.
- ASTM C 1202-05 (2005). *Standard Test Method for Electrical Indication of Concrete's Ability to Resist Chloride Ion Penetration*. American Society for Testing and Materials, West Conshohocken, PA, 6 pp.
- Banthia, N., Bentur, A., & Mufti, A. (1998). *Fiber reinforced concrete: present and future*. The Canadian Society for Civil Engineering.
- Beglarigale, A., & Yazıcı, H. (2013). The effect of alkali-silica reaction on steel fiber-matrix bond characteristics of cement based mortars. *Construction and Building Materials*, 47, 845-860.
- Bentur, A., & Mindess, S. (1990). *Fibre reinforced cementitious composites*. London: Elsevier Applied Science.
- Bentur, A., Diamond, S., & Mindess, S. (1985). The microstructure of the steel fibre-cement. *Journal of Materials Science*, 20(10), 3610-3620.

- Bentur, A., Mindess, S., & Diamond, S. (1985). Pull out processes in steel fiber reinforced cement. *International Journal of Cement Composites & Lightweight Concrete*, 7(1), 29-38.
- Bentur, A., Wu, S.T, Banthia, N., Baggott, R., Hansen, W., Katz, A., et al. (1995). *Fibre-matrix interfaces, High Performance Fibre Reinforced Cementitious Composites*. London: Chapman and Hall.
- Chan Y.W., & Chu, S.H. (2004). Effect of silica fume on steel fiber bond Characteristics in reactive powder concrete. *Cement and Concrete Research*, 34(7), 1167-1172.
- Chan, Y.W., & Li, V.C. (1997). Effects of transition zone densification on fiber/cement paste bond strength improvement. *Advanced Cement Based Materials*, 5(1), 8-17.
- Çolak, A. (2005). Properties of plain and latex modified Portland cement pastes and concretes with and without superplasticizer. *Cement and Concrete Research*, 35(8), 1510-1521.
- Cunha, V., Barros, J., & Sena-Cruz, J.M (2010). Pullout behavior of steel fibers in self-compacting concrete. *Journal of Materials in Civil Engineering*, 22(1), 1-9.
- Gao, J.M., Qian, C.X., Wang, B., & Morino K. (2002). Experimental study on properties of polymer-modified cement mortars with silica fume. *Cement and Concrete Research*, 32(1), 41-45.
- Gray, R.J. (1983). Experimental techniques for measuring fibre/matrix interfacial bond shear strength. *International Journal of Adhesion and Adhesives*, 3(4), 197-202.

- Kayali, O.A. (2004). Effect on high volume fly ash on mechanical properties of fiber reinforced concrete. *Materials and Structures*, 37(5), 318-327.
- Kim, J.H., & Robertson, R.E. (1997). Prevention of air void formation in polymer-modified cement mortar by pre-wetting, *Cement and Concrete Research*, 27(2), 171-176.
- Kim, J.J., Kim, D.J., Kang, S.T., Lee, J.H. (2012). Influence of sand to coarse aggregate ratio on the interfacial bond strength of steel fibers in concrete for nuclear power plant. *Nuclear Engineering and Design*, 252, 1-10.
- Lee, Y., Kang, S.T., & Kim J.K. (2010). Pullout behavior of inclined steel fiber in an ultra-high strength cementitious matrix. *Construction and Building Materials*, 24(10), 2030-2041.
- Lehmann, C., Fontana, P., & Muller, U. (2009). Evolution of phases and microstructure in hydrothermally cured Ultra-High Performance Concrete (UHPC). *Nanotechnology in construction* 3, 287-93.
- Neville, A.M. (1995). *Properties of Concrete*. England: Addison Wesley Longman Limited.
- Odler, I. (2004). Hydration setting and hardening of Portland cement. *Lea's chemistry of cement and concrete* (4th ed.) (241-398). UK: Elsevier Science & Technology Books.
- Ohama, Y. (1997). Recent progress in concrete-polymer composites. *Advanced Cement Based Materials*, 5(2), 31-40.
- Ohama, Y., (1998). Polymer-based admixtures. *Cement and Concrete Composites*, 20(23), 189-212.

- Pascal, S., Alliche, A., & Pilvin, P. (2004). Mechanical behaviour of polymer modified mortars. *Materials Science and Engineering A*, 380, 1-8.
- Pei, M., Kim, W., Hyung, W., Ango, A.J., & Soh Y. (2002). Effects of emulsifiers on properties of poly(styrene– butyl acrylate) latex-modified mortars. *Cement and Concrete Research*, 32(6), 837-841.
- Richard, P., & Cheyrezy, M. (1994). Reactive powder concretes with high ductility and 200 - 800 Mpa compressive strength. *American Concrete Institute*, 144, 507-18.
- Richard, P., & Cheyrezy, M. (1995). Composition of reactive powder concretes. *Cement and Concrete Research*, 25(7), 1501-11.
- Shannag, M.J., Brincker, R., & Hansen, W. (1997). Pullout behavior of steel fibers from cement-based composites. *Cement and Concrete research*, 27(6), 925-36.
- Silva, F.A., Mobasher, B., Soranakom, C., & Filho, R.D.T. (2011). Effect of fiber shape and morphology on interfacial bond and cracking behaviors of sisal fiber cement based composites. *Cement & Concrete Composites*, 33(8), 814-823.
- Tuyan, M., & Yazıcı H. (2012). Pull-out behavior of single steel fiber from SIFCON matrix. *Construction and Building Materials*, 35, 571-577.
- Wang, R., Wang, P.M., & Li, X.G. (2005). Physical and mechanical properties of styrene–butadiene rubber emulsion modified cement mortars. *Cement and Concrete Research*, 35(5), 900-906.
- Wu, H.C., & Li, V.C. (1999). Fiber/cement interface tailoring with plasma treatment. *Cement & Concrete Composites*, 21(3), 205-212.